Investigating the role of CBX2 in models of triple negative breast cancer

Chloe Warren

201501220

Thesis for the Masters by Research course in Biomedical Science

Supervisor: Dr Mark Wade

Second Supervisor: Dr Barbara Guinn

September 2019

Acknowledgments

I would like to thank Ella Waters for all of her support and encouragement throughout the project.

I would like to thank Dr Mark Wade for being a great supervisor and for all of his knowledge, support and guidance, without which I would not have been able to complete this project.

I am grateful to Dr Barbara Guinn for her knowledge and experience, which was very helpful throughout the project.

I would like to thank Dr Cheryl Walter for all of the extra resources, guidance and kind words throughout the project.

I would like to thank Rebecca Humphries for her support, advice and kind words during the project.

I would like to acknowledge Dr Pedro Beltran-Alvarez, Mrs Kathleen Bulmer and Josh Warnes for their assistance and helpful advice during the project.

I would like to thank Ellie Beeby for providing phase contrast microscopy training.

I would like to thank all of my family and friends for their unconditional love and support during this project, I could not have completed this project without their understanding, and I am incredibly grateful to have had them with me throughout.

Abstract

Breast cancer accounts for around 11,500 deaths per year in the UK in women. There are several subtypes of breast cancer including triple negative breast cancer (TNBC) which is categorised by a lack of oestrogen, progesterone and human epidermal growth factor 2 (HER2) hormone receptor expression. The prognosis for patients with TNBC is poor as it is an aggressive subtype of the disease that currently lacks any targeted therapeutics and is therefore hard to treat. The identification of novel therapeutic targets for TNBC is therefore crucial.

Epigenetics is the study of gene expression control via chemical modification of DNA and histone proteins. Recent studies have shown that altered histone modification is linked with cancer development. Epigenetic regulatory proteins may therefore be a source of novel therapeutic targets in cancer. CBX2 is an epigenetic reader protein and is part of the polycomb repressive complex 1 (PRC1). Expression of CBX2 is increased in TNBC compared to normal breast tissue indicating that it may play a role in the progression of this disease. This study aimed to investigate the function of CBX2 in TNBC by downregulating *CBX2* expression in TNBC cell line models by RNA interference (RNAi) and analysing phenotypic and gene expression changes. We identified that CBX2 is present in an active phosphorylated form in TNBC cells and that cell proliferation decreased when CBX2 was knocked down. We identified that the expression of cell cycle regulatory genes such as *Cyclin D1 (CCND1), CCND3, CCNA2 CDK1* and *CDK4* decreased when CBX2 was knocked down and RNA-Seq analysis in TNBC cells following CBX2 knockdown showed that differentially expressed genes were associated with the cell cycle and multiple oncogenic signalling pathways. These results suggest that CBX2 may play a key role in TNBC development and may therefore be a potential future therapeutic target.

Key words

Breast cancer

CBX2

PRC1

Triple negative breast cancer

Histone modifications

Post translational modifications

Contents

Abbreviation List

APS – Ammonium persulphate

BET – Bromodomain and extraterminal

BL1 - Basal-like 1

BL2 - Basal-like 2

BLBC - Basal-like breast cancer

BMI - B-lymphoma Mo-MLV insertion region 1 homolog

BRD - Bromodomain

BSA – Bovine serum albumin

CBX2 – Chromobox 2

CCND – Cyclin

CDK – Cyclin-dependent kinase

CDKN1A – Cyclin dependent kinase inhibitor 1A

CDKN2A – Cyclin dependent kinase inhibitor 2A

CIP – Calf intestinal phosphatase

ddH_20 – Double distilled water

DNA – Deoxyribonucleic acid

DTT – Dithiothreitol

DUB – Deubiquitinating enzymes

ER – Oestrogen receptor

EZH2 – Enhancer of Zeste 2

FBS – Foetal bovine serum

HAT – Histone acetyltransferase

HDAC – Histone deacetylase

HER2 – Human epidermal growth factor receptor 2

HPH – Human polyhomeotic homolog

IB – Immunoblot

IM - Immunomodulatory

LAR - Luminal androgen receptor

M - Mesenchymal

MAPK – Mitogen-activated protein kinase

MSL - Mesenchymal stem-like

mTOR – Mammalian target of rapamycin

NaCl – Sodium chloride

PBS – Phosphate buffered saline

PcG – Polycomb group complex

PCGF – Polycomb group factor

PI3K – Phosphoinositide 3-kinase

PMSF – Phenylmethane sulphonyl fluoride

PR – Progesterone receptor

PRC – Polycomb repressive complex

PRC1 – Polycomb repressive complex 1

PRC2 – Polycomb repressive complex 2

PTM – Post-translational modifications

PVDF – Polyvinylidene difluoride

qPCR – quantitative Polymerase Chain Reaction

RING – Really interesting new gene

SAP – Shrimp alkaline phosphatase

SDS – Sodium dodecyl sulphate

SDS-PAGE – Sodium dodecyl sulphate polyacrylamide gel electrophoresis

siRNA – Small interfering Ribose Nucleic Acid

TEMED – Tetramethylethylenediamine

TNBC – Triple negative breast cancer

TSG – Tumour suppressor gene

WR – Working reagent

Table of Figures

Table of Tables

1. Introduction

1.1 Cancer

Cancer is defined as a collection of diseases which are caused by uncontrollable cell division (Cancer Research UK). There are over 200 types of cancer and in the UK 1 in 2 people will be diagnosed with cancer during their life (Cancer Research UK). Some cancers are more common than others and the risk of developing different cancers can vary between different populations, age groups and between men and women. There are many known risk factors which can increase the likelihood of developing cancer, including inherited genetic mutations and exposure to carcinogenic agents which can cause genetic mutation. Hanahan and Weinberg described the Hallmarks of Cancer in 2011 highlighting that genome instability and mutation is a key driver of cancer progression (Figure 1.1, Hanahan and Weinberg, 2011).

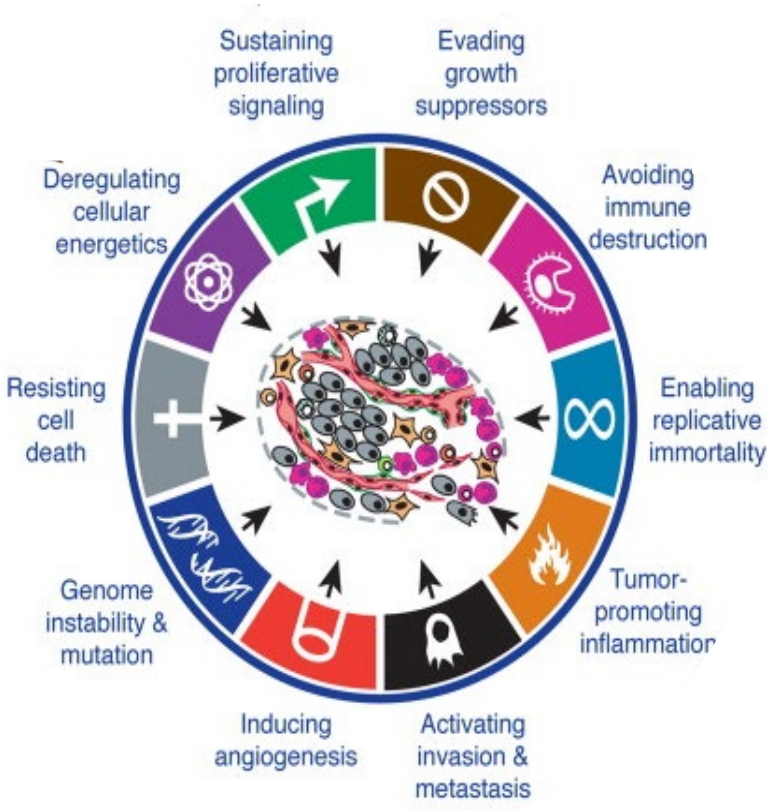

Figure 1.1: The hallmarks of cancer as described by Hanahan and Weinberg. 10 hallmarks described and the possible targeted therapeutic methods used in each case (Hanahan and Weinberg, 2011).

Genomic instability refers to high levels of mutation within a genome. Usually, this includes changes to the nucleic acid sequence and differences in chromosomal arrangement. Genomic instability is a feature of a majority of human cancers, and can drive cancer progression due to the development of the other hallmarks of cancer.

In health, there is a balance between the number of proto-oncogenes and tumour suppressor genes (TSG). Oncogenes are genes which code for proteins capable of inducing cancer *in vivo* or transforming cells in culture when either mutated or expressed at high levels. Genes which have the potential to become oncogenes are called proto-oncogenes. Usually, proto-oncogenes become oncogenes when they undergo a gain-of-function mutation (Lodish, et al., 2000). There are three mechanisms which usually contribute to oncogene formation; point mutations in a proto-oncogene, translocation causing the proto-oncogene to be under the control of a different promotor causing overexpression, and gene amplification of a DNA segment containing the proto-oncogene resulting in overexpression (Lodish, et al., 2000). TSGs inhibit tumour formation often by controlling cell proliferation or inducing cell death. Mutations can occur that cause the TSG to stop functioning or being expressed. In contrast to oncogenes, it is the inactivation of the TSG which contributes to the formation and progression of tumours (Copper, 2000). Often, numerous mutations are required in a cell causing concurrent proto-oncogene activation and TSG inactivation for cell transformation (Lee and Muller, 2010). Control of expression of oncogenes and TSG is an important mechanism in the normal function of cells, as well as in the formation of cancer. There are changes within a cell which promote higher levels of expression of oncogenes and reduce levels of expression of TSGs, which can eventually lead to cancer (Chow, 2010).

1.1.1 Types of cancer

In 2018, the most common types of cancer in men were lung cancer, prostate cancer and colorectal cancer. These contributed 44.4% of all of the cancers seen in men in the same year. In women, it is well known that breast cancer is the most common type of cancer. Breast cancer contributed 25.4% of all cancers diagnosed as new cases in 2018 (World Cancer Research Fund, 2018). Over a quarter of all cancer diagnoses in women are breast cancer and breast cancer accounts for 15% of all cancer related mortalities in women which clearly highlights the need for novel research into the cause and subsequent treatment of this disease (Cancer Research UK, 2016) (Figure 1.2).

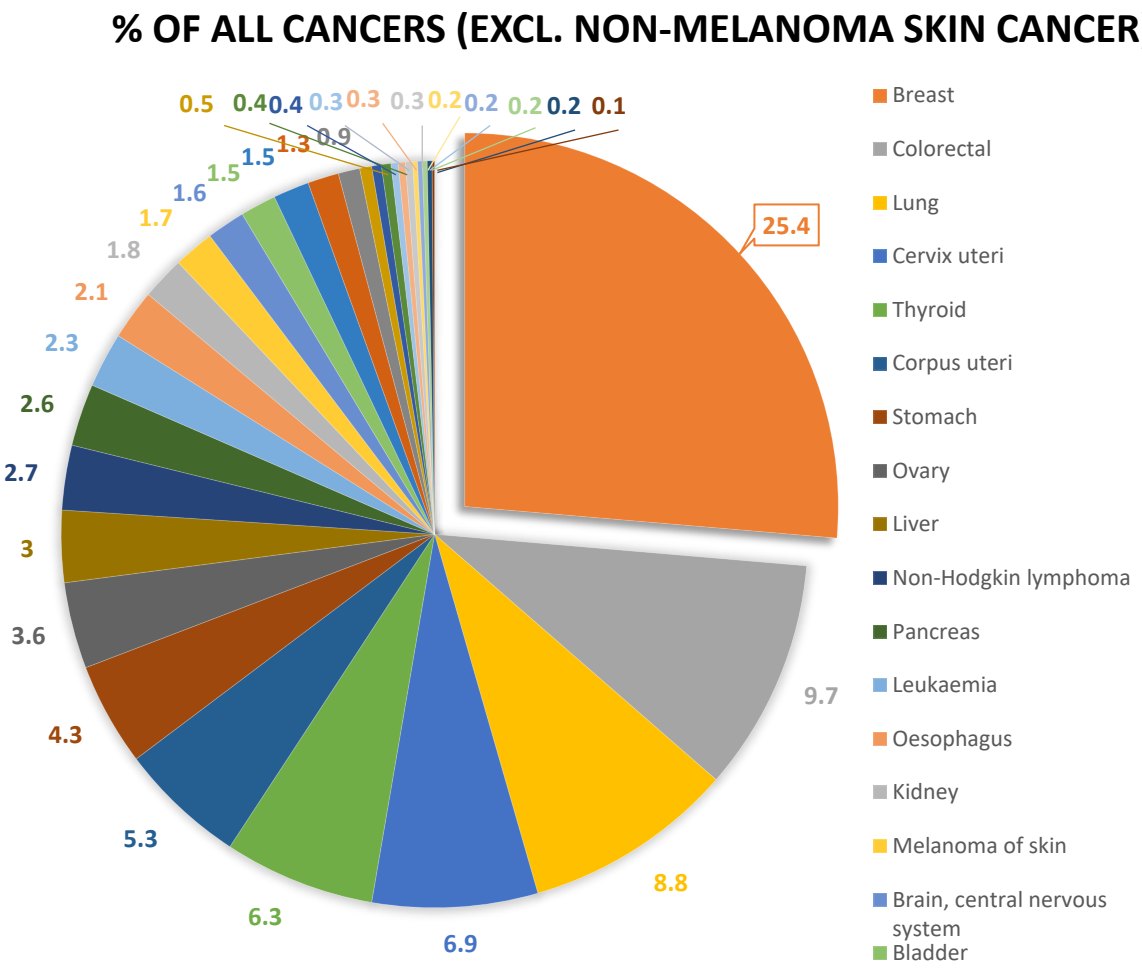

Figure 1.2: Incidence of cancer in women. Incidence of 31 types of cancer in women as of 2018, excluding non-melanoma skin cancer. Incidence shown in percentage of total new recorded cases of cancer in women in 2018 (8,218,216). Breast cancer accounts for 25.4% of all new recorded cases (World Cancer Research Fund, 2018).

1.2 Breast cancer

Breast cancer occurs due to uncontrolled growth of breast cells. This usually occurs in the lobule cells where the milk is produced, or in the mammary ducts. Occasionally breast cancer can develop in the stroma but this is less common. The vast majority (85-90%) of breast cancers occur due to a sporadic mutation, whilst only 5-10% of breast cancer cases occur due to a hereditary mutation (Breastcancer.org, 2018). Breast cancer is a heterogeneous disease outlined by a high degree of difference and diversity in tumours between each patient with breast cancer and sometimes between cells within the same tumour (Turashvili and Brogi, 2017).

1.2.1 Types of breast cancer

There are several sub-types of breast cancer. The classic breast cancer sub-types are based upon expression of hormone receptors and are classified as oestrogen receptor (ER) positive-, progesterone receptor (PR) positive-, Human epidermal growth factor receptor 2 (HER2) positive- and triple negative breast cancer (TNBC), which do not express any receptors.

Around 80-90% of breast cancers are ER/PR positive (ER+/PR+) or overexpress HER2 (HER2+) (Saraiva et al., 2017). In breast tissue, oestrogen facilitates cell proliferation via binding to the oestrogen receptor (ER) (Russo and Russo, 2006). The ER drives tumour growth in ER+ tumours and this has allowed targeted hormone based therapies directed at the ER to be developed such as tamoxifen for ER+ tumours (Bulut and Altundag, 2015). Tamoxifen is a competitive antagonist which competes with oestrogen for the ER and reduces oestrogen-induced effects by blocking ER signalling, thereby inhibiting ER+ breast cancer growth (Shagufta and Ahmad, 2018).

Human epidermal growth factor receptor 2 (HER2) is a tyrosine kinase and oncogene which usually controls the growth and repair of breast cells. In approximately 20% of breast cancers, the *HER2* gene is overexpressed meaning that the number of HER2 receptors increases, which causes uncontrolled growth and division of breast cells. Due to the presence of a specific oncogenic driver in HER2+ breast cancers, targeted therapies have been developed. Trastuzumab, more commonly referred to as Herceptin is a commonly used treatment for HER2+ cancers (Gutierrez and Schiff, 2011). Herceptin

is a humanized monoclonal antibody which is directed against the extracellular domain IV of HER2 (Vu and Claret, 2012). There are several proposed mechanisms of action of Herceptin. Firstly, studies have suggested that HER2 is degraded through the recruitment of a tyrosine-kinase ubiquitin ligase called c-Cbl. Upon the binding of Herceptin to HER2, c-Cbl is recruited which in turn ubiquitinates HER2 causing its proteosomal degradation (Klapper et al., 2000). Another suggested mechanism of action of Herceptin is an antibody-dependent cellular cytotoxic response. Clynes et al., (2000) suggested that cells overexpressing HER2 could be 'coated' with Herceptin which caused these cells to become targets to natural killer cells in a CD16-mediated manner. Following this, Arnould et al., (2006) confirmed this theory as upon treatment with Herceptin, an increase in the levels of natural killer cells and cytotoxic proteins was seen. This also could explain why those tumours with a higher overexpression of HER2 respond better to this form of treatment. Finally, the most well-known mechanism of Herceptin action is by mediating the PI3K-AKT and MAPK signalling pathways. Junttila et al., (2009) suggested that Herceptin interferes with the dimerization of HER2 and therefore inhibits HER2 activation along with AKT phosphorylation. This leads to suppression of growth. In addition to this, Nagata et al., (2004) and Zhang et al., (2011) suggested that when Herceptin binds HER2, this blocks tyrosine kinase Src signalling which leads to an increase in PTEN activity. This also leads to suppression of the PI3K-AKT signalling pathway and as a result reduces cell growth and proliferation.

In TNBC, all of the above receptors are not present. TNBC can be therefore more difficult to treat than other subtypes of breast cancer because there are no receptors present to target during therapy. There is also a large degree of heterogeneity between types of TNBC tumours (Mills et al., 2018) (to be discussed in section 1.2.2).

As well as subtyping breast cancer by hormone receptor status it has been identified that there are in fact 5 intrinsic molecular subtypes of breast cancer according to differences in gene expression pattern (Sørlie et al., 2001). 8,102 genes were analysed from 85 microarray experiments and 427 genes were identified as having different expression levels between different tumours compared with the levels between the same tumours. The tumour subtypes were identified using hierarchical clustering. These are Luminal A, Luminal B, HER2 overexpression, Basal and Normal-like. These intrinsic

subtypes along with hormone receptor expression and tumour grades provide information to determine the likely prognosis of patients with different tumour types as well as to develop therapeutic treatments specific to the type of breast cancer diagnosed. The data in table 1.1 is derived from a study of tumours obtained from the University of British Columbia and Washington University at St Louis (UBC-WashU series) from 357 patients with invasive breast carcinomas (Cheang et al., 2009). This shows the prevalence of the different molecular subtypes, their link with associated hormone receptor status and tumour grade and predicted subsequent patient outcomes, adapted from Dai et al., 2015.

Table 1.1: intrinsic subtypes of breast cancer, including receptors present and outcome.

Intrinsic Subtype	Receptors	Grade	Outcome	Prevalence
Luminal A	ER+, PR+, HER2-, KI67-	1-2	Good	23.7%
Luminal B	ER+, PR+, HER2+/-, KI67+	2-3	Intermediate	38.8% 14%
HER2 overexpression	ER-, PR-, HER2+,	2-3	Poor	11.2%
Basal	ER-, PR-, HER2-, basal marker+	3	Poor	12.3%
Normal-like	ER+, PR+, HER2-, KI67-	1-2-3	Intermediate	7.8%

1.2.2 Triple negative breast cancer

TNBC makes up around 10-20% of all breast cancers (Saraiva et al., 2017). In general, TNBC has a poorer prognosis than hormone receptor positive breast cancers (Kumar and Aggarwal, 2015). TNBC are more heterogeneous than other cancers and therefore have many different and diverse characteristics. TNBC can be categorised with regards to the morphological appearance of the cells. These are; infiltrating ductal carcinoma, medullary carcinoma, adenoid cystic carcinoma, myoepithelial carcinoma, squamous carcinoma, metaplastic carcinoma, apocrine carcinoma, secretory carcinoma, carcinoma arising with microglandular adenosis and not otherwise specified (Hon et al., 2016). Of these, the prognosis of medullary carcinoma is classified as good, and the prognosis of adenoid cystic carcinoma upon tumour removal is classified as very good due to the fact that it is very slow growing (Hon et al., 2016). TNBC is generally a more aggressive cancer than other types of breast cancer but there are some subtypes which are less aggressive. TNBC can be also be categorised into 6 subtypes based on their gene expression profiles. These are basal-like 1 (BL1), basal-like 2 (BL2), immunomodulatory (IM), mesenchymal (M), mesenchymal stem-like (MSL), and luminal androgen receptor (LAR) (Santonja et al., 2018) (Figure 1.3).

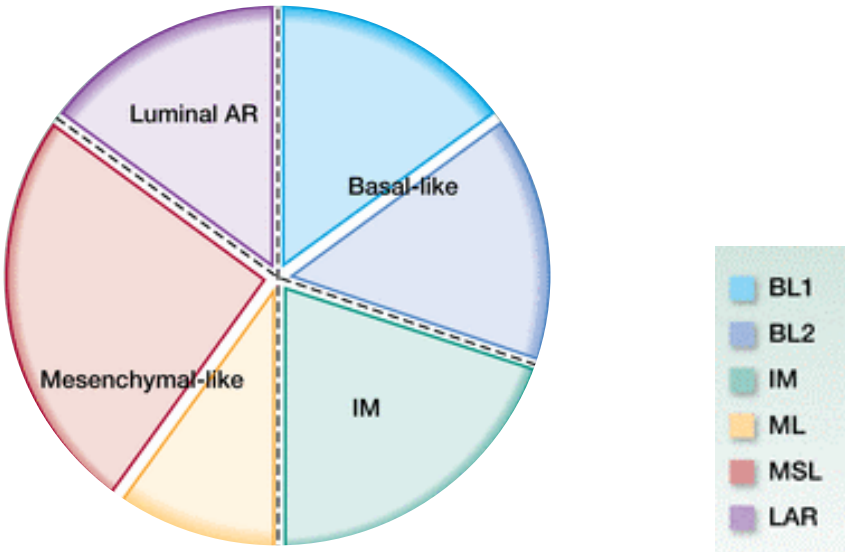

Figure 1.3: Types of triple negative breast cancer. TNBC can be divided into Basal like (Basal-like 1 [BL1] and Basal-like 2 [BL2]), Immunomodulatory (IM), Mesenchymal-like (mesenchymal [M] and mesenchymal stem-like [MSL]), and Luminal androgen receptor (LAR) (adapted from Turner and Reis-Filho, 2013).

Basal-like breast cancers (BLBC), so called because of the markers of basal type cells expressed, is considered to be the same as TNBC, however, not all TNBC express basal markers (Hon et al., 2016). TNBC that do express basal markers have a poorer prognosis than those that do not. Whilst BLBC is aggressive, when treated with chemotherapy, it has a longer disease-free survival than other types of TNBC. TNBC are often also classified as claudin-low types of breast cancers. This breast cancer subtype represents around 25-39% of all TNBC cases and was found to be similar to BLBC following molecular cluster analysis (Hon et al., 2016). Claudin-low breast cancer, so called due to lacking expression of claudin-3, -4, and -7 which are tight junction components, is often associated with poor prognosis, and poor sensitivity to chemotherapy (Hon et al., 2016). Due to the lack of receptors on the surface of TNBC tumours, there are no targeted treatment for these tumours as there are for ER+/PR+ or HER2+ breast cancers. As such, the only treatment currently for TNBC both in the early stages and the late stages is chemotherapy. Due to the heterogeneity of TNBC not all tumours will react the same way to chemotherapy and some tumours are more or less sensitive to chemotherapy than others. This highlights the need for new, targeted therapeutic approaches to be developed and new therapeutic targets need to be discovered.

1.3 Epigenetics and cancer.

Epigenetics is the study of the changes seen in organisms which occur due to a change in the level of gene expression rather than mutations in the genetic sequence (Simmons 2008). Epigenetic modification can occur on histone proteins and affect the structure of chromatin and therefore gene expression. In some cases, the expression of TSG is reduced, and the expression of oncogenes is increased which can, therefore, increase the likelihood of a tumour forming (You et al., 2012).

1.3.1 Histone proteins and chromatin structure

DNA is packaged into the cell in a structure called chromatin. Chromatin is made up of a DNA-protein structural subunit called the nucleosome. Around 147 base pairs of DNA wraps twice around an octamer of the histone proteins, called the histone core, creating a nucleosome. The histone core is comprised of two copies each of histone H2A, H2B, H3 and H4 (Figure 1.4). The H1 histone binds to linker DNA which is a sequence up to 80 nucleotides long and its role is to bind to the nucleosome core particle. H1 molecules have a central globular domain as well as flexible N- and C-terminal ends. Linker DNA is the stretch of DNA between histone cores. The H1 histone is extremely variable, which is, in part, due to the large number of subtypes of the H1 histone as well as the vast amount of post translational modifications (PTMs) which can impact the structure of the H1 histone (Hergeth and Schneider, 2015). In addition to the core histones and linker DNA, there are projections of amino acids which protrude from the surface of histones. These are called histone tails and, like the histone core, can be subject to PTMs which can affect the structure of chromatin (Bowman and Poirier, 2015).

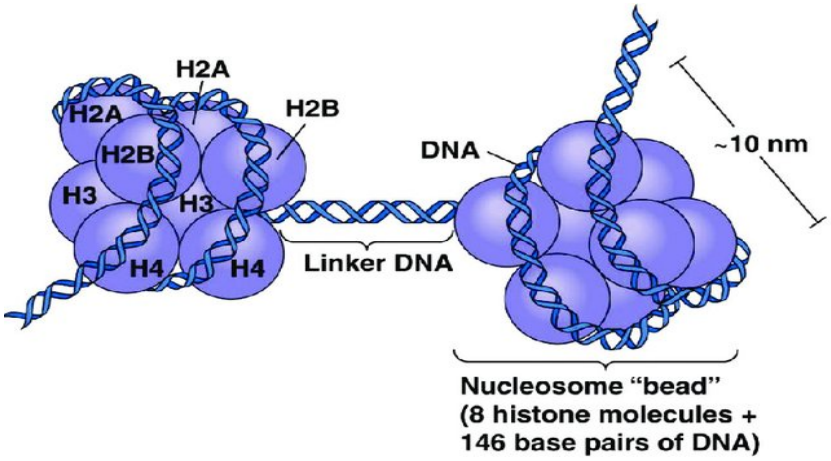

Figure 1.4. The nucleosome structure (Caputi et al., 2017).

Chromatin exists in two forms, heterochromatin and euchromatin. Heterochromatin is highly conserved and the genes located in heterochromatic regions are usually inaccessible to RNA polymerase II (RNAPolII), therefore meaning that the gene cannot be transcribed (Feher, 2012). Alternatively, euchromatin is less conserved and has a looser structure. This means that the genes located in these regions are accessible to transcriptional machinery and can be expressed. Areas of heterochromatin are referred to as being in a repressed chromatin state whereas areas of euchromatin are referred to as being in an active chromatin state (Pieterman et al.,2014) (Figure 1.5). The movement between heterochromatin and euchromatin in the genome is therefore an important regulator of gene expression.

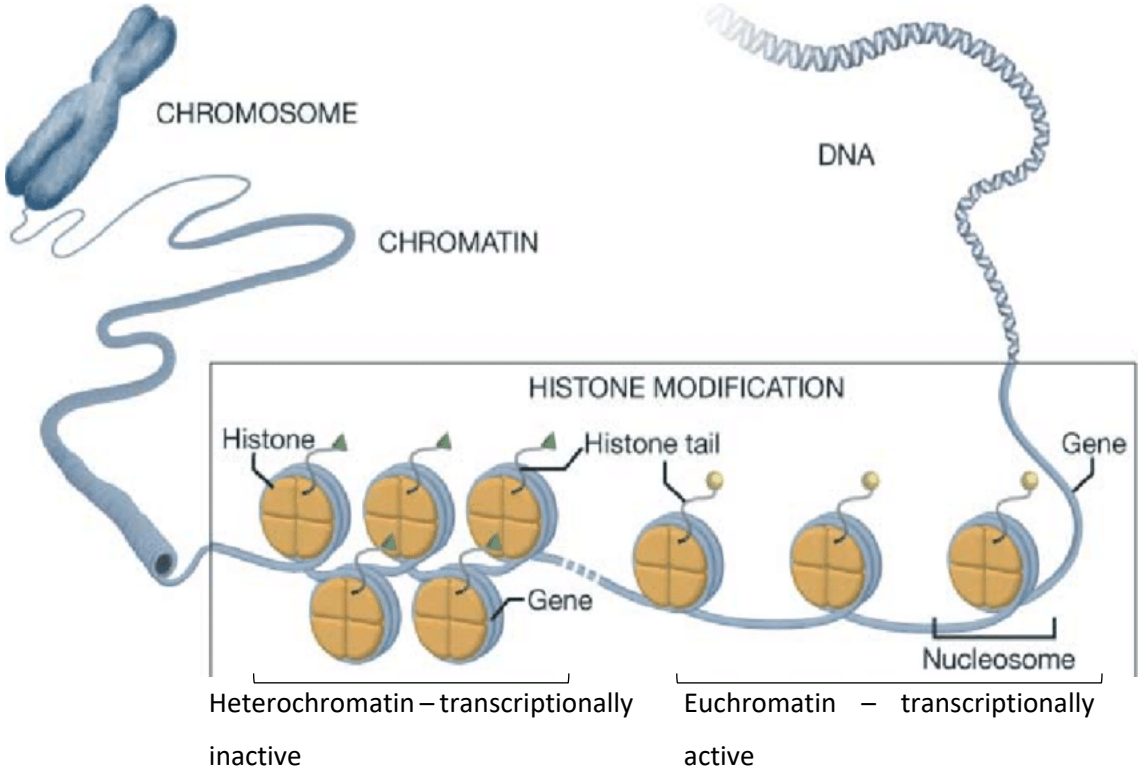

Figure 1.5: Chromosome structure. Structure of the chromosome showing the different types of chromatin and highlighting the difference between heterochromatin and euchromatin. Green triangles and yellow circles represent histone modifications which can lead to different chromatin activation states (Adapted from Pieterman et al., 2014).

1.3.2 Post translational modifications

Post translational modifications (PTM) are an example of epigenetic modification that occur on histones, control chromatin state and are therefore an important mechanism for regulation of gene expression. PTMs predominantly occur on the histone tails (Figure 1.6) which protrude from the histone and are facilitated by chromatin-modifying enzymes. Histone tails are comprised of amino acids such as lysine (K) and arginine (R). The histone modifications occur on the N-terminal tails of H2B, H3 and H4 along with the C-terminal tail of H2A. Common modifications which can occur on these histone tails include lysine acetylation, lysine mono-, di-, and tri-methylation and arginine methylation (Weaver et al., 2017).

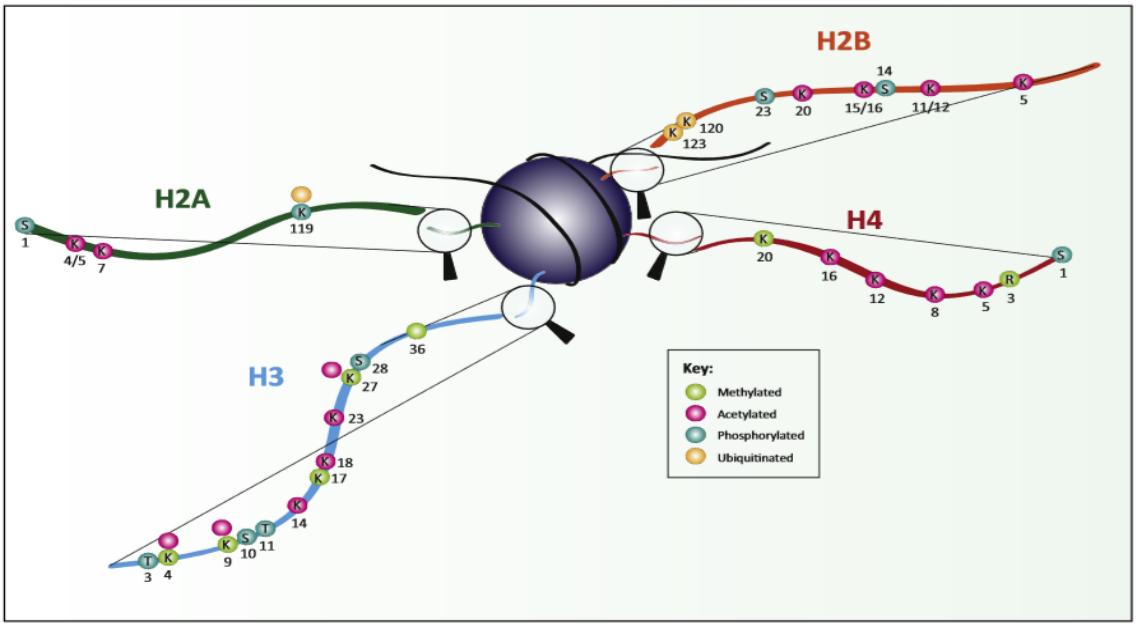

Figure 1.6: Histone structure. Histone tails comprised of amino acids such as lysine (K), serine (S) and threonine (T) and their associated PTMs. Specific PTMs (methylation, acetylation, phosphorylation and ubiquitination) and which amino acids they occur on are detailed on the diagram. Numbers identify the position of specific amino acids on the histone tails (Lawrence et al., 2016).

Chromatin-modifying enzymes can be divided into three categories; writers, readers and erasers (Kouzarides et al., 2007). Writers are enzymes which are capable of adding PTMs to amino acid residues, erasers are enzymes which can remove PTMs and readers are enzymes which have specialised domains which are capable of recognising epigenetic PTMs (Biswas and Rao, 2018). These modifications can cause compaction or relaxation of the chromatin structure and therefore can impact the accessibility of transcription

machinery such as RNA polymerase II (Orphanides and Reinberg, 2000). Regulation of writers, readers, erasers and other chromatin-modifying proteins is essential to ensure that only the correct genes are being expressed at the appropriate time. These proteins play many roles in normal tissue such as to maintain the identity of the cells, to regulate differentiation and development as well as to ensure that genome integrity is intact (Alexander et al., 2017).

There are many types of histone PTMs which frequently occur on histone tails. One such modification is acetylation. This is facilitated by histone acetyl transferases (HATs) and these modifications are removed by histone deacetylases (HDACs). HATs use acetyl coA cofactor to transfer an acetyl group to the ε-amino group of the lysine side chains. This process neutralises lysine's positive charge which can weaken the electrochemical bond between positively charged histone proteins and negatively charged DNA, thereby relaxing the chromatin structure (Bannister and Kouzarides, 2011). Histone acetylation is therefore associated with euchromatic regions of the genome and transcriptional activation and histone deacetylation is associated with heterochromatin and transcriptional repression. There can be an interaction between HDACs and methyl-binding proteins (MBPs), with the most widely studied example being methyl-CpG binding protein 2 (MeCP2). This protein recruits HDAC containing complexes to methylated gene promotors. In turn, this leads to deacetylation which causes heterochromatin formation. This subsequently results in the inaccessibility of transcriptional machinery to the promotor regions of the genes leading to transcriptional repression (Ropero and Esteller, 2007).

Another histone PTM is phosphorylation. Phosphorylation predominantly occurs on serines, threonines and tyrosines on histone tails. Generally, kinases transfer a phosphate from ATP to the hydroxyl group on the targeted side chain of amino acids. Phosphatases remove the phosphate from the serine, threonine or tyrosine. The addition of a phosphate group induces a negative charge which affects chromatin structure. When phosphorylation occurs, the DNA-histone electrochemical bond is weakened allowing access to transcription machinery and promoting DNA repair and transcription. Phosphorylated histone residues can also reduce binding of the adjacent methylated lysine with the relevant binding protein (Zhang et al., 2016).

Ubiquitination involves the addition of a ubiquitin molecule by ubiquitin ligases. The function of histone ubiquitination is less widely studied than other types of histone modification, but despite this, it is known that monoubiquitination of H2A is correlated with gene silencing and monoubiquitination of H2B is correlated with transcriptional activation. Three enzymes work to catalyse the ubiquitination of residues on histones, commonly lysine residues (Dikic and Robertson, 2012). These enzymes are known as E1, E2 and E3 ligases. E1 is the ubiquitin-activating enzyme. Ubiquitin becomes attached to this via a thiodiester bond. E2 is the conjugating enzyme which removes the ubiquitin molecule from the E1 enzyme and E3 is the ligase enzyme which binds to the target protein and then can attach the ubiquitin either directly or indirectly (Dikic and Robertson, 2012). These modifications can also be removed by deubiquitinating enzymes (DUBs). Generally, H2A and H2B are monoubiquitinated however it has also been discovered that H3, H4 and the linker histone H1 can also be ubiquitinated, albeit less commonly (Cao and Yan, 2012). The E3 ligases associated with ubiquitinating histone H2A are called RING1 and RING2. The most well studied E3 ligase is RING1B. This ubiquitin ligase facilitates the ubiquitination of lysine 119 on histone 2A (H2AK119Ub) and this was the first histone ubiquitination modification to be studied. In a previous study into the role of H2AK119ub in transcription in HeLa cells it was found that depletion of RING1B causes the level of H2A monoubiquitination to fall both globally and at promotors of specific genes (Cao and Yan, 2012). H2AK119ub is associated with heterochromatin therefore if the RING proteins are not expressed, and H2AK119 is not ubiquitinated, chromatin is less condensed and therefore genes can be expressed (Saksouk et al., 2015). Breast cancer type 1 susceptibility gene (BRCA1) can also function as a potential E3 ubiquitin ligase on histone H2A. H2A ubiquitin ligase can be found in transcription repressor complexes such as polycomb repressive complex 1 (PRC1) amongst others. It has been determined that RING1B mediated H2Aub is necessary for polycomb targeted gene silencing (Cao et al. 2015).

Methylation is another PTM which can occur on histones. Unlike acetylation and phosphorylation, methylation does not change the charge of the histone protein. Histone methylation by methyltransferase enzymes generally occurs on the side chains of lysine and arginine. Lysines can be mono-, di- or tri-methylated whereas arginines can be mono-, asymmetrically, or symmetrically di-methylated. Whilst methylation was

originally thought to be irreversible, it is now known that it can be reversed by demethylases. It is suggested that epigenetic reader proteins can recognise methylation marks and recruit other molecules to change the chromatin structure and transcription state (Greer and Shi, 2012). Methylation can sometimes lead to silencing of genes and sometimes can lead to activation of genes. For example, histone H3 lysine 4 (H3K4) can be methylated and this in turn leads to transcriptional activation. High levels of H3K4me1, H3K4me2 and H3K4me3 are found at transcription start sites and high levels of histone acetylation along with H3K4met are found at promotor regions of active genes (Barski et al., 2007). Conversely, histone 3 lysine 27 (H3K27) methylation leads to silencing of genes and is mediated by enzymes in the polycomb group (PcG) such as the Enhancer of Zeste 2 protein (EZH2) in the polycomb repressive complex 2 (Martin and Zhang, 2005).

1.3.3 Histone modifications and cancer

Dysregulation of histone modifications have been shown to be involved in cancer formation and progression. For example, levels of H3K9me3 and H4K20me3, which are repressive histone marks, are increased in breast cancer tissue compared to normal breast tissue indicating that the genes which regulate these PTMs behave differently in cancer cells (Katz et al., 2014). In turn, the presence or absence of certain histone modifications can be used to predict the prognosis of some cancer types. For example, a pancreatic cancer study of 195 patients found that tumours with low levels of H3K4me2, K3K9me2 and H3K18ac had worse overall survival and relapse-free survival (Manuyakorn et al., 2010). This was validated using tumour microarray analysis and Kaplan-Meier survival curves showed lower median survival times for each low histone level, indicating that the level of histone modification can predict prognosis of pancreatic cancer (Manuyakorn et al., 2010).

There are many histone modifying enzymes which have been shown to be involved in cancer. These enzymes are responsible for modifying both histone and non-histone proteins, both of which can play a role in cancer development and progression. Many of these non-histone substrates which the histone modifying enzymes modify are involved in gene regulation (Zhang and Dent, 2005). For example, KDM3A is a lysine demethylase and high expression is correlated with poor prognosis in colorectal cancer, as well as

overexpression being associated with renal cell carcinoma (Uemura et al., 2010 and Guo et al., 2011). KDM3A can also regulate the expression of YAP1. YAP1 functions as a transcriptional regulator and facilitates cell proliferation gene transcription whilst suppressing apoptotic gene transcription (Wang et al., 2019). KDM4B is also a lysine demethylase and is overexpressed in gastric cancer. Importantly, KDM4B is required for the proliferation and formation of metastatic tumours in breast cancer (Kawazu et al., 2011). In addition, LSD1 was the first lysine demethylase identified and is specific to modifying H3K4 and H3K9. LSD1 is overexpressed in many cancers including prostate carcinoma, bladder cancer, neuroblastoma and, importantly, TNBC (Lim et al., 2010). EZH2, which is a component of the PRC2 complex, is overexpressed or amplified in a variety of cancers, including but not limited to breast cancer (Bracken et al., 2003). EZH2 can undergo a gain-of-function mutation which increases the specificity of the SET domain in EZH2 to H3K27me3 causing accumulation. This can then lead to gene silencing and EZH2 catalyses the malignant transformation seen in cancer cells (Audia and Campbell, 2016). This small sample of epigenetic regulatory proteins that have been shown to play a role in cancer provides evidence that dysregulation of histone PTM is important for cancer development. It also suggests that epigenetic regulatory proteins may be effective novel therapeutic targets to treat many different cancer types.

1.4 Epigenetic Reader Proteins

Epigenetic (epi) reader proteins recognise one or more histone modifications and have also been shown to play a role in cancer. BRD4 is an example of an epireader protein involved in cancer. BRD4 recognises histone acetylation and is in the bromodomain and extraterminal (BET) family which also includes BRD2, BRD3 and BRDT. BRD4 binds to acetylated lysine residues including H4K16ac via two conserved bromodomains, BD1 and BD2. BRD4 is involved in transcription by recruiting positive transcription elongation factor P-TEFβ to regions of the chromatin with acetylated histone marks. The P-TEFβ complex is made up of cyclin-dependent kinase 9 (Cdk9) and Cyclin T (CycT) and this complex promotes elongation after RNAPolII pauses transcription shortly after transcription initiation by phosphorylating negative elongation factors in RNAPolII. This in turn allows initiation of productive elongation at the signal of P-TEFβ to ensure that the mRNA produced is full length and properly processed (Itzen et al., 2014). Disrupting the protein-protein interactions between BRD4 and acetylated lysine residues have been shown to block cell proliferation in cancer (Liu et al., 2017). BET inhibitors such as JQ1 and I-BET reversibly bind to the bromodomains and prevent them from interacting with lysine acetylation. When there is binding of JQ1 or I-BET to the bromodomain pocket of BRD4, it displaces the protein and therefore causes the removal of RNAPolII, resulting in target gene expression being stopped. BET inhibitors have been shown to be promising for cancer treatment, they inhibit the transcription of oncogenes which should prevent the tumour from growing. One study investigating the effects of BET in oral squamous cell carcinoma found that cells treated with either JQ1 or IBET underwent cell death after 72 hours. This was determined using cleaved-poly (ADP-ribose) polymerase (-PARP) as a common marker of cell death (Baldan et al., 2019). Experiments have also been conducted into the relevance of BET inhibitors in TNBC, and dependence of TNBC tumours on BRD4 was confirmed by RNA interference experiments. Cell viability of TNBC cell lines MDA-MB-231 and SUM159 transfected with a control short hairpin RNA (shRNA) or one of two independent shRNAs targeting BRD4 was analysed after four days and cell viability decreased in the BRD4 targeted cells. These studies into BRD4 provide an example of where targeting an epigenetic reader protein has an effect on TNBC tumour growth (Shu et al., 2016). This means that there may be potential for other epigenetic reader proteins to be targeted in therapy for TNBC tumours.

1.5 PRC1 and CBX2

The Polycomb Repressive Complex 1 (PRC1) is comprised of polycomb proteins which are epigenetic regulatory proteins. The complex has roles in development, senescence and cancer. The components of PRC1 are polycomb group factor (PCGF) proteins, Really Interesting New Gene (RING) proteins which function as E3 ligases, human polyhomeotic homolog (HPH) proteins and chromobox (CBX) proteins. There are six PCGF proteins which can be involved in the complex, two RING proteins, three HPH proteins and five CBX proteins (Figure 1.7). The PRC1 complex has a high level of heterogeneity due to the vast amount of different ways that the complex can be made up using different combinations of proteins from each group (Aloia et al, 2013). The PRC1 complex whilst initially believed only to be involved in transcriptional repression, may also play a role in transcriptional activation shown by knockdown of RING1B which resulted in both upregulation and downregulation of genes (Gil and O'Loghlen, 2014). In addition to this, a study by Chen et al., (2018) showed that RING1B is recruited to active enhancers and is associated with positively regulating their expression.

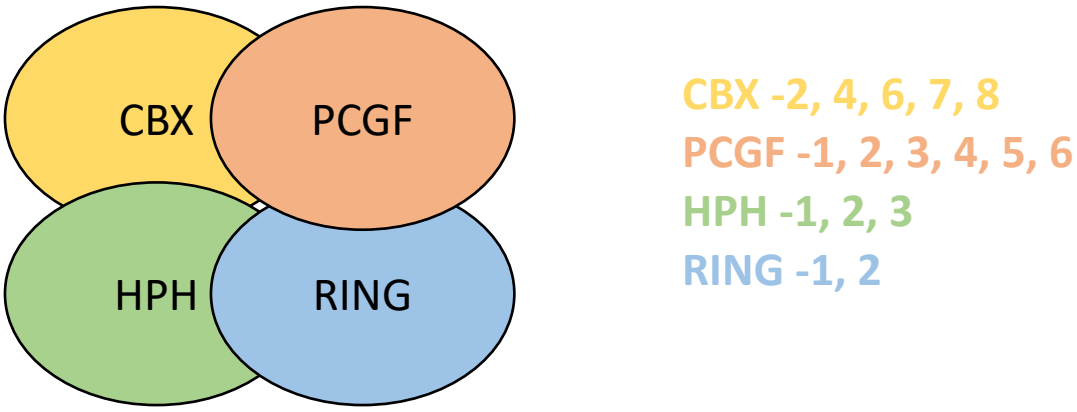

Figure 1.7: Components of the PRC1 complex. PRC1 is comprised of a combination of CBX proteins, PCGF homologs, HPH proteins and RING proteins.

CBX proteins are epi-reader protein components of the PRC1 complex. CBX proteins recognise the PRC2-mediated trimethylation of lysine 27 on histone 3 (H3K27me3) via chromobox domains. Chromobox domains are regions of chromobox proteins which recognise histone modifications (Nichol et al., 2016). Upon recognition of H3K27me3, the E3 ligase RING proteins of the PRC1 complex catalyse the monoubiquitination of histone H2A at lysine 119 (H2AK119ub) (Jin et al., 2011). This monoubiquitination, commonly recognised as a transcriptional repressive mark, leads to chromatin

condensation and can result in the formation of heterochromatin which means that the promotor regions of genes are inaccessible to transcription machinery and therefore transcription does not occur (Gil and O'Loghlen, 2014).

1.5.1 CBX2 in cancer

A meta-analysis performed by Clermont et al. (2014) suggested the oncogenic role of one particular CBX protein called CBX2. Clermont et al. demonstrated that in 25 studies analysed, 3848 patients showed upregulation of CBX2 in cancer tissues compared to 0 patients showing downregulation, indicating that CBX2 has a functional role in a number of types of cancer including breast (Figure 1.8).

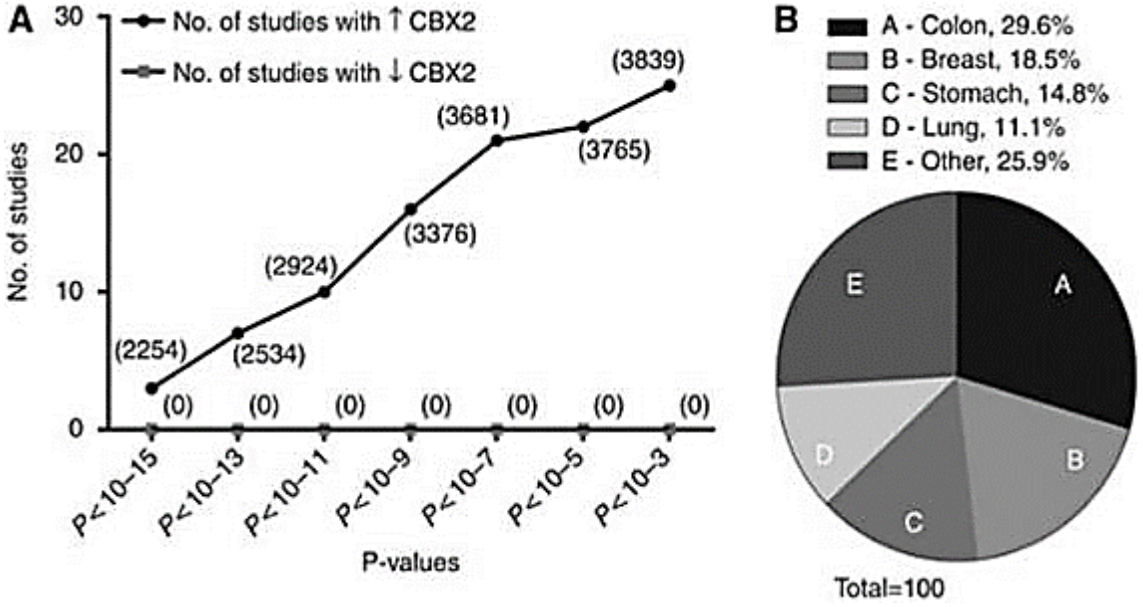

Figure 1.8: Upregulation of CBX2 in cancerous compared to normal tissues. A – studies showing up- or down-regulation of CBX2 in cancerous tissues. B – most frequent locations of tissues showing CBX2 upregulation across 3848 patients (Clermont et al., 2014).

The meta-analysis also showed that there were very low levels of mutation in CBX2 and the ones that were identified would not be functionally relevant. This, coupled with the high expression of CBX2 in colon, stomach, lung and breast tissues indicate that the normal function of CBX2 is of importance in tumour cells. 9 of the 25 studies showed that, when looking at clinical indicators of tumour progression such as metastasis, the levels of CBX2 were increased in metastatic tumours compared to primary tumours. Breast cancer accounted for two of these nine studies, indicating that further research needs to be undertaken into the role of CBX2 in breast cancer (Clermont et al., 2014).

CBX2 has previously been shown to have roles in cancer formation and development. In animal models with CBX2 knockout, multiorgan hypocellularity is seen due to lack of proliferation (Clermont et al., 2016). This indicates that CBX2 promotes proliferation, which could explain tumour formation when CBX2 is overexpressed. For example, the overexpression of CBX2 was shown in a prostate cancer (PCa) study performed by Clermont et al., (2016) which used the LTL313H/LTL313B PDX model of metastatic and non-metastatic PCa. Both metastatic and non-metastatic xenografts were derived from two independent needle biopsies of the same PCa tumour. Microarray analysis was performed from the RNA which was harvested from both the metastatic and non-metastatic cells to identify genes which were differentially expressed. CBX2 was highly upregulated in the metastatic (LTL313H) cells compared with the non-metastatic (LTL313B) cells. Further to this, qPCR confirmed a 3.2 fold upregulation in CBX2 in LTL313H compared with LTL313B. CBX2 upregulation was associated with known markers of poor prognosis in PCa including lower patient age, higher Gleason grade and a positive nodal status. This was determined using multivariate analysis of variance (MANOVA). Two metastatic PCa cell lines C4-2 and LNCaP were transfected with siRNAs targeted to CBX2 and after 55 hours of growth, phenotypic changes began to occur. After 96 hours, a majority of cells had detached from the plate and stopped proliferating suggesting that CBX2 knockdown affects cell viability. This was confirmed with an MTT assay of cell viability. CBX2 depletion induced PCa cell death *in vitro* and the gene expression of genes which were related to PCa progression differed when CBX2 was not present. This suggests that CBX2 is important in tumour progression in PCa and that CBX2 could be a useful therapeutic target (Clermont et al., 2016). These results could suggest CBX2 involvement in other cancer types.

1.5.2 CBX2 in breast cancer

CBX2 has been shown to be highly expressed in basal-type breast cancers, which often include TNBC (Chan et al., 2018). As TNBC are hardest to treat due to the lack of markers, this makes CBX2 an interesting protein to study as a potential therapeutic target (Liang et al., 2017). The levels of expression of CBX2 were found to be higher in breast tumour tissues than adjacent normal tissues (Chen et al., 2017). In addition to this, the expression of CBX2 has been shown to be significantly higher in basal-like subtypes compared with luminal subtypes of breast cancer, indicating a potentially important role

in TNBC (Liang et al., 2017). The level of expression of CBX2 was found to be inversely correlated with prognosis in breast cancer patients (Liang et al., 2017). This is supported by the findings that suggest that CBX2 upregulation and amplification are significantly correlated with a lower rate of overall survival in breast cancer along with higher metastatic rate in many types of cancer, particularly breast cancer (Clermont et al., 2014; Liang et al., 2017). In the aforementioned meta-analysis performed by Clermont et al, the overexpression of CBX2 in breast cancer accounted for 18.5% of cases, second only to colon cancer at 29.6% (Clermont et al., 2014). High mRNA levels of CBX2 was associated with shorter relapse-free survival in breast cancer patients who received adjuvant chemotherapy only. An elevated level of expression of CBX1 and CBX2 was correlated with worse prognosis in patients treated only with adjuvant chemotherapy designed to prevent relapse and extend survival, suggesting that CBX1 and CBX2 may play a role in chemoresistance (Liang et al., 2017). Pique et al., (2019) found that high CBX2 expression in breast cancer was associated with poor prognosis in the 1084 patients studied. They also found that CBX2 was enriched in basal-like tumours as well as HER2- tumours. In addition to this, they found a positive relationship between the aggressiveness of the tumour subtype and the proportion of patients who expressed CBX2 in each subtype (Pique et al., 2019).

2. Hypothesis, aims and objectives

2.1 Hypothesis

CBX2 has a role in triple negative breast cancer (TNBC) and is a potential therapeutic target.

2.1.1 Aims

1. Optimise knockdown of CBX2 in TNBC cell lines.
2. Identify the localisation of CBX2 in TNBC cell lines.
3. Determine the effect of CBX2 knockdown on expression of cell cycle regulatory genes.
4. Investigate the effect of CBX2 knockdown on levels of global histone modifications.
5. Investigate the effect of CBX2 knockdown on cell viability in TNBC cell lines.
6. Investigate the role of CBX2 in non-transformed, non-tumorigenic breast epithelial cell line.

2.2 Ethical considerations

The cell lines used in this project were sourced from ATCC in accordance with the ethical guidelines outlined in the Human Tissue Act of 2004. The donor remained anonymous for the duration of the project and onwards. All cells were obtained with consent from the donor. Control Of Substances Hazardous to Health (COSHH) forms were completed prior to any and all experiments involving these cell lines.

3. Materials and methods

3.1 Cell culture

Adherent MDA-MB-231 (ATCC HTB-26) and HS-578T (ATCC HTB-126) TNBC cell lines were cultured in RPMI 1640 media and DMEM media respectively (Gibco, UK). Adherent MCF10A (ATCC CRL-10317) immortalised breast epithelial cells were grown in DMEM F-12 media (Gibco, UK). All media used for growth was supplemented with growth serum and antibiotics. RPMI 1640 media and DMEM media (Gibco, UK) were supplemented with 10% foetal bovine serum (FBS) (Gibco, UK), 1% glutamine (Gibco, UK) and 1% penicillin and streptomycin (Gibco, UK). DMEM F-12 media (Thermofisher) was supplemented with 5% horse serum (Thermofisher), 1% penicillin and streptomycin (Gibco, UK), 1% cholera toxin (Sigma), 20ng/ml EGF (Gibco, UK), 0.5ug/ml hydrocortisone (Sigma) and 10ug/ml insulin (Sigma). The cells were grown in either T75 or T175 flasks (Sarstedt, Germany). 12ml of relevant media was added to T75 flasks and 30ml of relevant media was added to T175 flasks. This media was changed every three days. The cell were incubated in a humidified incubator with 5% CO_2 at 37°C (Nuaire, UK).

3.1.1 Trypsinisation

All flasks and tubes obtained from Sarstedt, UK unless otherwise stated.

When the cells reached around 80% confluency, they were trypsinised. 1X phosphate-buffered saline (PBS), trypsin-EDTA (Lonza, UK) solution and media were warmed to 37°C prior to use. The media was removed from the flask. Following this, the cell monolayer was washed with 8ml of warmed PBS which was made up from 200ml ddH_20 and 1 PBS tablet (Fisher, UK) and autoclaved for sterility. Following this, 3ml of warmed trypsin (diluted 1:30 in sterile PBS) was added to a T75 flask. 5ml of trypsin was added to T175 flasks. The flasks were incubated at 37°C for between 2 and 5 minutes to allow the cells to detach. When using MCF-10A cells, warmed trypsin was used diluted 1:10 in sterile PBS and the flasks were incubated at 37°C for 15 minutes as these cells took longer to detach from the flask surface than the TNBC cell lines. Once the cells had detached from the surface of the flask, the trypsin was neutralised with 12ml of relevant media for a T75 or 10ml for a T175. The cells were transferred to a 50ml falcon tube (Sarstedt, Germany) and then centrifuged for 3 minutes at 0.4 x g (Eppendorf, 5702

centrifuge). This created a cell pellet, and the media was removed from this pellet and discarded. The cell pellet was resuspended in 5ml of fresh media. For routine cell culture, cells were added to fresh media in new T75/T175 flasks at cell dilutions between 1:5 and 1:12.

3.1.2 Cell counting

Once the cells had been resuspended in 5ml of relevant media and pipetted up and down to ensure a single cell monolayer, the cells were counted. 20µl of cells was added to a haemocytometer (Neubauer). The cells were counted using a light microscope.

3.2 Transfections

The cells were grown until 80% confluent and then trypsinised. The cells were counted and then placed at a specific cell density and transfected with small interfering ribonucleic acids (siRNA). The control siRNA used was a scrambled siRNA (siSCR) which is non-silencing. In addition, three independent siRNAs targeting CBX2 were used; siCBX2-1, siCBX2-3 and siCBX2-4 (Table 3.1) Firstly, a master mix was made for each siRNA. The master mixes contained siRNA (50µM stock), RNAiMAX lipofectamine (Thermofisher, UK) and phenol red free RPMI-1640 (basal media) (Gibco) at a ratio of 1:2:100. These master mixes were left to combine at room temperature for around 20 minutes. Following this, the cells were trypsinised as above. Once the cells had been counted, the number of cells needed for each experiment could be calculated. The relevant number of cells were diluted in fresh full media. For a Western blot, 75,000 cells/ml were used for all cell lines. For MTS assays, 25,000 cells/ml were used for all cell lines. For all RNA-based experiments, 75,000 cells/ml were used for all cell lines. For a reverse transfection, 100µl of the transfection master mix was added to the centre of the wells of a 6 well plate and then 2ml of the cell suspension was dispensed onto the master mix generating a final siRNA concentration of 25nM. These cells were then left to grow for 72 hours or 96 hours depending on the experiment they were needed for. Alternatively, for a forward transfection, 2ml of the cells were dispensed into the wells at the relevant density for the experiment and grown for 24 hours. After 24 hours, siRNA master mixes were made as described above. 100µl of the master mix was added to the wells and then the cells were incubated for 72 hours. For a reverse transfection into a

96 well plate, 5µl of the transfection master mix was added to the centre of the wells and then 100µl of the cell suspension was dispensed onto the master mix generating a final siRNA concentration of 25nM. These 96 well plates were placed into the incubator and left to grow for the appropriate amount of time depending on the experiment used for. For a forward transfection, 100µl of cells were added to the wells and then placed into the incubator for 24 hours. Following this, the siRNA master mixes were made as described above and 5µl was added to each relevant well. The 96 well plates were returned to the incubator and grown for the appropriate amount of time for the experiment they were needed for.

Table 3.1. siRNAs used for transfections, their sequences and the company and catalogue numbers.

siRNA name	Sequence 5'-3'	Company	Catalogue number
siSCR	UUCUCCGAACGUGUCACGU	Sigma	HA11411080
siCBX2-1	AGGAGGUGCAGAACCGGAA	Sigma	HA11411074
siCBX2-3	GCAAGGGCAAGCUGGAGUA	Sigma	HA11411076
siCBX2-4	CAAGGAAGCUCACUGCCAU	Sigma	HA11411078

3.3 Western blot

3.3.1 Protein lysis

After the cells were counted as described above (Section 3.1.2), 2ml of cells were added to each well of a 6 well plate (Sarstedt, Germany). The plates were incubated for 72 hours prior to lysis. After 72 hours, the media was removed from the wells and the wells are washed with 1ml of warmed PBS. Following this, the cells are lysed using a lysis buffer (125mM Tris-HCl pH 6.8, 10% glycerol and 2% (w/v) SDS and beta-mercaptoethanol). The lysis buffer added to each well depended on the confluency of the wells as determined from observing the cells down the microscope prior to lysis. The SDS buffer was added at volumes between 100μl and 200μl to each well and incubated on a rocker for 5 minutes. Following this, the wells were scraped and the cell lysates were added to Eppendorf tubes. These were then stored at -20°C until they were needed for western blot experiments.

3.3.2 Gel electrophoresis

Proteins were separated by molecular weight using sodium dodecyl sulphate polyacrylamide gel electrophoresis (SDS-PAGE). A resolving gel of either 10% or 15% acrylamide (depending on the size/weight of the proteins of interest) was cast. For western blots used to confirm CBX2 knockdown, a 10% gel was used and for western blots used for histone modifications, a 15% gel was used. The gels were composed of acrylamide, deionised water, buffers containing Tris and SDS, APS and TEMED (the latter two are required for the polymerisation of the gel and as such are added last) (Table 3.2, Table 3.3).

Table 3.2: Composition of buffer A and buffer B for 200ml total volume.

	Buffer A (pH 8.8)	Buffer B (pH 6.8)
Tris (g)	18.16	6
SDS (g)	0.4	0.4

Table 3.3: Composition of running and stacking gel.

	Running		Stacking
	10%	15%	
Acrylamide	3.3ml	5ml	830 µl
ddH_20 (ml)	1.67	0	1.67
Buffer A (ml)	5	5	0
Buffer B (ml)	0	0	2.5
APS (µl)	100	100	50
TEMED (µl)	12	12	7.5

The running gel was pipetted into 1.5mm separated glass plates up to approximately 2cm from the top of the glass plates in a gel cast holder. In order to ensure a level gel and to ensure that there were no bubbles in the running gel, 200µl of isopropanol was added to the top of the running gel. After the running gel had set, the isopropanol was poured off and the stacking gel was added on top. Before the stacking gel set, a comb was placed into the gel. Depending on the experiment and amount of samples required per gel, either a 10-well comb or a 15-well comb was used. Once the stacking gel had set, the gel was placed in a gel electrophoresis holder and placed into an electrophoresis tank. Running buffer was added to submerge the gels. 1x running buffer was made up of 800ml ddH_20 and 200ml 5x running buffer stock (Table 3.4). Following this, 5µl of either Spectra protein ladder or PageRuler pre-stained protein ladder (Thermofisher, UK) with markers of known molecular weight was added to the first well of the gel in order to aid in the identification of the protein bands produced. The samples were boiled at temperatures in excess of 80°C for 10 minutes and then spun down in a centrifuge. Following this, the protein lysate samples at volumes between 5µl and 35µl depending on the relevant experiment were loaded into the gel. The gels were run using a powerpack (Biorad). This process was performed at 140V for ~60 minutes for a 10% gel and slightly longer for a 15% gel.

3.3.4 Transfer

Once the gels finished running, the proteins were transferred to a polyvinylidene difluoride (PVDF) membrane (GE Healthcare Life Sciences). This was performed using a transfer cassette (Biorad). Firstly, a sponge was placed onto the black side of the transfer cassette. Next, 2 pieces of Whatman paper were placed on top of the sponge. The gel was removed from the glass plates using a gel releaser (BioRad) and placed onto the Whatman paper with the protein ladder on the right hand side (ensures correct orientation on membrane post-transfer). The PVDF membrane was placed on top of the gel followed by 2 more pieces of Whatman paper. A glass roller was used to ensure that there were no bubbles between the PVDF membrane and the gel. Finally, a sponge was added to the Whatman paper and the cassette was closed. The transfer cassette was placed into a tank and transfer buffer was added to cover the cassette. The 1x transfer buffer was composed of 800ml ddH_20, 100ml 10x transfer buffer (Table 3.4) and 100ml methanol. A magnetic stirrer was added to the tank and the tank was placed onto a magnetic plate to keep the transfer buffer circulating during transfer. An ice pack was added to the tank to prevent overheating. The transfer was performed at 100V for 1 hour.

Table 3.4: Composition of running buffer stock, transfer buffer stock and TBS stock.

	Running Buffer (5x)	Transfer Buffer (10x)	TBS (10x)
Tris (g)	30	30.28	24.2
Glycine (g)	144	112.6	0
SDS (g)	5	0	0
NaCl (g)	0	0	8.8

3.3.5 Antibody incubation and visualisation

Following transfer, the membrane was washed 3x10 minutes in tris-buffered saline with 0.1% Tween (Thermofisher) (TBS/T) which was 900ml ddH_20, 100ml 10x TBS stock (Table 3.4) and 1ml Tween. Next, the membrane was blocked in 5% milk (5g of milk powder in 100ml TBS/T) for 1 hour. The membrane was then incubated in a 50ml falcon tube (Sarstedt, Germany) with primary antibodies diluted in 5ml of 5% milk to an appropriate concentration against the protein of interest overnight at 4°C (Table 3.5). The next day,

the membrane was washed in TBS/T 3x10 minutes. Following this, the membrane was incubated in secondary antibodies raised against the animal that the primary antibody came from (Table 3.5). These antibodies were diluted in 5ml of 5% milk at an appropriate concentration for the protein of interest. The membrane was incubated in secondary antibody at room temperature on a roller for 1 hour. Following this, the membrane was washed 2x10 minutes in TBS/T and 1x10 minutes in TBS. The secondary antibody contained a horseradish peroxidase (HRP) conjugate. A chemiluminescence reagent (ECL) (Biorad) was added to the membrane which bound to the horseradish peroxidase (HRP) conjugate. 500µl of ECL A and 500µl of ECL B (light sensitive) were diluted in 2ml of TBS. 1ml of the ECL mixture was added to each membrane which was placed between 2 sheets of parafilm. The reaction between the ECL and the HRP produced a signal, which was detected by the ChemiDoc XRS+ imager (Biorad). The bands detected were then compared to the molecular weight protein ladder to identify each protein visualised.

Table 3.5. Antibodies used along with concentrations, catalogue numbers, companies and animals raised in

Antibody	Concentration	Catalogue number	Company	Animal raised in
CBX2	1:5,000	ab80044	Abcam	Rabbit
Alpha Tubulin	1:10,000	66031-1-Ig	Proteintech	Mouse
GAPDH	1:5,000	Ab97046	Abcam	Mouse
H3Pan	1:20,000	C15310135-20	Diagenode	Rabbit
H3K27me3	1:20,000	C15410069-10	Diagenode	Rabbit
H3K27ac	1:1,000	C15410174	Diagenode	Rabbit
H2APan	1:20,000	C15410166-10	Diagenode	Rabbit
H2AK119ub	1:5,000	C15410002-10	Diagenode	Rabbit
IgG	1:1250	C15410206	Diagenode	Rabbit
Apoptosis cocktail Primary	1:250	ab136812	Abcam	Rabbit and Mouse
Apoptosis cocktail Secondary	1:100	ab136812	Abcam	Goat
Anti-rabbit Secondary	1:1,000-1:10,000	HAF008	R&D Systems	Goat
Anti-mouse Secondary	1:10,000	HAF007	R&D Systems	Goat

3.4 RNA extraction

RNA was extracted from previously siRNA-transfected cells using a variety of methods. Two methods of RNA extraction were used in this project. Both methods used filter pipette tips to prevent contamination with nucleases.

3.4.1 Phenol-chloroform extraction

The first method that was used involved using phenol and chloroform to extract the RNA. The RNA was extracted from transfected cells using Ribozol lysis reagent (VWR International, UK). This denatures the cell-cell bonds as well as the cell-plate bonds and caused the cells to be lysed releasing protein, DNA and RNA. First, once the cells had been grown for 72 hours in a 6 well plate, the media was removed and discarded. Next, 1ml of warmed PBS was added to each well to wash the cells. This was removed and 500μl of Ribozol was added to each well, lysing the cells. The plate was placed on the rocker for five minutes to allow full lysis of cells. Following this, the wells were scraped using a pipette tip to ensure all cells lysed and the Ribozol-cell solution was transferred to RNase-free Eppendorf tubes (Thermofisher, UK). These were then incubated on ice for 10 minutes. After this, 200μl of chloroform was added to each Eppendorf tube and the tubes were shaken vigorously for 15 seconds and then incubated on ice for two minutes. The tubes were then centrifuged for 15 minutes at 12,000 x g and 4°C (MicroStar 17R, VWR, UK). Once the samples had been centrifuged, the phases had been separated leaving the RNA in the clear aqueous phase. The aqueous phase was transferred carefully to another RNase-free Eppendorf tube ensuring not to aspirate any other phases as these would contaminate the RNA and the remaining phases were discarded. After this, 250μl of isopropanol was added to each tube, and the tubes were inverted five times. The tubes were incubated at room temperature for 10 minutes followed by a 10 minute centrifugation at 12,000 x g and 4°C. This produced a small, white pellet of RNA. The supernatant was discarded taking care not to dislodge the pellet and then the pellet was washed with 500μl of 75% ethanol. The samples were briefly vortexed and then centrifuged for 10 minutes at 7,500 x g and 4°C. This was repeated to ensure the pellet was clean. After the final centrifuge step, all of the ethanol was removed from the pellet and the tubes were placed on a heat block set to 37°C for 10 minutes with the lids of the tubes open to dry the pellet. Following this, 30μl of

molecular grade water was added to each pellet and then the samples were heated at 55°C for 10 minutes.

3.4.2 Qiagen RNeasy Mini kit

Another method to extract RNA is to use the Qiagen RNeasy Mini kit (74104). This method can produce higher purity and therefore higher quality samples. For this reason, the samples generated for RNA-sequencing (RNA-seq) were obtained using this method. In this method, the cells were lysed directly in the 6-well plate after 72 hours. 350µl of buffer RLT was added to each well and then the wells were scraped with a cell scraper. The solution was transferred to RNase-free Eppendorf tubes and vortexed to homogenise the sample. 350µl of 70% ethanol was added to each tube and mixed by pipetting up and down. A maximum of 700µl was transferred to the spin columns in 2ml collection tubes. The tubes were centrifuged for 15 seconds at 8,000 x g. During this step, the RNA remained in the filter within the spin column, while the remaining solution was collected in the collection tube. This was then discarded ensuring that no liquid touched the filter within the spin column. 700µl of buffer RW1 was added to the spin column in the 2ml collection tube and centrifuged for 15 seconds at 8,000 x g. The flow-through was again discarded and 500µl of buffer RPE was added to the spin column. The tube was inverted to ensure that the wash buffer covered all sides. The spin columns were centrifuged for 15 seconds at 8,000 x g and the flow-through discarded again. Following this, 500µl of buffer RPE was added and centrifuged for 2 minutes at 8,000 x g. Next, the spin column was carefully placed into a new, clean 2ml collection tube and centrifuged for one minute at maximum speed to ensure all flow-through was removed from the membrane. 30µl of RNase-free water was added directly to the membrane taking care not to touch the sides of the spin column. The spin column was placed into a new 1.5ml collection tube and centrifuged for one minute at 8,000 x g. This step eluted the RNA from the membrane. The spin column was discarded. Following both of these methods, the RNA was analysed using the ND-100 programme and the Nanodrop 2000 (Thermofisher, UK). The concentration of RNA (ng/µl), DNA/protein contamination (260:280) and ethanol/isopropanol contamination (260:230) were determined using this method.

3.4.3 Reverse transcription

Complementary DNA (cDNA) was generated from RNA to be used for quantitative-PCR (qPCR) experiments. Using the concentration of RNA as determined using the Nanodrop, the volume needed for 1μg of RNA was calculated. This volume was made up to 12.7μl with molecular grade water. The RNA samples were then heated at 55°C for 5 minutes and then centrifuged for ~10 seconds and placed on ice. Meanwhile, a master mix of reverse transcription reagents was made up in an Eppendorf tube. The master mix contained 1μl of oligo dT primer (0.5μg/μl) (bound to the poly A tail to ensure that only the mRNA is reverse transcribed), 2μl of dNTPs (10mM) which include the four bases needed to generate the strands of cDNA, 4μl of reverse transcriptase (RT) buffer (1ml stock) and 0.3μl of the Reverse transcriptase (RT) enzyme (200u/μl) (Promega) per sample. 7.3μl of this master mix was added to each of the RNA samples. Next, the samples were heated for 1 hour at 37°C and then heated for 5 minutes at 100°C to denature the RT enzyme and stop the reaction. Finally, 180μl of molecular grade water was added to each sample. The cDNA was then ready to be used in qPCR experiments.

3.5 Quantitative PCR (qPCR)

Real time (RT) quantitative PCR (qPCR) was used to measure the amplification of target DNA molecules in real time and to facilitate the gene expression analysis (Promega). Master mixes were made for each gene of interest on ice. The master mixes contained 5μl SYBR Green (Sigma), 2.2μl of molecular grade water and 0.4μl of the relevant forward and reverse primers per reaction (Table 3.6). In addition, Rox dye (100x stock) diluted to 1x was added to either the SYBR Green stock or the master mixes prior to use to act as a reference. Prior to using any primers or new samples of cDNA a standard curve was performed. The control cDNA sample for the relevant experiments was diluted 1:5, 1:10, 1:20, and 1:50 with molecular grade water. Each master mix was vortexed to ensure complete mixing before being loaded into the 96-well PCR plate (Applied Biosystems). 8μl of each master mix was loaded into the plate in triplicate. Then, 2μl of each cDNA sample was loaded into the top of the plate in triplicate. Molecular grade water was added as a negative control. Once the plate was loaded, a clear coverslip was added to ensure that the samples did not mix when heated. The plate was spun down in a microplate PCR plate spinner (Labnet). Then, the PCR plate was loaded

into the StepOne Plus qPCR machine and the parameters of the qPCR run were inputted into the StepOne software. The experiment type chosen depended on the experiment. Either 'Quantitation - Standard Curve' or 'Quantitation - Comparative CT (ΔΔCT)' was chosen. Regardless of the experiment type chosen, the 'Reagent' chosen was Sybr Green Reagents (With melt curve), the 'Speed' chosen was ~2 hours and the 'Template' chosen was cDNA (2-step RT-PCR). The reaction volume per well was 10µl. The run method began with a 'Holding Stage' which was performed at 95°C for 10 minutes to denature the DNA double strands. Following this, the temperature was decreased to 60°C to facilitate the annealing of the primers to the DNA strands. This was the 'Cycling Stage' and there were 40 cycles. Each cycle took approximately 1 minute. The optimum temperature for polymerisation of the strands was around 68-72°C (Enzo Lifesciences). Finally, a melt curve was generated to determine the levels of dissociation of double stranded DNA which occurred when the temperature increased. When the qPCR was finished, the amplification results could be analysed using StepOne software (Applied Biosystems) and the data exported to Excel for further analysis.

Table 3.6. Forward and reverse primers used for qPCR along with sequences and companies.

Primer name	Forward (F)/Reverse (R)	Sequence	Company
RPL13A	F	CCTGGAGGAGAAGAGGAAAGAGA	Sigma
	R	TTGAGGACCTCTGTGTATTTGTCAA	
CBX2	F	GCTCCAAAGCCAGACTAACA	IDT
	R	CAGGGACAGACATCCTCATTTC	
CDK1	F	CCTAGCATCCCATGTCAAAAACTTGG	Sigma
	R	TGATTCAGTGCCATTTTGCCAGA	
CDK2	F	GCTAGCAGACTTTGGACTAGCCAG	Sigma
	R	AGCTCGGTACCACAGGGTCA	
CDK4	F	AGATTGCCCTCTCAGTGTCCA	Sigma
	R	TGGAAGGAAGAAAAGCTGCC	
CCNA2	F	AGCTGCCTTTCATTTAGCACTCTAC	Sigma
	R	TTAAGACTTTCCAGGGTATATCCAGTC	
CCND1	F	ACTACCGCCTCACACGCTTC	Sigma
	R	AGTCCGGGTCACACTTGATCA	
CCND3	F	ATTCTGCACCGGCTCTCTC	Sigma
	R	GCTTCGATCTGCTCCTGACA	
CCNE2	F	CGGCCTATATATTGGGTTGG	Sigma
	R	ACGGCTACTTCGTCTTGACA	
CDKN1A	F	CAGCATGACAGATTTCTACC	Sigma
	R	CAGGGTATGTACATGAGGAG	
CDKN2A	F	AGCATGGAGCCTTCG	Sigma
	R	ATCATGACCTGGATCGG	

3.6 Immunoprecipitation

Immunoprecipitation (IP) involves isolating a protein of interest using Dynabeads and antibodies specific for the protein of interest. Cells were grown at a density of 1 million cells per 10cm^2 plate. After 72 hours, the media was removed from the plates and the cells were washed with warmed PBS. The cells were scraped using a cell scraper to ensure all cells removed from the plate. The cell-PBS solution was transferred to 15ml falcon tubes. These were then centrifuged at 0.4 x g for 3 minutes and the supernatant was discarded. The remaining cell pellets were resuspended in 1ml of lysis buffer (Table 3.7) to lyse cells and release proteins in the sample.

Table 3.7. Composition of lysis buffer.

Reagent	Amount	Stock concentration
Tris (pH 7.5)	250µl	1M
Sodium Chloride (NaCl)	188µl	4M
H_20	4.315ml	
Dithiothreitol (DTT)	5µl	1M
Phenylmethane sulphonyl fluoride (PMSF)	50µl (17.4mg PMSF stock in 1ml methanol)	
NP40 (non-ionic surfactant)	50µl	
Protease inhibitor cocktail III (Fisherscientific – 12841640)	50µl	

The samples were transferred to Eppendorf tubes and incubated on ice for 30 minutes. The samples were centrifuged for 3 minutes at full speed (13.3 xg). The supernatant was transferred to a new Eppendorf tube and 50μl of this supernatant was transferred to another new Eppendorf tube and frozen to be used as the input sample. Antibodies against CBX2 and IgG were added depending on the concentrations. The CBX2 antibody stock was 1mg/ml and so 2μl of antibody was added to one sample. The IgG negative control antibody stock was 5mg/ml so 0.4μl was added to the other sample. The Eppendorf tubes were covered with Parafilm and placed on a rotator for 2 hours at 4°C. Whilst the samples were incubating, 25μl of Dynabeads were added to each of two Eppendorf tubes with 1ml of 1% Triton X-100 detergent in TBS. Using a magnet, the Dynabeads were collected on one side of the Eppendorf tube and the Triton X-100 was removed. 1ml of 1% Triton X-100 was added to repeat the wash up to a total of 3 washes. Following this, the Dynabeads were resuspended in 30μl of Triton X-100 to prevent them from drying out whilst the samples were incubating. Once the samples had incubated for 2 hours, the Triton X-100 was removed from the Dynabeads and they were resuspended in the cell-antibody samples. These Eppendorf tubes were re-covered in Parafilm and incubated on the rotator overnight at 4°C. During this incubation, the antibodies bound to the Dynabeads. The next day, the magnet was used to collect the Dynabeads to one side of the Eppendorf tube, and the supernatant was transferred to a new Eppendorf tube and labelled as flowthrough and frozen. The Dynabeads were washed 3 times with Triton X-100 as before, ensuring that the supernatant was removed following the final wash. 20μl of the input and the flowthrough were transferred to new Eppendorf tubes and 6μl of SDS sample buffer was added. 30μl of SDS sample buffer was added to each of the IgG, CBX2 and Dynabead samples. These samples were all boiled for 10 minutes at around 70°C and were then ready to be used on a 10% gel in a Western blot.

3.7 Apoptosis assay

Cells were transfected with siSCR, siCBX2-1, siCBX2-3 and siCBX2-4 in 3 6-well plates to be harvested at the 24 hour, 48 hour and 72 hour time points. Once the cells had grown for either 24, 48 or 72 hours, the media was removed from the wells and transferred to 15ml falcon tubes relative to each siRNA transfection condition. The wells were washed with 1ml of warmed PBS. The PBS was removed and transferred to the relevant 15ml falcon tube. The media and PBS was retained to account for floating cells in the media. Next, the 15ml falcon tubes were centrifuged at 0.4 x g for 3 minutes and the supernatant was discarded. The volume of SDS sample buffer to be added to each well of the 6 well plate was determined by looking at the relative confluency of the wells in comparison to siSCR, taking into account the floating cells. SDS sample buffer was added to each well and this cell-SDS sample buffer solution was transferred to the 15ml falcon tubes containing the cell pellets pipetting up and down to resuspend the pellet. The samples were transferred to Eppendorf tubes and frozen until required for western blotting. The antibodies used for these apoptosis assays (Table 3.6) included markers of apoptosis cleaved poly-ADP ribose polymerase (PARP), cleaved caspase and procaspase 3, and beta actin as a loading control.

3.8 MTS assay

An MTS assay (197010, Abcam) is a colorimetric method used to quantify the relative amount of viable cells. This method can be used to assess cell proliferation, viability and cytotoxicity. The method of action in an MTS assay is that viable cells reduce MTS tetrazolium to a formazan dye which is soluble in media. The reduction is thought to take place by dehydrogenase enzymes found in metabolically active cells which rely on NADPH to reduce the MTS tetrazolium (Abcam). Firstly, transfection master mixes were made for each siRNA used. Next, the cells were split (described in section 3.1.2) and counted. The cells were diluted to 25,000 cells per ml as 2,500 cells were required per well. The assay was performed in 96-well tissue culture plates and 4 plates were required per assay for 4 time points; 24 hours, 48 hours, 72 hours and 96 hours. Following this, 5µl of each siRNA master mix was added to the relevant wells. All siRNAs were added in triplicate. Non-transfected (NT) wells were also included to determine the effect of the transfection process on cell viability. This was also performed in triplicate. Next, 100µl of the diluted 2,500 cells/well cell dilution was added to the 12 wells required for the NT, siSCR, siCBX2-3 and siCBX2-4 conditions along with a border of media or cells if enough left over after the cells were added to the treated wells. This was done to prevent evaporation of the cells in the middle and to ensure conditions remained consistent throughout all conditions. The plates were then incubated at 37°C and 5% CO_2. After the plates had been incubated for the appropriate amount of time, MTS reagent was added to each of the 12 wells at 10% of the volume of the well. In this case, 10µl was added to the NT condition along with 10.5µl to the siSCR, siCBX2-3 and siCBX2-4 conditions. The plate was incubated at 37°C and 5% CO_2 for 3 hours. Following this, the plate was read at 490nm using an ELISA plate reader (Synergy 2, BioTek) and KC4 software. The data from this was then analysed using Microsoft Excel. Following all time points, the readings were normalised to the 24 hour time point and a graph was plotted.

3.9 Cytoplasmic and Nuclear extraction

Cell pellets of 1 million cells were used to generate cytoplasmic extracts and nuclear extracts. 100µl of cytoplasmic extraction reagent 1 (CER1) was added to 2 pellets of 1 million cells. The samples were vortexed for 15 seconds and pooled into a single Eppendorf tube. The sample was incubated on ice for 10 minutes. Following this, 11µl of CER II was added to the sample and vortexed for 5 seconds. This was then incubated for 1 minute on ice. The sample was vortexd for another 5 seconds and then centrifuged at maximum speed for 5 minutes. During this the cytoplasmic fraction of the cells were released. The supernatant was immediately transferred to a clean, pre-chilled Eppendorf tube forming the cytoplasmic extract. Immediately following this, the cell pellet was resuspended in 100µl of nuclear extraction reagent (NER) and vortexed for 15 seconds. The sample was placed on ice and vortexed for 15 seconds every 10 minutes for 40 minutes. The sample was centrifuged at full speed for 10 minutes and the supernatant was transferred to a new, clean, pre-chilled Eppendorf tube. This formed the nuclear extract. The remaining pellet contained the insoluble chromatin fraction which remained once the cytoplasmic and nuclear extracts had been removed. SDS sample buffer was added at a ratio of 1:5 to the sample. 40µl of SDS sample buffer was added to the cytoplasmic extract, 20µl was added to the nuclear extract and 50µl was added to the chromatin fraction. These samples were then ready to be used on a 15% gel for Western blotting.

3.10 Dephosphorylation

To determine whether the form of CBX2 seen in western blotting is phosphorylated, a dephosphorylation experiment was performed. Two phosphatases were used to dephosphorylate CBX2; shrimp alkaline phosphatase (SAP) and calf intestinal alkaline phosphatase (CIP).

3.10.1 SAP protocol

Cell pellets of approximately 1 million cells were used for these experiments and these were lysed in RIPA buffer (10ml stock) (Table 3.8).

Table 3.8. Composition of RIPA buffer for 10ml.

	RIPA
Tris-HCl	500µl
NaCl (4M)	375µl
NP40	100µl
Sodium deoxycholate	50µg
SDS	10µg

For the SAP experiments, an alkaline phosphatase reaction buffer was made composed of 50ml Tris-HCl pH 9 and 0.5M $MgCl_2$. 1ml of RIPA buffer was added to two Eppendorf tubes along with 10mM of sodium fluoride (NaF). The pellets were lysed in the RIPA buffer. All samples were incubated on ice for 30 to 60 minutes. Following this, 200µl of alkaline phosphatase reaction buffer was added to each Eppendorf tube. 64µl of rSAP was added to one of the tubes. The samples were heated at 37°C for at least 3 hours. Then, SDS sample buffer was added at a ratio of 1:5 to the sample. The samples were then frozen and ready to be used on a western blot.

3.10.2 CIP

Cell pellets of approximately 1 million cells were used for these experiments and these were lysed in co-immunoprecipitation (Co-IP) lysis buffer (Table 3.7). Prior to the beginning of this experiment, the protein in the cell pellets was quantified using a BCA assay. For the CIP experiments, a 100ml stock of CIP buffer was made and adjusted to a

pH of 7.9 at 25°C (Table 3.9). 20-30µg of protein as calculated using the BCA standard curve was added to 2 Eppendorf tubes. The protein lysate in both Eppendorf tubes was resuspended in 10µl of CIP buffer per 1µg of protein and 1 unit of CIP per 1µg of protein was added to one of the Eppendorf tubes. The samples were heated at 37°C for up to 60 minutes. Following this, SDS buffer was added to both samples at a ratio of 1:5. The samples were then ready to be used in western blotting.

Table 3.9. Composition of CIP buffer.

Reagent	Amount
NaCl (4M stock)	2.5ml
Tris-HCl (1M stock)	5ml
MgCl2 (0.5M stock)	2ml
DTT (1M stock)	100µl

3.11 Bicinchoninic acid assay (BCA)

A BCA is used to quantify protein in a sample as compared to a serial dilution of bovine serum albumin (BSA) standard. Prior to dephosphorylation by CIP, a BCA was performed on protein lysates from cell pellets of 1 million cells from the MDA-MB-231 cell line (Pierce BCA protein assay kit ThermoFisher). The BCA was performed in a 96-well plate. First, the cell pellets were resuspended in Co-IP lysis buffer (Table 3.7) and incubated on ice for 60 minutes to allow cells to lyse and proteins to be released. Meanwhile, a serial dilution of BSA standard was made according to Table 3.10.

Table 3.10. Preparation of BSA standards

Vial	Volume of diluent (µl)	Volume and source of BSA (µl)	Final BSA concentration (µg/ml)
A	0	300 of stock	2000
B	125	375 of stock	1500
C	325	325 of stock	1000
D	175	175 of B	750
E	325	325 of C	500
F	325	325 of E	250
G	325	325 of F	125
H	400	100 of G	25
I	400	0	0

Next, the BCA working reagent was prepared according to the following formula. (number of standards + number of unknowns) x (number of replicates) x (volume of working reagent per sample) = total volume of working reagent required. The working reagent (WR) was prepared by mixing reagent A and reagent B at a ratio of 50:1. Next, 25µl of each sample and standard was added to the relevant wells of the 96-well plate. The ratio of sample to WR was 1:8. If there was not enough sample, 10µl could have been added changing the sample:WR ratio to 1:20. Next, 200µl of WR was added to each well and the plate was mixed on a plate shaker for 30 seconds. The plate was then covered in aluminium foil and incubated at 37°C 5% CO_2 for 30 minutes. Following the 30 minute incubation, the plate was cooled to room temperature and then read at or

close to 562nm on an ELISA plate reader. From the readings from the plate reader, the standard curve was plotted. Using the equation generated from the standard curve graph, the concentration of the unknown samples was calculated. The volume needed for 20-30µg (as was required for the CIP protocol) was calculated and added to 2 Eppendorf tubes and placed on ice or frozen until needed for the CIP protocol.

3.12 RNA-Sequencing

MDA-MB-231 cells were transfected (3.2 Transfections) with siSCR, siCBX2-3 and siCBX2-4. The cells were incubated for 72 hours. Following this, RNA was extracted using the Qiagen RNeasy Mini kit (as in section 3.4.2). The Qiagen RNeasy Mini kit was used preferentially over the phenol-chloroform method due to the higher quality of RNA which could be extracted using the Qiagen kit. In addition, the values for DNA/protein contamination (260:280) and the values for the ethanol/isopropanol contamination (260:230) were higher using the Qiagen kit indicating higher purity achieved using this kit. The RNA samples were then sent to Novogene™ where the cDNA library was generated and sequencing and bioinformatic analysis performed.

3.13 Statistical analysis

Students T-test statistical method was used during analysis of qPCR data.

4. Results

4.1 Reduction of CBX2 mRNA expression using CBX2 targeting siRNA.

qPCR was performed to determine the efficiency of *CBX2* mRNA knockdown. MDA-MB-231 and HS-578T TNBC cells were transfected with small interfering RNA (siRNA). Three independent *CBX2* knockdown siRNAs were used along with a scrambled (SCR) siRNA as a non-silencing control. The cells were grown for 72 hours before RNA extraction was performed. cDNA was generated from this RNA and then qPCR was performed using primers specific for *CBX2* and *RPL13A* (as a normalising control gene) to validate the CBX2 knockdown (Figure 4.1).

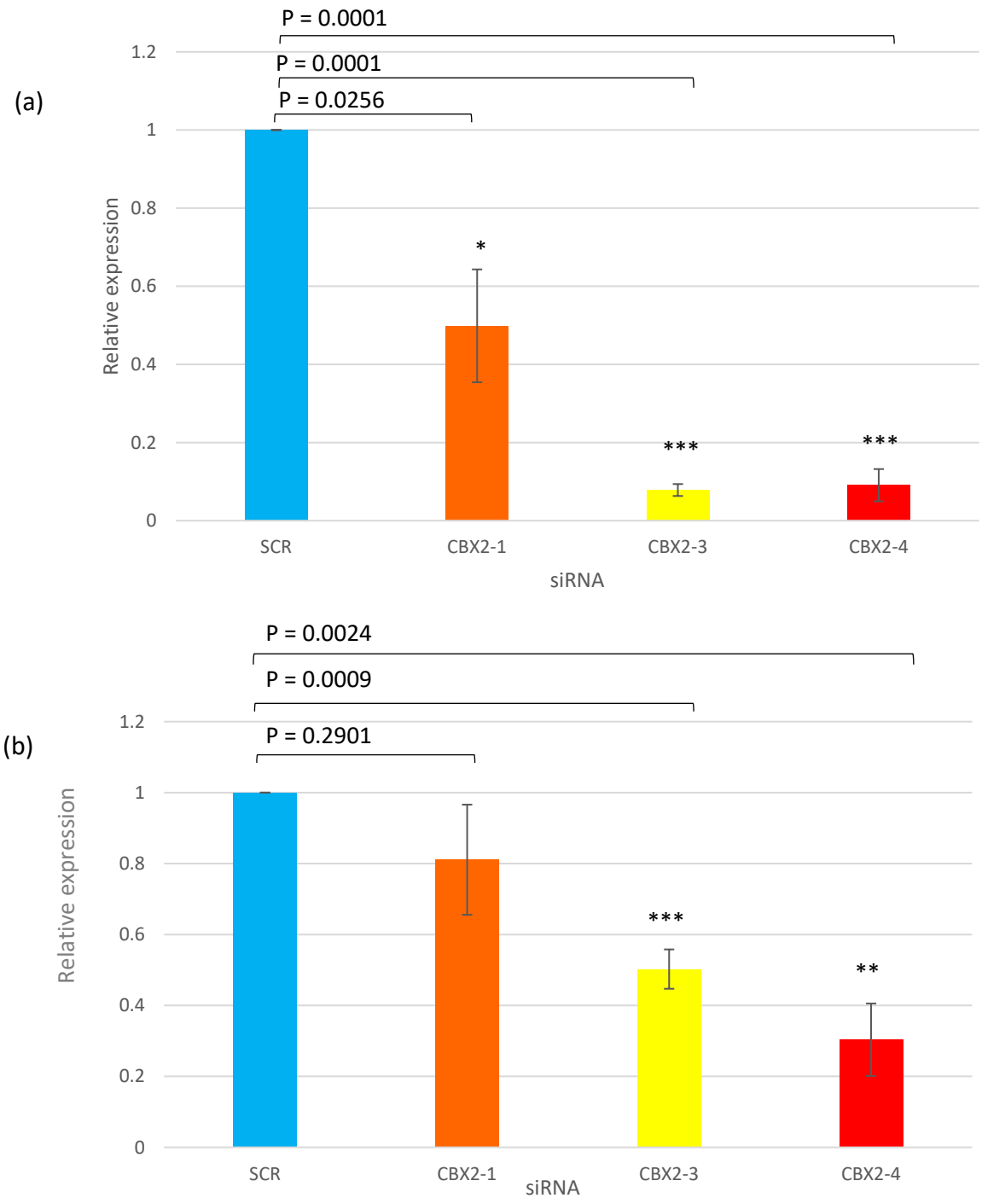

Figure 4.1: Relative CBX2 mRNA expression in MDA-MB-231 and HS-578T cells following siRNA mediated knockdown as determined by qPCR. Relative expression indicated on the left of the graphs. Error bars represent standard error. (a) represents MDA-MB-231 cells, N=3 (b) represents HS-578T cells. A student's T test was used to determine level of significance. N=3. $P<0.05$. * = significant, ** = very significant, *** = extremely significant.

In MDA-MB-231 cells, the expression of *CBX2* in the siCBX2-1, siCBX2-3 and siCBX2-4 transfected cells is significantly decreased in comparison to the expression of *CBX2* in the siSCR transfected cells. Expression was decreased by approximately 90% using siCBX2-3 and siCBX2-4 in comparison to approximately 50% using siCBX2-1 indicating that the knockdown was more efficient using siCBX2-3 and siCBX2-4 than siCBX2-1. In HS-578T cells, the expression of *CBX2* in the siCBX2-3 and siCBX2-4 transfected cells was significantly decreased by approximately 50% and 70% respectively in comparison to the expression of *CBX2* in the siSCR condition There is no significant difference between the expression of *CBX2* in the siCBX2-1 transfected cells which was decreased by approximately 20% in comparison to the expression of *CBX2* in the siSCR condition again indicating that knockdown using this siRNA is not efficient.

4.2 Reduction of CBX2 protein expression using CBX2 targeting siRNA

Following the analysis showing *CBX2* mRNA knockdown western blot analysis was undertaken to assess whether the siRNAs targeted to *CBX2* could successfully knock down CBX2 protein in MDA-MB-231 and HS-578T TNBC cells. Cells were transfected with a non-silencing scrambled control (siSCR) or one of 3 independent CBX2 knockdown siRNAs (siCBX2-1, siCBX2-3 or siCBX2-4). The transfected cells were cultured for 72 hours as previously described before being lysed in SDS lysis buffer. The protein lysates were run on a western blot using antibodies specific for CBX2 and alpha tubulin (used as a loading control) to determine if knockdown of CBX2 had been successful (Figure 4.2, Figure 4.3).

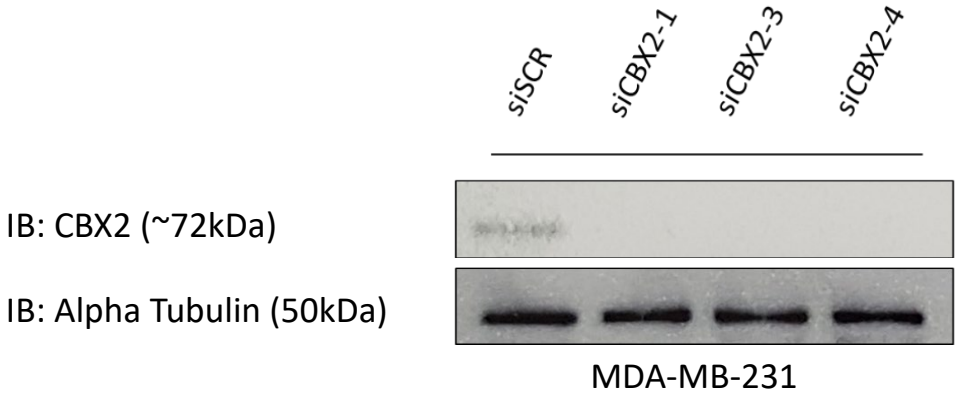

Figure 4.2: CBX2 protein knockdown in MDA-MB-231 cells. Antibodies used and molecular weights observed indicated on the left of the blots (IB = immunoblot). The siRNAs that were used in each transfection condition are indicated on the top of the blots over the relevant lanes.

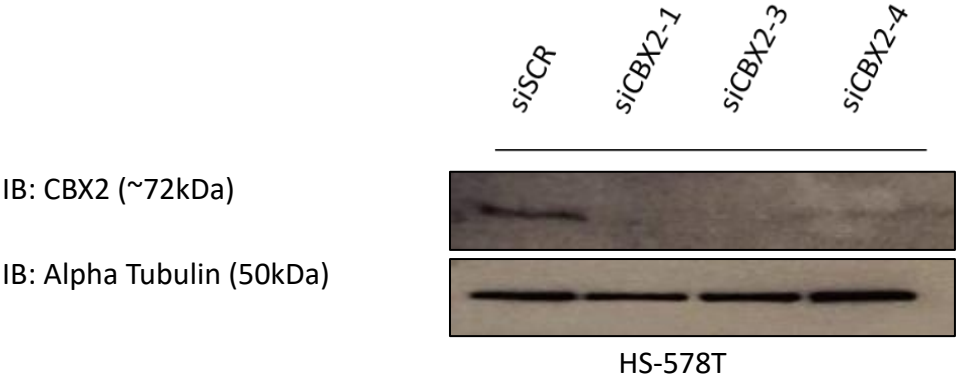

Figure 4.3: CBX2 protein knockdown in HS-578T cells. Antibodies used and molecular weights observed indicated on the left of the blots (IB = immunoblot). The siRNAs that were used in each transfection condition are indicated on the top of the blots over the relevant lanes.

The band in the siSCR transfected lysates indicates that CBX2 is present. The absence of bands in the remaining lanes indicate that there is no CBX2 present, and therefore that the knockdown of CBX2 was successful. The alpha tubulin serves as a loading control to confirm that the loading of all of the samples was equal, therefore the effect of knocking down CBX2 on the band suspected to be for CBX2 was genuine. The CBX2 band as seen in the siSCR lane is at a higher molecular weight (~72kDa) than expected from previous literature in which the height of CBX2 is 56kDa. Studies by Hatano et al., (2010) and Kawaguchi et al., 2017 however have shown that CBX2 is phosphorylated and this phosphorylated form of CBX2 is seen using western blotting at ~72kDa. We therefore next investigated if the band observed in this study is also a phosphorylated form of CBX2.

4.3 Investigation of CBX2 phosphorylation

4.3.1 Cell fractionation experiments

In previous studies, it has been shown that phosphorylated CBX2 has a higher affinity to H3K27me3 and that CBX2 is phosphorylated in order to translocate to the nucleus (Kawaguchi et al., 2017). In order to investigate whether the identified CBX2 band (figure 4.3) at 72kDa is present in the nucleus, we performed a nuclear and cytoplasmic extraction followed by a western blot analysis. Protein extracts from each cell fraction were probed for CBX2 and α-tubulin which is a cytoplasmic specific protein to test if the extraction was successful (Figure 4.4).

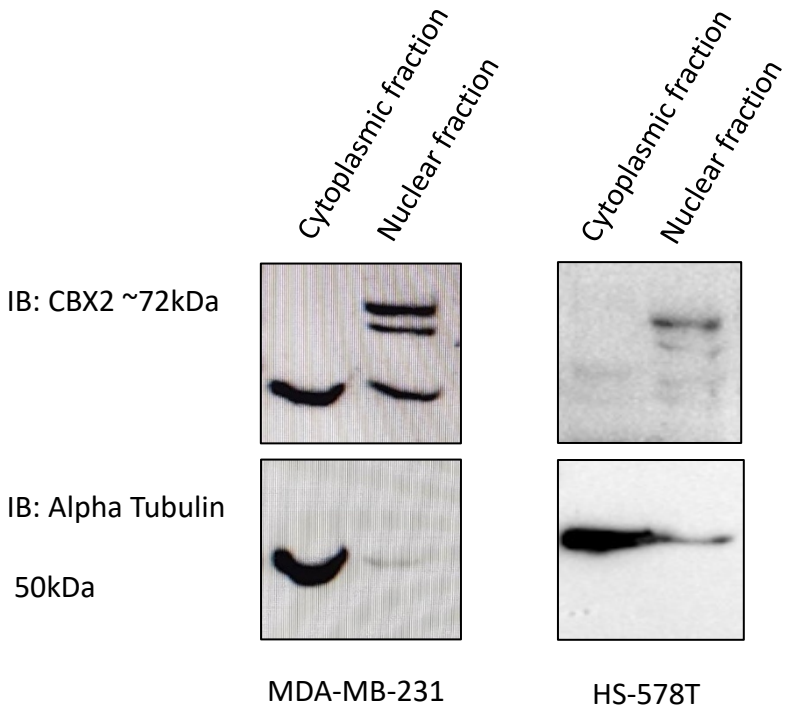

Figure 4.4: Cytoplasmic and nuclear extractions and detection of CBX2 in MDA-MB-231 and HS-578T cells. Antibodies used and molecular weights observed indicated on the left of the blots (IB = immunoblot). Lysates from different cell fractions are indicated on the top of the blots over the relevant lanes.

The bands seen at ~72kDa for CBX2 were only seen in the nuclear fraction confirming that the proposed phosphorylated form of CBX2 is present the nucleus. This is supported by previous studies by Hatano et al., (2010). Alpha tubulin was used as a marker for the cytoplasmic fraction and to confirm that the fractionation was successful. Bands seen at 50kDa for alpha tubulin were predominantly seen in the cytoplasmic fraction indicating that the fractionation was successful. There was, however, a small amount of alpha tubulin seen in the nuclear fraction indicating that the fractionation was not 100% efficient. The second band seen at around 70kDa was unidentified, but it could be that another CBX family member was detected due to having a similar structure. Another possibility is that this is non-specific binding, but this needs further investigation to be able to identify this band.

4.3.2 CBX2 dephosphorylation

Following the cytoplasmic and nuclear extraction, a dephosphorylation experiment was performed to confirm that the band that we have seen at ~72kDa was a phosphorylated form of CBX2. Shrimp alkaline phosphatase (SAP) and calf intestinal alkaline phosphatase (CIP) were used to dephosphorylate CBX2 (Figure 4.5 and Figure 4.6). Previous studies using murine models along with HEK293T cells have found that CBX2 is phosphorylated (Kawaguchi et al, 2017). Experiments showed that CBX2 was endogenously expressed at 72kDa but when cell lysates were treated with phosphatase (SAP) the molecular weight of CBX2 reduced. The study also found that the phosphorylation of CBX2 is critical for binding to H3K27me3, and therefore important in transcriptional regulation (Kawaguchi et al., 2017). In this study, cell pellets of 1 million cells were incubated with SAP and a western blot was performed to determine if the proposed molecular weight of CBX2 changes when dephosphorylated (Figure 4.5).

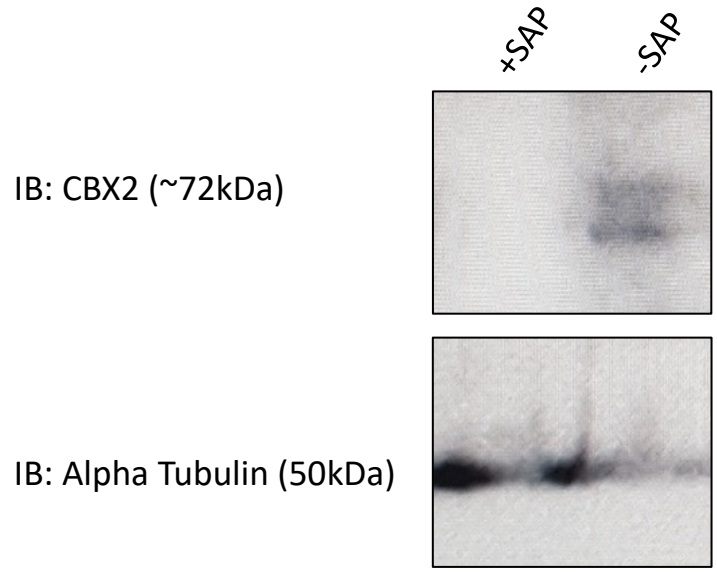

Figure 4.5. Dephosphorylation of CBX2 in MDA-MB-231 cells using SAP. SAP = shrimp alkaline phosphatase. Antibodies used and molecular weights observed indicated on the left of the blots (IB = immunoblot). Samples and treatments indicated on the top of the blots over the relevant lanes.

The CBX2 band seen in the -SAP condition was at the pre-observed height of 72kDa. No bands were seen in +SAP conditions. The alpha tubulin antibody was used to show equal protein loading between samples. This shows that protein has been loaded into each lane, despite not showing even bands. This western blot analysis suggests that the band for CBX2 observed at 72kDa represents a phosphorylated form of CBX2, however this protocol was difficult to optimise. Due to this, another method of dephosphorylating proteins was performed. The concentration of protein in pellets of 1 million cells was calculated and 2 aliquots of 20ug of protein were set aside. These were treated with protease inhibitor and one sample was incubated with CIP. A western blot was performed to determine if this method could dephosphorylate CBX2 and produce a band at the expected CBX2 molecular weight (Figure 4.6).

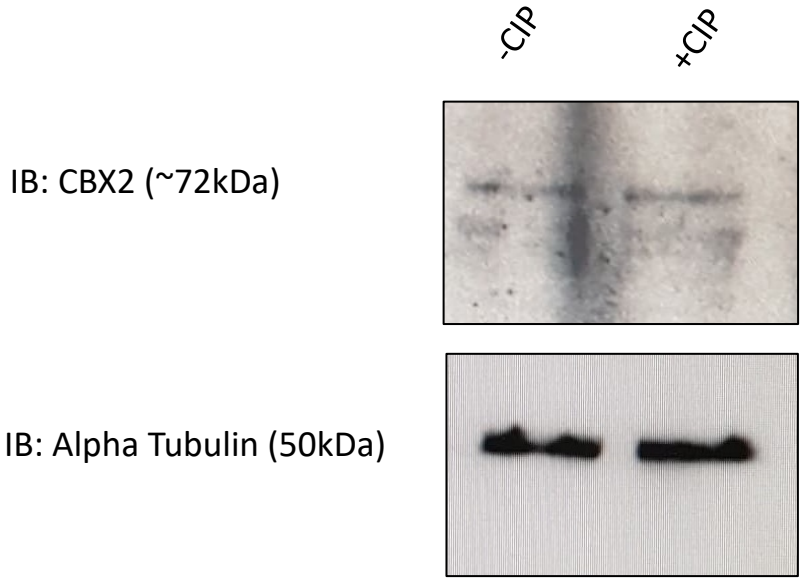

Figure 4.6. Dephosphorylation of CBX2 in MDA-MB-231 cells using CIP. CIP = calf intestinal alkaline phosphatase. Antibodies used and molecular weights observed indicated on the left of the blots (IB = immunoblot). Samples and conditions indicated on the top of the blots over the relevant lanes.

Bands seen at 72kDa for CBX2 in the -CIP sample and, unexpectedly, the +CIP sample, too. The blot was probed for alpha tubulin as a protein loading control and the bands produced were even. The CBX2 in these samples does not seem to have been dephosphorylated which is not consistent with the result observed using SAP. This experiment was only performed once due to time constraints and therefore needs further optimising.

4.4 CBX2 affects levels of global histone modifications.

It has been established in previous literature that the PRC1 complex plays a role in transcriptional repression. Therefore, the effect of CBX2 knockdown on global histone marks related to PRC1 activity as well as histone marks which are related to transcriptional activation or repression through chromatin remodelling was investigated. A western blot was performed using an siSCR transfected cell protein lysate and cell lysates from cells transfected with 3 independent CBX2 targeting siRNAs; CBX2-1, CBX2-3 and CBX2-4. The blots were probed for different histone marks including H3K27me3, H3K27ac, and H2AK119ub. H3K27me3 is the modification which is recognised by CBX2, H3K27ac is a transcriptionally activating mark occurring on the same lysine residue and H2AK119ub is the modification which the PRC1 facilitates to cause gene silencing. Antibodies specific for unmodified histones (H2A-pan and H3-pan) were used as a loading control (Figure 4.7, Figure 4.8).

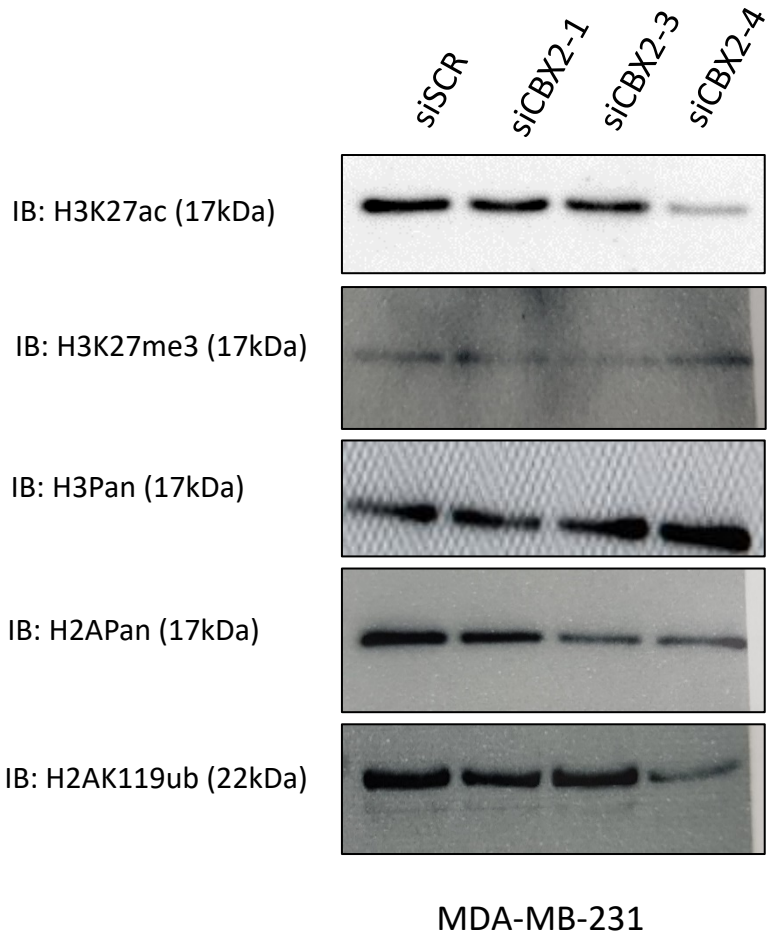

Figure 4.7: Histone western blots. MDA-MB-231 cell line. Antibodies used and molecular weights observed indicated on the left of the blots (IB = immunoblot). The siRNAs that the cells were transfected with are indicated on the top of the blots over the relevant lanes.

The level of acetylation decreased in the cells transfected with siCBX2-4 in comparison to the cells transfected with siSCR. The level of histone H3 K27 acetylation appears to be equal in the cells transfected with siCBX2-1 and siCBX2-3 in comparison to the cells transfected with siSCR. The level of histone H3K27 methylation appears to be equal in the cells transfected with siSCR, siCBX2-1, siCBX2-3 and siCBX2-4. The level of histone H2AK119 ubiquitination decreased in the cells transfected with siCBX2-4 in comparison to the cells transfected with siSCR. The level of ubiquitination appears to be equal in the cells transfected with siCBX2-1 and siCBX2-3 in comparison to the cells transfected with siSCR.

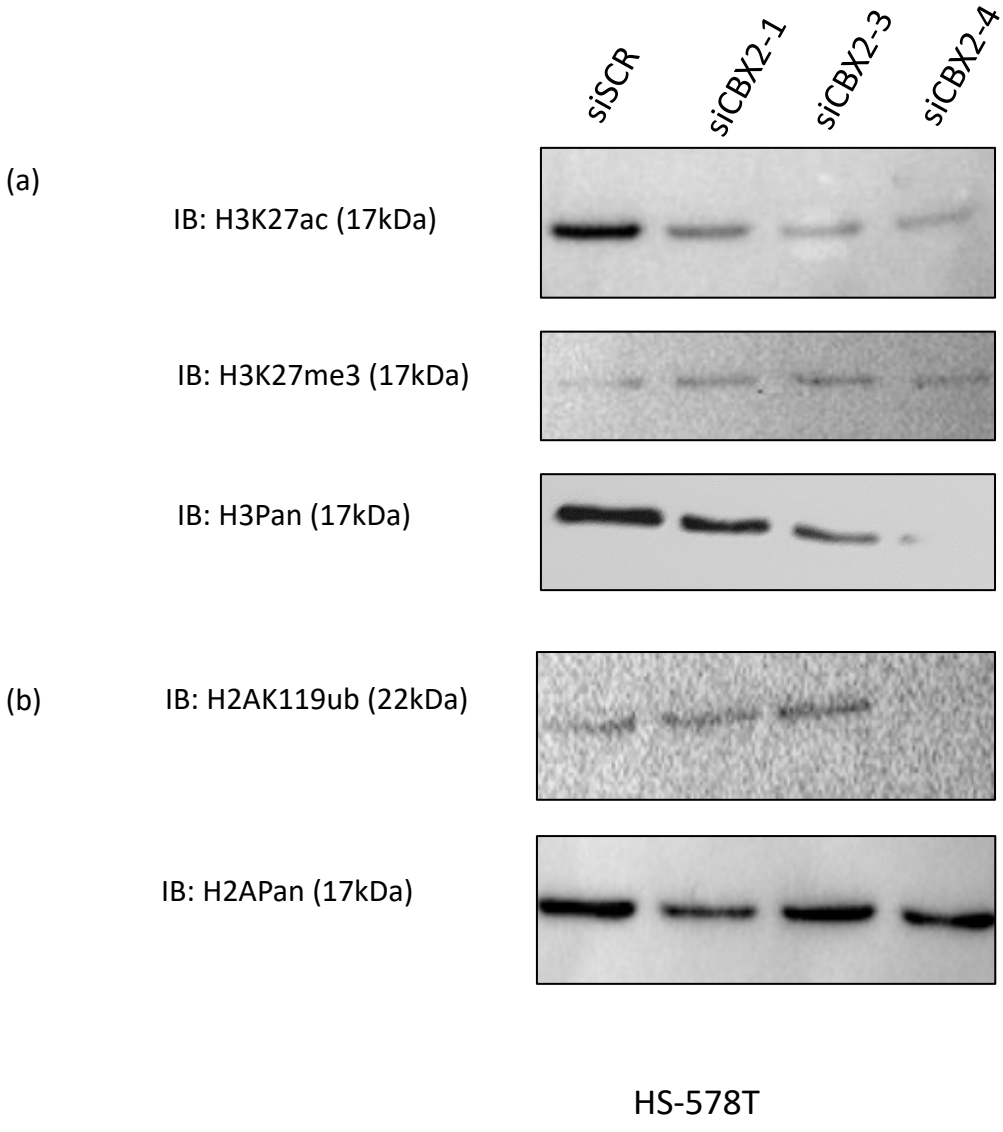

Figure 4.8: Histone western blots. HS-578T cell line. Antibodies used and molecular weights observed indicated on the left of the blots (IB = immunoblot). siRNAs transfected with indicated on the top of the blots over the relevant lanes. (a) represents blots from an independent repeat. (b) represents blots from a separate independent repeat.

The level of acetylation decreased in HS-578T cells transfected with siCBX2-1, siCBX2-3 and siCBX2-4 in comparison to cells transfected with siSCR. The level of methylation appeared to be equal between the cells transfected with siSCR, siCBX2-1, siCBX2-3 and siCBX2-4. The level of ubiquitination decreased in cells transfected with siCBX2-4 in comparison to cells transfected with siSCR. The level of ubiquitination appeared to be equal between the cells transfected with siCBX2-1 and siCBX2-3 in comparison to the cells transfected with siSCR.

4.5 CBX2 knockdown affects cell proliferation – MTS assay

Following the CBX2 knockdown analysis, an MTS assay was performed to assess the effect of CBX2 knockdown on cell growth. MDA-MB-231 and HS-578T cells were seeded in 4x 96 well plates at a density of 2500 cells/well and transfected with either siSCR, siCBX2-3 or siCBX2-4. Additionally, non-transfected wells were seeded. A plate was analysed every 24 hours. All experiments were performed in triplicate (Figure 4.9).

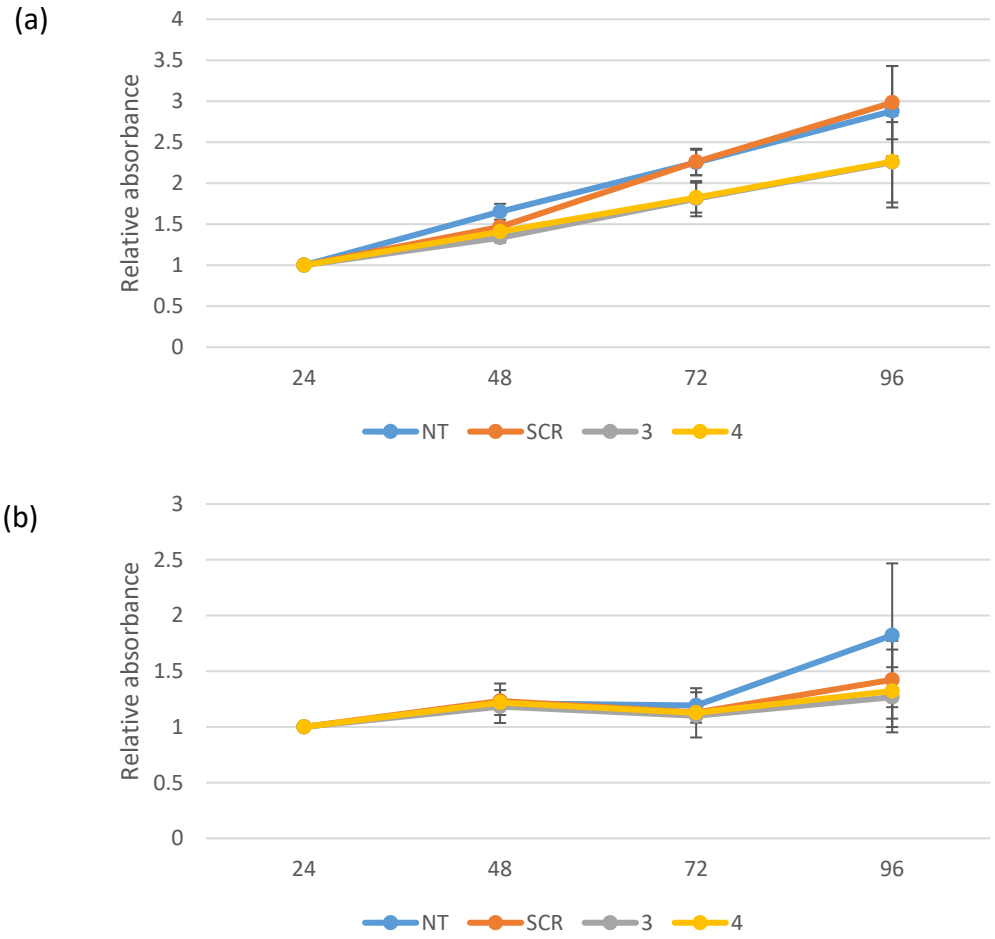

Figure 4.9. MTS cell viability assay in MDA-MB-231 and HS-578T cells. Relative absorbance normalised to 24 hours indicated on the left of the graphs. Error bars represent standard error. (a) represents MDA-MB-231 cells mean values from N=3. (b) represents HS-578T cells mean values from N=2.

In the MDA-MB-231 cell line, cell growth decreased in cells transfected with siCBX2-3 and siCBX2-4 over 96 hours although the difference was not significant. After 96 hours, the relative absorbance seen in non-transfected cells and cells transfected with siSCR was around 3-fold higher than at the 24 hour normalised value. In contrast, the relative absorbance seen in cells transfected with siCBX2-3 and siCBX2-4 was only around 2-fold higher than at the 24 hour normalised value, indicating reduced cell proliferation when CBX2 is knocked down. In the HS-578T cell line, cells did not appear to start to grow until between 72 and 96 hours. Transfection with siSCR, siCBX2-3 and siCBX2-4 appeared to have slightly affected growth at 96 hours in comparison to the non-transfected cells. The cell viability for the cells transfected with siSCR was very slightly higher than the cells transfected with siCBX2-3 and siCBX2-4.

4.6 CBX2 knockdown reduces cell proliferation – phase contrast microscopy

The reduction in cell proliferation was not significant when measured by MTS assay however, phase contrast microscopy images appear to show a bigger difference in cell growth and viability. MDA-MB-231 and HS-578T TNBC cell lines were used for the majority of experiments. All were transfected with either siSCR non-silencing siRNA or one of three independent siRNAs targeted to CBX2; siCBX2-1, siCBX2-3 or siCBX2-4. Cells were cultured for 72 hours prior to imaging. There was an observable decrease in the number of cells seen in siCBX2-1, siCBX2-3 and siCBX2-4 transfected cells compared to siSCR transfected cells, with the biggest effect being seen in siCBX2-4 transfected cells. Cells in the siSCR condition were adherent, cells in siCBX2-4 condition were rounded and floating indicating cell death. In HS-578T cells, the amount of cells decreased between siSCR and siCBX2-1, siCBX2-3 and siCBX2-4. Cells were adherent in the siSCR condition however, cells in siCBX2-4 were rounded and detached (Figure 4.10).

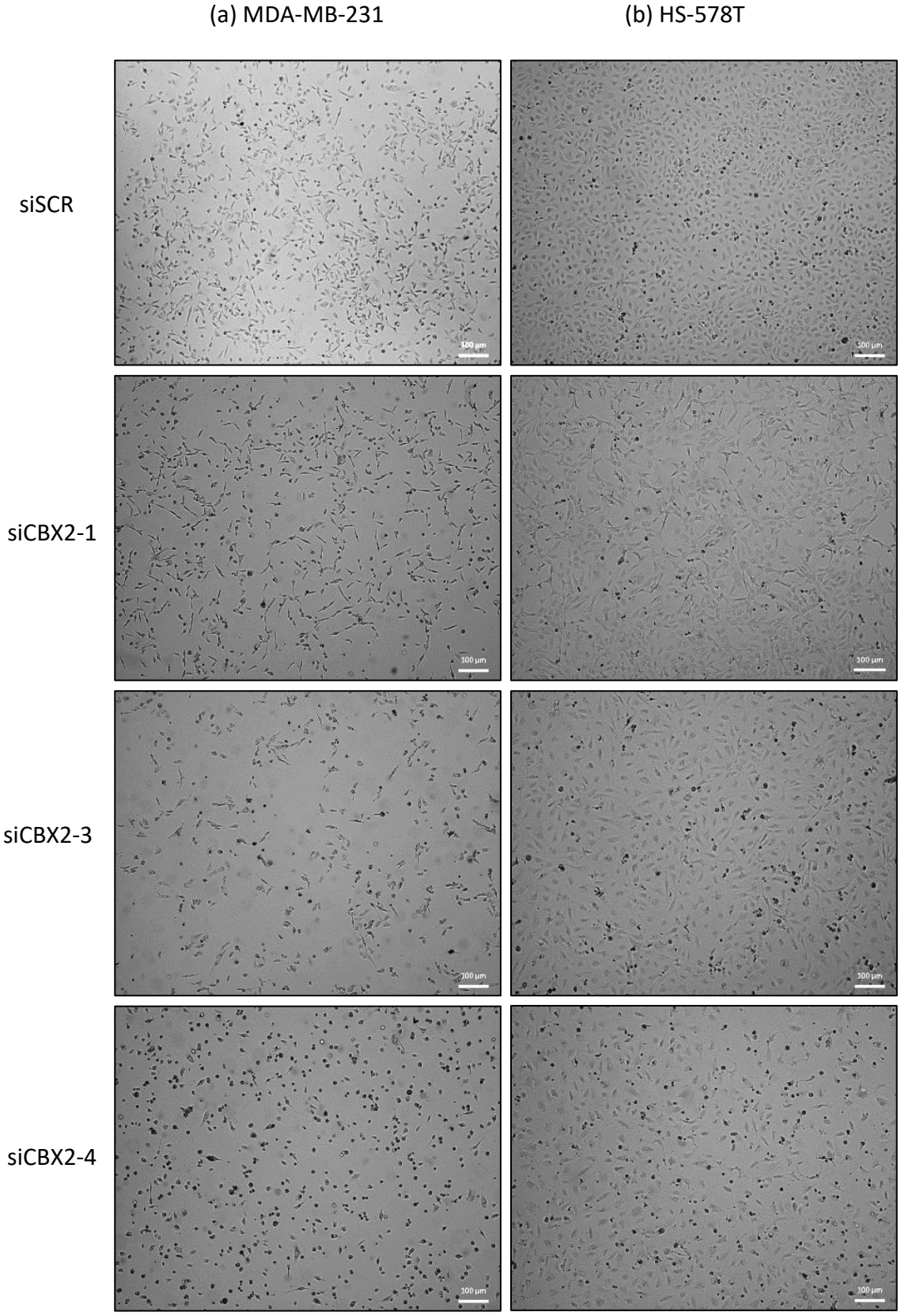

Figure 4.10. Phase contrast microscopy images of MDA-MB-231 (a) and HS-578T (b) cells 72 hours post-transfection with siSCR, siCBX2-1, siCBX2-3 or siCBX2-4.

4.7 CBX2 knockdown induces apoptosis

The phase contrast microscopy images showed that the cells appeared rounded and there was a high proportion of detached cells in those cells transfected with siCBX2-1, siCBX2-3 and siCBX2-4 compared to those cells transfected with siSCR. To determine if cells with CBX2 knocked down were undergoing apoptosis (programmed cell death) or entering a state of senescence, apoptosis assays were performed. MDA-MB-231 were seeded in 3 6-well plates at a density of 75,000 cells/ml and transfected with either siSCR, siCBX2-1, siCBX2-3 or siCBX2-4. The cells were grown for 72 hours in total, with the protein being harvested every 24 hours (See 3.3.1 Protein lysis). Following this, a western blot was performed, and the membrane was probed with an apoptosis cocktail antibody (Abcam) (Figure 4.11).

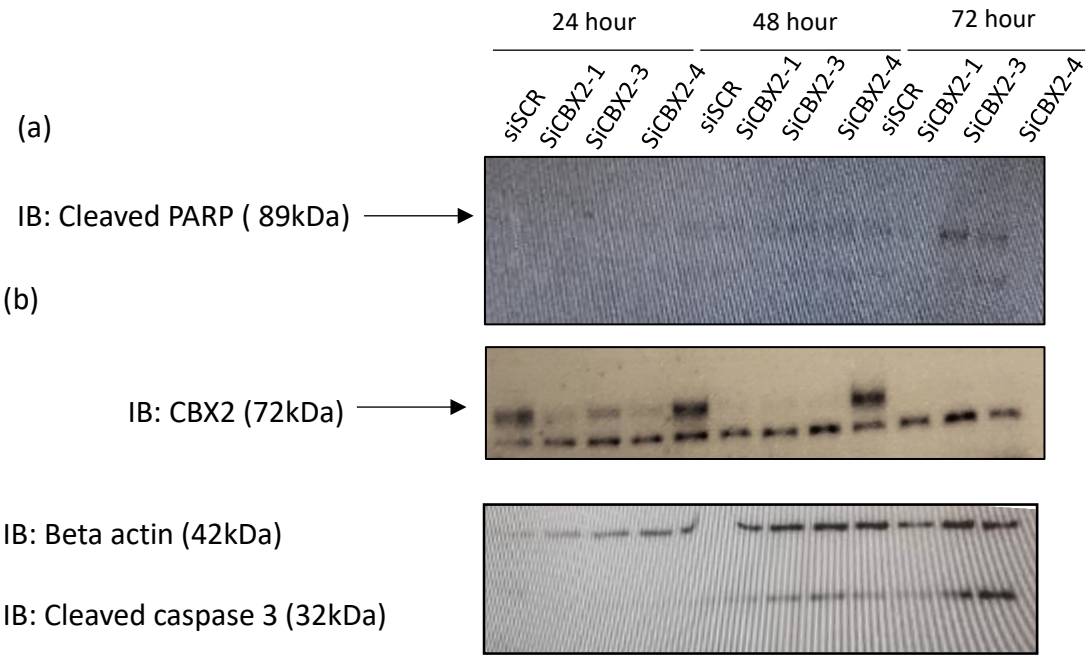

Figure 4.11. Apoptosis time course performed in MDA-MB-231 cells. Antibodies used and molecular weights observed indicated on the left of the blots (IB = immunoblot). Samples and conditions indicated on the top of the blots over the relevant lanes. (a) represents an independent repeat. (b) indicates a separate independent repeat.

Expression of cleaved PARP increased at 72 hours in cells transfected with siCBX2-3 and siCBX2-4 and was otherwise not visibly present on the western blot indicating an increase in apoptotic cells. CBX2 was expressed in cells transfected with siSCR at all time points. CBX2 knockdown was not as pronounced in cells transfected with siCBX2-1, siCBX2-3 and siCBX2-4 at 24 hours in comparison to 48 and 72 hours. Beta actin expression was approximately equal across all time points although an anomalous band was seen for siSCR transfected cell lysates at the 48 hour timepoint. Expression of cleaved caspase 3 also increased in siCBX2-3 and siCBX2-4 in both 48 hour and 72 hour time points indicating an increase of cells undergoing apoptosis.

4.8 CBX2 affects expression of cell cycle regulatory genes

Following the phenotypic data which suggested that CBX2 knockdown reduced cell viability along with data previously collected in Dr Mark Wade's laboratory has indicated that upon knocking down CBX2, MDA-MB-231 triple negative breast cancer cells arrest in G2 phase of the cell cycle, possibly triggering apoptosis (data unpublished). qPCR was performed using cDNA generated from RNA extracted from MDA-MB-231 and HS-578-T cells transfected with either siSCR, siCBX2-1, siCBX2-3 or siCBX2-4 and grown for 72 hours to investigate the effect of CBX2 knockdown on cell cycle regulatory gene expression. The genes tested were*; CDK1, CDK2, CDK4, CCNA2, CCNE2, CCND1*, *CCND3.* Following the amplification data from a standard curve, it was decided that the genes to be tested with the knockdown samples would be *CDK1, CDK4, CCNA2, CCND1* and *CCND3* (Figure 4.12).

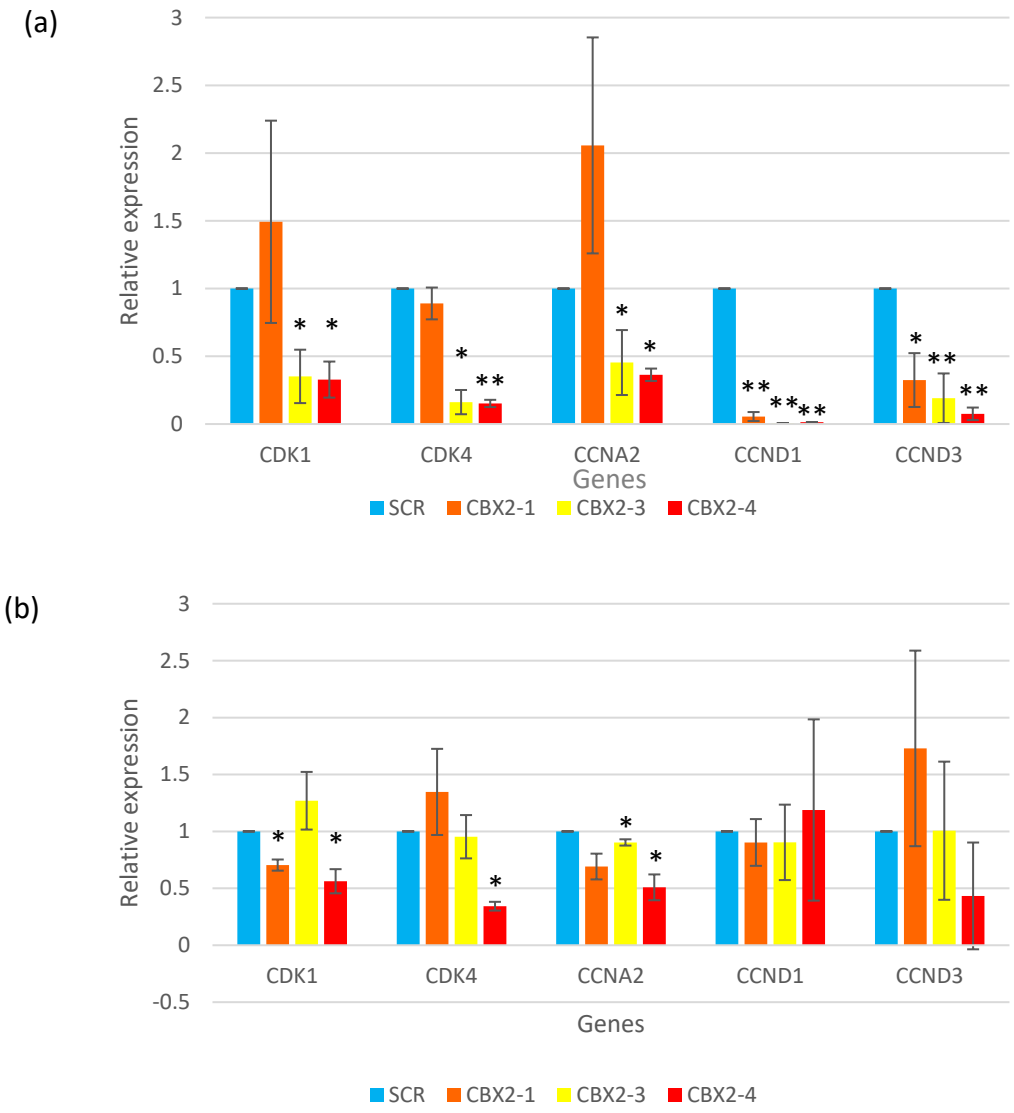

Figure 4.12. Effect of CBX2 knockdown on expression of cell cycle regulatory genes in MDA-MB-231 and HS-578T cells. Relative mRNA expression indicated on the left of the graphs. Error bars represent standard error. (a) represents MDA-MB-231 cells, N=3 (b) represents HS-578T cells. A student's T test was used to determine level of significance. N=3. P<0.05. * = significant, ** = very significant, *** = extremely significant.

In MDA-MB-231 cells, the expression of pro-proliferative cell cycle regulatory genes *CDK1, CDK4, CCNA2, CCND1* and *CCND3* decreased when CBX2 was knocked down with siCBX2-3 and siCBX2-4 when compared to siSCR. Expression of *CDK1* and *CCNA2* increased when CBX2 was knocked down with siCBX2-1 and expression of *CDK4, CCND1* and *CCND3* decreased under the same conditions when compared to siSCR. In HS-578T cells, the expression of *CDK1, CDK4, CCNA2* and *CCND3* decreased when CBX2 was

knocked down with siCBX2-4. The expression of *CCND1* increased under the same conditions. This supports the MTS data which showed little change in cell viability in HS-578T cells but showed a reduction in growth in MDA-MB-231 cells.

4.9 CBX2 knockdown also affects growth and viability of non-transformed breast epithelial cells

To determine whether CBX2 had the potential to be used as a therapeutic target in TNBC, we next determined the effect that CBX2 knockdown had on non-tumorigenic, non-transformed breast epithelial cells. For this investigation, we used MCF-10A cells. Firstly, we performed a western blot analysis to confirm that CBX2 is expressed and that transfection with CBX2 targeting siRNA reduces CBX2 expression (Figure 4.13).

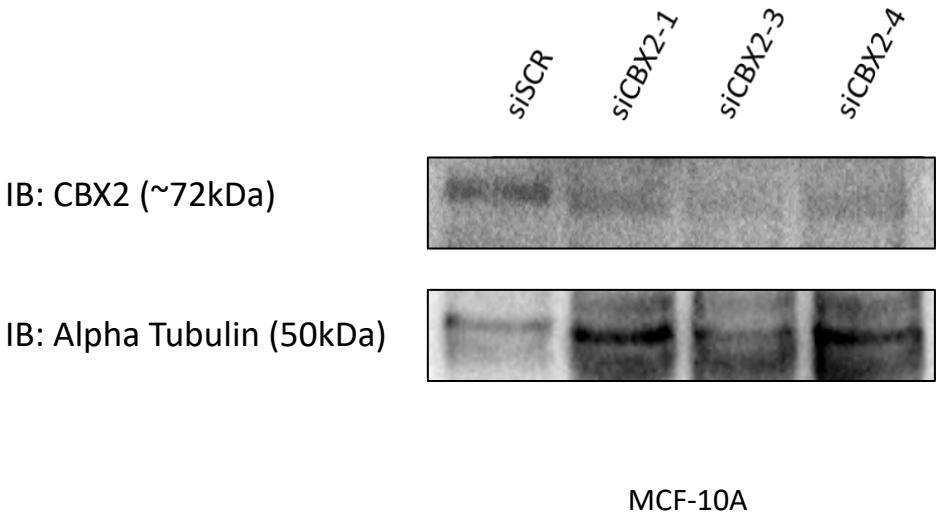

Figure 4.13. CBX2 knockdown in MCF-10A cells. Antibodies used and molecular weights observed indicated on the left of the blots (IB = immunoblot). siRNAs transfected with indicated on the top of the blots over the relevant lanes.

The bands seen at 72kDa determined to be CBX2 in TNBC cell lines appeared in all lanes in MCF-10A cells however appear fainter in cell lysates from cells transfected with CBX2-targetting siRNAs. The alpha tubulin was used as a loading control and confirms that protein had been loaded into all lanes, despite these bands not being even. However, this blot was only performed once, therefore this western blot needs further optimising for this cell line. Following the Western blot analysis, an MTS assay was performed in order to assess the impact of CBX2 knockdown on cell viability (Figure 4.14).

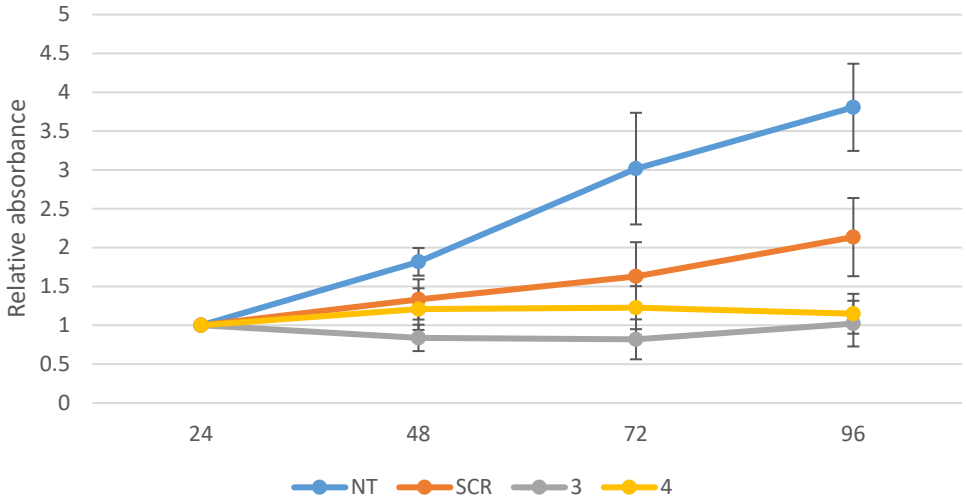

Figure 4.14. CBX2 knockdown effect on cell viability in MCF-10A cells. Relative absorbance normalised to 24 hours indicated on the left of the graphs. Error bars represent standard error. N=3.

In cells transfected with siSCR, siCBX2-3 and siCBX2-4, the cell viability decreases in comparison to non-transfected cells over 96 hours, although this was not significant. After 96 hours, the relative absorbance in non-transfected cells was around 4-fold higher than the 24 hour normalised absorbance. However, the relative absorbance in the cells transfected with siSCR was around 2-fold higher than the 24 hours normalised absorbance and the relative absorbance in the cells transfected with siCBX2-3 and siCBX2-4 did not appear to change from 24 hours to 96 hours. The cells transfected with siCBX2-3 and siCBX2-4 had a relative absorbance of around 4-fold lower than in the non-transfected cells. Finally, cell counts were taken to determine whether CBX2 knockdown affected cell growth and proliferation despite the MTS data (Figure 4.15).

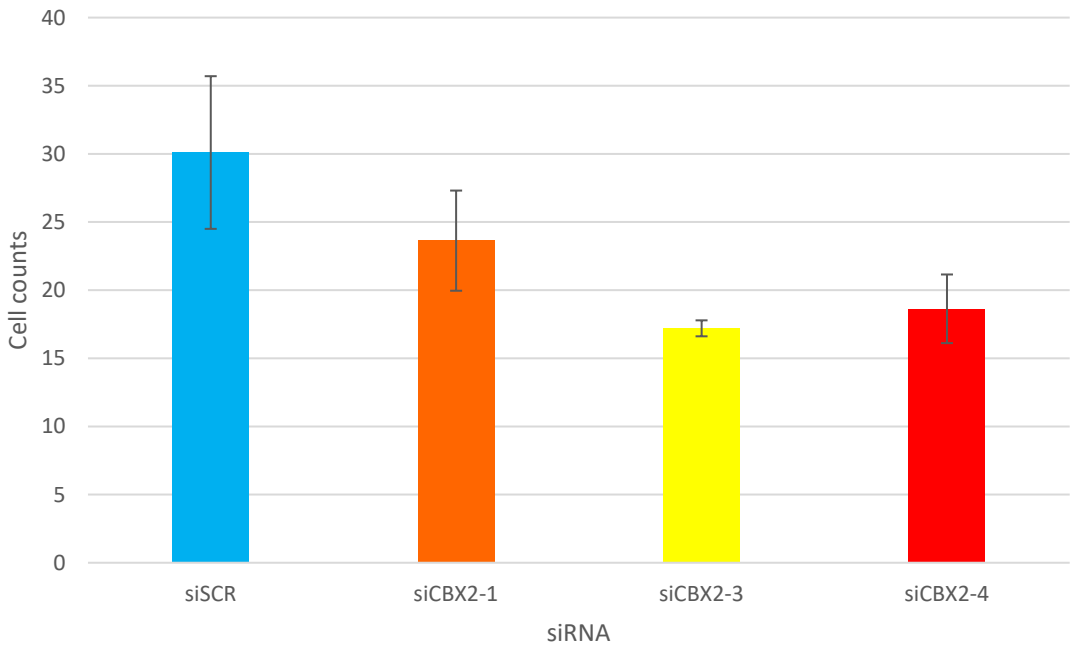

Figure 4.15. Cell counts for MCF-10A cells 72 hours post-transfection. All counts performed in triplicate and an average taken. Error bars represent standard error. A student's T test was used to determine level of significance. P=<0.05. * = significant, ** = very significant, *** = extremely significant.

This indicates that CBX2 knockdown reduces cell growth. However, the reduction in cell count is not significant in any condition. Phase contrast microscopy images were taken to observe the changes seen in MCF-10A cells upon CBX2 knockdown (Figure 4.16). The cells appear larger and more rounded slightly in cells transfected with siCBX2-3 and siCBX2-4 compared with cells transfected with siSCR. Overall, this indicates that CBX2 knockdown reduces cell growth.

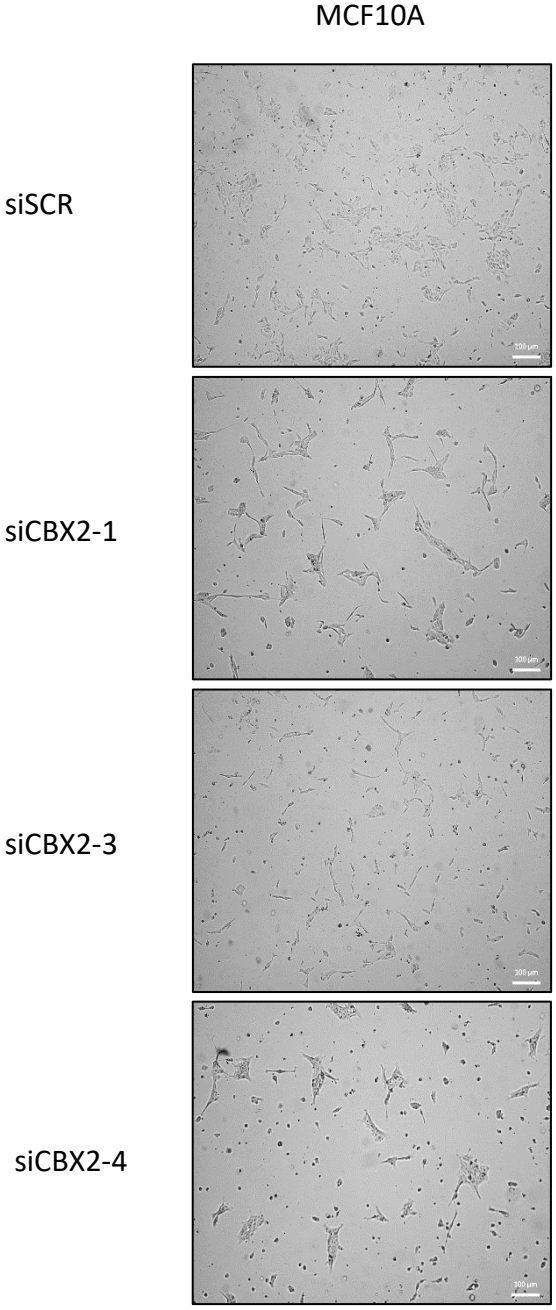

Figure 4.16. Phase contrast microscopy images of MCF-10A cells 72 hours post-transfection with siSCR, siCBX2-1, siCBX2-3 or siCBX2-4.

4.10 RNA-sequencing

RNA-sequencing (RNA-seq) was performed in MDA-MB-231 cells to determine the effect of CBX2 knockdown on global gene expression and therefore indicate which genes CBX2 regulates and which cell processes it is involved in controlling. All graphs and data generated by Novogene™. Firstly, the samples were tested for quality control and a graph was generated showing the correlation between the biological repeats of each sample and between different samples in different condition. The similarity between the biological repeats are all above 0.97 whereas the similarities between the samples from different conditions are lower, all being around 0.88. This indicates that the samples generated were consistent between biological repeats and that no samples were mixed up. As all of the figures are above 0.86, these samples were considered of a high enough quality to be analysed (Figure 4.17).

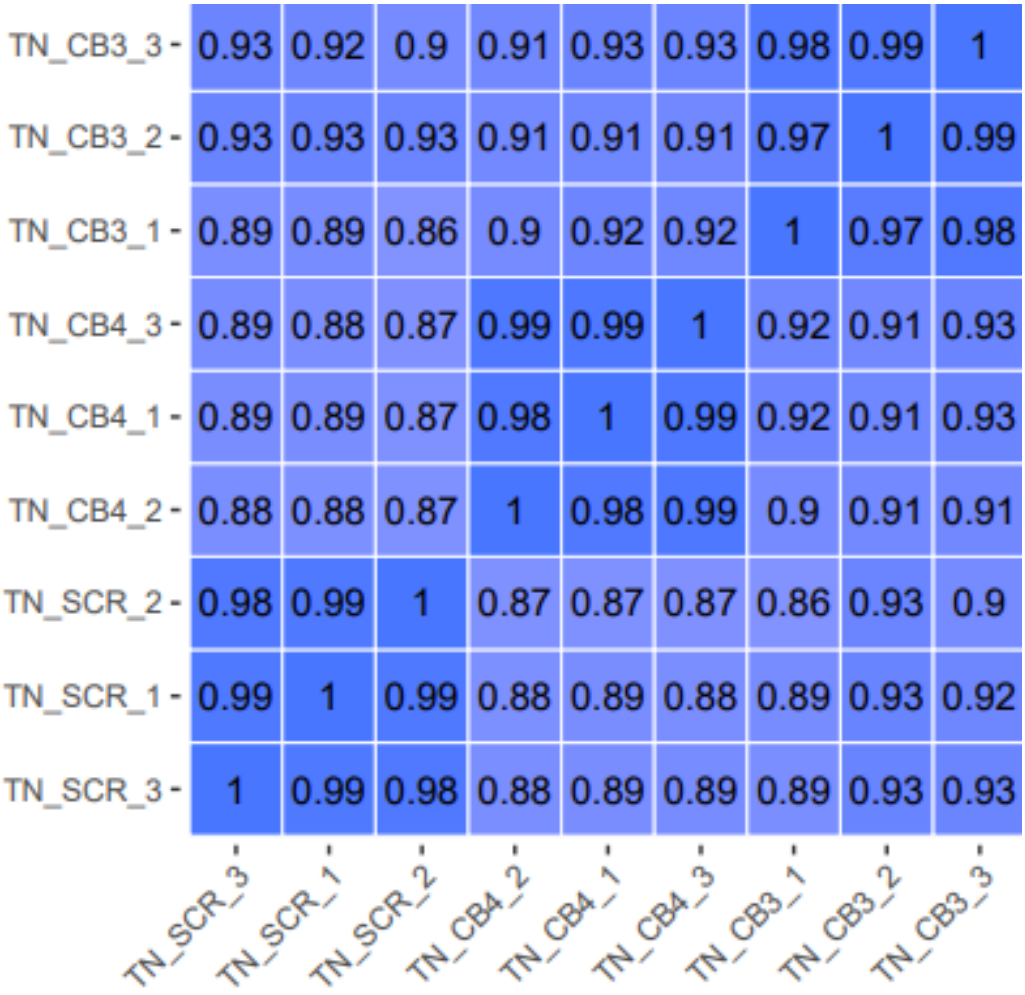

Figure 4.17. A Pearson correlation coefficient of triplicates of each siRNA used. All have an R^2 value of at least 0.8 meaning that they are significant.

A heat map was generated to show the gene expression profile for all genes in each sample (Figure 4.18). The SCR samples 1, 2 and 3 cluster together indicating that the biological replicates are consistent. The siCBX2-3 transfected samples (CB3 samples) 1, 2 and 3 also cluster together, as do the siCBX2-4 transfected samples (CB4 samples 1, 2 and 3). This again indicates consistency and that all samples were not mixed up. The gene expression profiles of the SCR and CB3 samples are more closely correlated than the SCR and CB4 gene expression profiles. Both the correlation coefficient map and the heat map indicate that the biological repeats were consistent and that the samples were not mixed up.

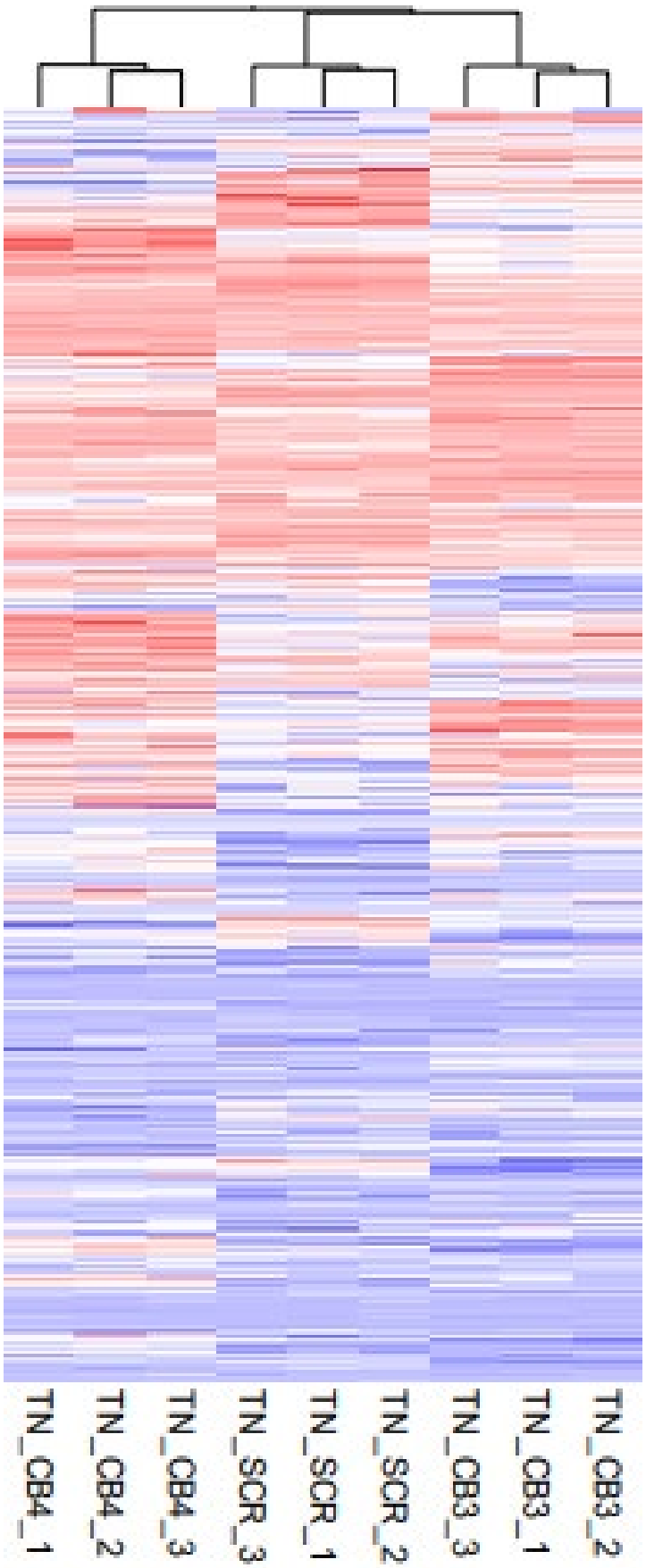

Figure 4.18. Heat map showing the similarities between the profiles for siSCR, siCBX2-3 and siCBX2-4 in MDA-MB-231 cells. The blue lines indicate low expression and the red lines indicate high expression.

The analysis of the RNA-seq data was received at the very end of this project and hence only analysis into siCBX2-3 transfected cells was conducted due to time constraints. The analysis for the siCBX2-4 transfected samples was not performed during this project. Following the quality control tests, a volcano plot was generated showing that when comparing the gene expression profiles of those cells transfected with siSCR to those cells transfected with siCBX2-3, there are 4864 genes significantly upregulated and 1986 genes significantly downregulated (Figure 4.19). The x axis shows the log adjusted fold change of all of the differentially expressed genes. The further these genes were from 0 meant that there was a bigger change in expression when CBX2 was knocked down. The y axis shows the log adjusted p values of all of the differentially expressed genes. The further these genes were up the scale meant that they were more statistically significant.

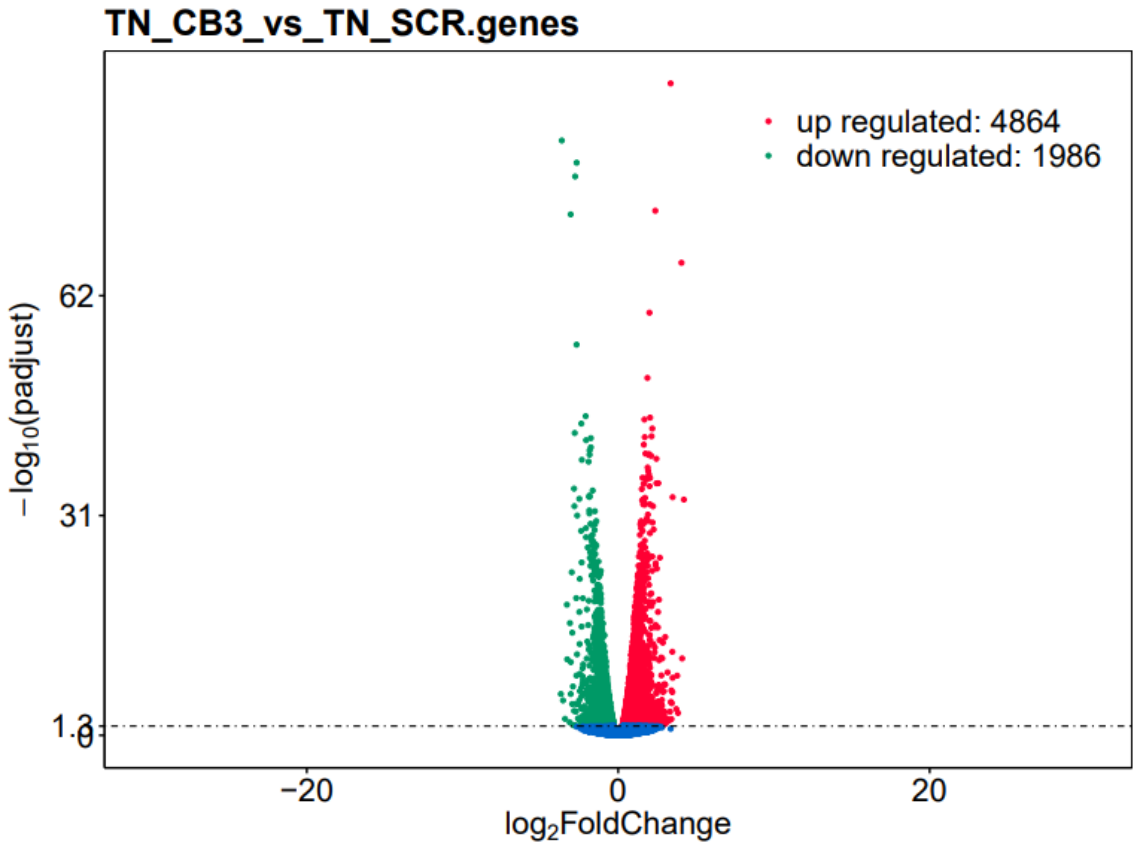

Figure 4.19. Volcano plot of differentially expressed genes between SCR samples and CBX2-3. Comparison between cells transfected with siSCR (TN_SCR) and cells transfected with siCBX2-3 (TN_CB3).

This data correlates with the fact that CBX2 is a transcriptional repressor. Following this, Kyoto Encyclopaedia of Genes and Genomes (KEGG) gene ontology analysis was performed on differentially expressed genes. This highlighted the top 20 pathways that the differentially expressed genes identified in the volcano plot were involved in. Particular pathways of interest identified were the "Cell Cycle" pathway, the "mTOR signalling pathway", the "PI3K-AKT signalling pathway" and "Pathways in cancer" (Figure 4.20).

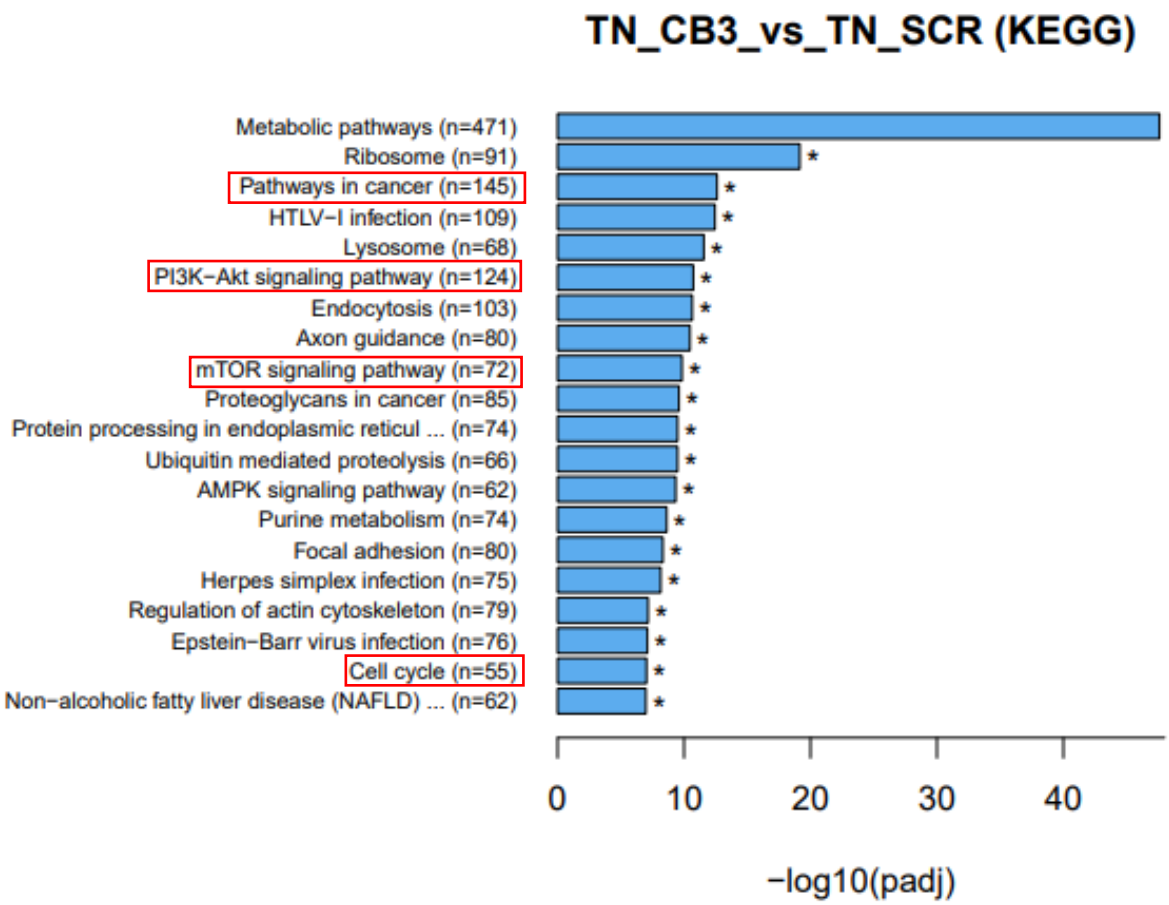

Figure 4.20. KEGG pathway analysis graph. The top 20 pathways that the differentially expressed genes were associated with were highlighted. Specific pathways of interest highlighted with red boxes.

These pathways are of interest because some of them are oncogenic signalling pathways further highlighting that CBX2 plays a role in cancer. In addition, this data supports the cell cycle regulatory gene expression data and the proliferation data gained using the TNBC cell lines.

As the PI3K—AKT signalling pathway was identified in the top 20 pathways, this was further investigated (Figure 4.21). On the right-hand side of the graph are pathways and processes which are controlled by the PI3K-AKT signalling pathway.

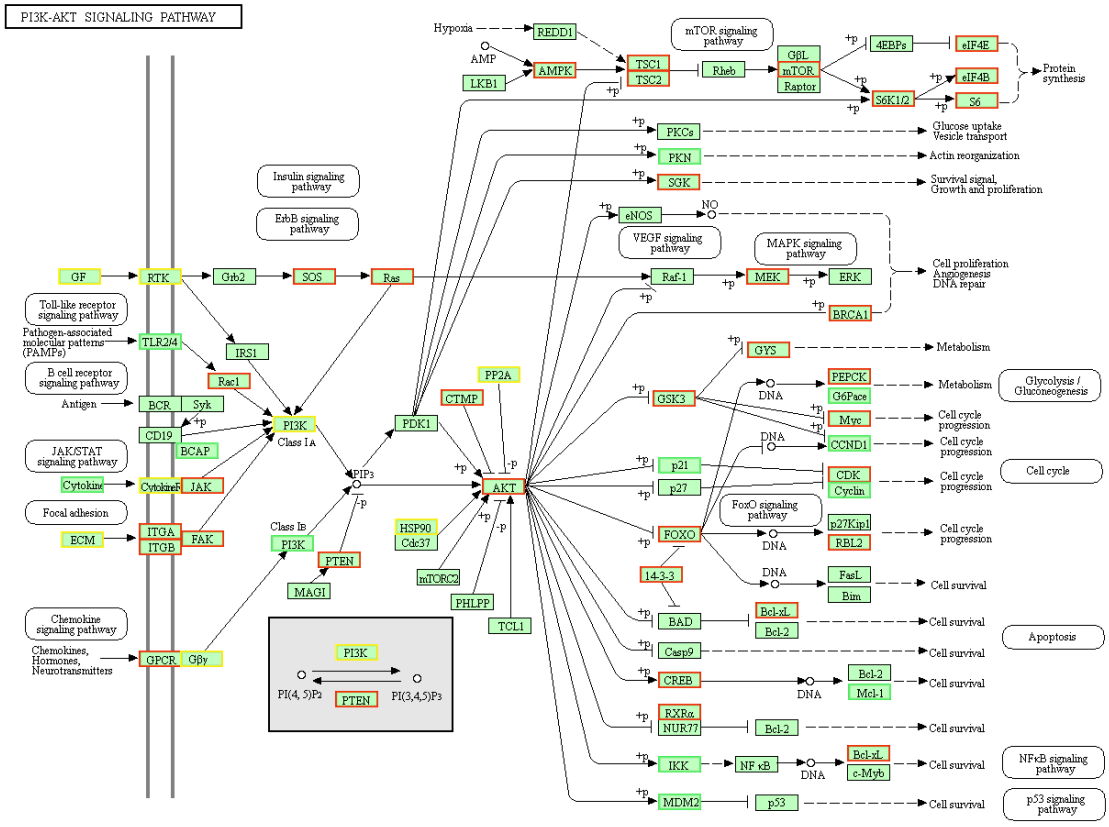

Figure 4.21. PI3K-AKT signalling pathway analysis. Differentially expressed genes highlighted. The red boxes indicate genes which are upregulated when CBX2 is knocked down. The green boxes indicate genes which are downregulated when CBX2 is knocked down and the yellow boxes indicate multiple protein subsets where some genes were upregulated and some were downregulated when CBX2 was knocked down.

PTEN is highlighted in red indicating that the expression was upregulated when CBX2 was knocked down. *PTEN* is a negative regulator of the PI3K-AKT signalling pathway and *PTEN* is usually downregulated in cancer. CCND1 is highlighted in green indicating that the expression was upregulated when CBX2 was knocked down. This correlates with the KEGG pathway analysis which showed that some of the differentially expressed genes were associated with the cell cycle. The mTOR signalling pathway was also identified as an oncogenic signalling pathway which some of the differentially expressed genes were associated with. *AMPK, TSC1* and *TSC2* TSG involved in inhibiting the mTOR signalling

pathway were upregulated when CBX2 was knocked down. This analysis is preliminary and more investigation needs to be done on the RNA-seq data.

4.11 Immunoprecipitation.

An immunoprecipitation experiment was performed and optimization was started on this protocol to be able to perform chromatin immunoprecipitation (ChIP) in the future to investigate whether CBX2 is directly regulating any of the genes identified from the RNA-seq data. CBX2 was immunoprecipitated from samples and the western blot analysis showed that the band for CBX2 was present at 72kDa. This band was not seen in the IgG control sample confirming that the band seen represented CBX2. In the input control lane, the band for CBX2 is also at 72kDa (Figure 4.22).

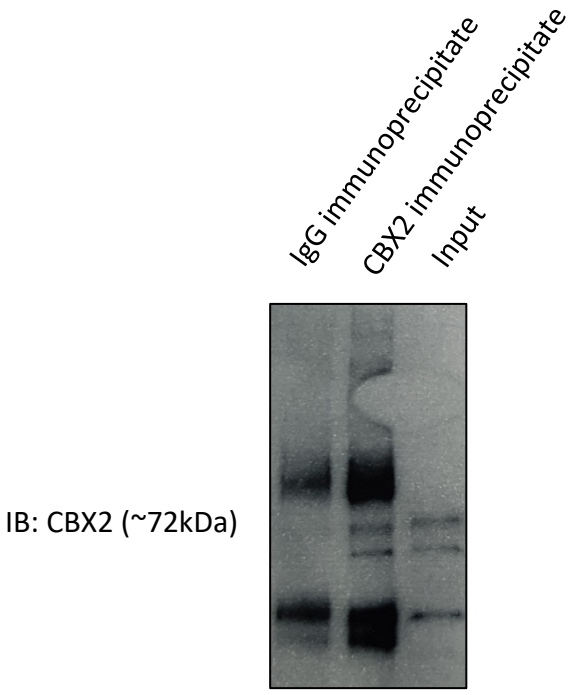

Figure 4.22. Immunoprecipitation western blot using MDA-MB-231 cells and protein A beads. Bands were seen at 72kDa for CBX2 in an input control lane and CBX2 antibody immunoprecipitate lane. No bands were seen in IgG control antibody lane indicating that CBX2 was precipitated from the sample and this band did relate to CBX2.

5. Discussion

Due to the lack of targeted therapeutics available for TNBC, and the poor prognosis of people with TNBC, it is important to try and identify novel therapeutic options to treat this disease. The epi-reader protein CBX2 is upregulated in basal breast cancers when compared to normal breast tissues (Chen et al., 2018). The majority of these basal tumours are TNBC suggesting that CBX2 may be a potentially novel therapeutic target for TNBC tumours (Alluri and Newman, 2014). CBX2 has been suggested as a possible therapeutic target in various cancer types such as prostate cancer (PCa) (Clermont et al., 2014 and Clermont et al., 2016). The aim of this study was therefore to assess the role of CBX2 in models of TNBC and begin validation of it as a potential novel therapeutic target.

In this study, we have identified CBX2 in an active phosphorylated form in TNBC cell lines. In addition to this, we have determined that CBX2 knockdown reduces growth and that CBX2 is involved in oncogenic signalling pathways, regulating the expression of cell cycle genes.

Very recently, Piqué et al., (2019) showed in basal breast cancer cell lines that CBX2 knockdown reduces breast cancer growth, validating our findings that CBX2 has a role in basal breast cancer progression.

CBX2 recognises H3K27me3 using a chromodomain which potentially could be targeted by small molecule inhibitors. Stuckey et al., (2016) showed that chromodomains can be targeted using UNC3866, which is a PRC1 chromodomain inhibitor that had a high affinity for CBX2 orthologues CBX4 and CBX7, indicating that it may also be possible to specifically target the chromodomain of CBX2.

5.1 CBX2 is phosphorylated in TNBC cells

CBX2 knockdown was confirmed in TNBC cells using siRNAs targeted to CBX2; siCBX2-1, siCBX2-3 and siCBX2-4. Multiple siRNAs were used rather than a single oligonucleotide to ensure that any results gained were not due to off target effects, but rather due to the CBX2 knockdown itself. First, *CBX2* knockdown was shown at the mRNA level using qPCR and then shown at the protein level using Western blot analysis. When the Western blot analysis was performed, it was noted that the band for CBX2 was seen consistently at 72kDa which contrasted with the expected molecular weight of CBX2 of

55kDa, as shown in protein databases (Uniprot and the antibody manufacturers instructions (Abcam). In addition to the western blot analysis, immunoprecipitation also showed the band for CBX2 at 72kDa. Hatano et al., (2010) also identified a CBX2 band at approximately 72kDa. They hypothesised that CBX2 at this molecular weight was a phosphorylated form and used a phosphatase called CIP on protein lysates from F9 cells to perform a dephosphorylation. They showed that following treatment, CBX2 was detected at a lower molecular weight indicating that the form of CBX2 seen at 72kDa is indeed phosphorylated. Recently, a study performed by Kawaguchi et al., (2017) also indicated that CBX2 is phosphorylated in HEK239T human embryonic kidney cells. In the study, they used SAP instead of CIP to dephosphorylate protein lysates and found that, in the sample not treated with SAP the molecular weight of CBX2 was 72kDa. In the sample treated with SAP CBX2 was observed at 55kDa. The study also found that the phosphorylated form of CBX2 was found *in vivo* and is the active transcriptionally repressive form of CBX2. CBX2 is active when in the nucleus as this is where the H3K27me3 is recognised and therefore where CBX2 promotes the ubiquitination of H2AK119 via the PRC1 complex, and therefore the condensation of chromatin. Phosphorylation of CBX2 increased the affinity for H3K27me3 binding, and dephosphorylation of CBX2 inhibited its transcriptional repressive activity. As the active form and the form found *in vivo* was identified in the present study, our study could be more representative of the way CBX2 acts in tumours which may be important for future target validation experiments.

Unfortunately, in this study, we could not fully replicate previous results using SAP treatment however we did obtain results that were suggestive that the CBX2 band we identified was phosphorylated. Following SAP treatment, protein bands were not consistently seen using Western blot analysis at ~55kDa (the molecular weight of non-phosphorylated CBX2) despite exposing the blot for a longer period of time than previously used. A faint band was observed at 72kDa in the non-treated sample whereas no band was observed in the sample treated with SAP which is suggestive of the phosphorylation of CBX2. While this result was not conclusive, it does appear to corroborate the findings of the previous studies including Hatano et al., (2010) and Kawaguchi et al., (2017). To attempt to gain more conclusive results using SAP treatment, we increased the number of cells that were in each pellet from 1 million to 2 million and

eventually to 3 million per pellet. In addition to this, we also lysed the cells in a lower amount of lysis buffer to increase the concentration and incubated these cells for a longer period of time in the lysis buffer. Finally, we loaded a higher volume of sample onto the acrylamide gel, using 35µl of sample instead of the usual 10µl or 15µl of sample. Despite these troubleshooting attempts, a conclusive result could not be gained. CIP treatment was also used as opposed to SAP treatment. Whilst bands were seen on a Western blot while using CIP instead of SAP, there was no apparent difference between the sample treated with CIP and the sample not treated with CIP. This experiment was also only performed once due to time constraints, so again, this result is not conclusive.

Using a nucleosome pull-down assay, the study by Kawaguchi et al., (2017) also found that the phosphorylation of CBX2 is essential to facilitate the translocation of CBX2 to the nucleus. This again emphasises the importance of phosphorylation of CBX2 in the activity of CBX2. In this study, we found that CBX2 at 72kDa is found in the nuclear fraction which supports these findings. The fractionation was not always 100% efficient as seen with a small amount of alpha tubulin present in the nuclear fraction. This may have been as a result of pipetting error between fractions and could potentially be improved by ensuring all of one fraction is removed before continuing. In future it might also be useful to probe the membranes for a specific nuclear marker. In a future study, a marker such as PARP for the nuclear fraction could be used.

5.2 CBX2 knockdown affects levels of global histone modifications

Following the phosphorylation experiments, it was important to investigate the effect of CBX2 knockdown on the level of global histone modifications. The phosphorylated form of CBX2, upon translocation to the nucleus, reads the H3K27me3 mark as added by the PRC2 complex. Once read, CBX2 induces the PRC1 complex to monoubiquitinate H2AK119 (Jin et al., 2011). Study of the effect of CBX2 on these global histone modifications would indicate whether CBX2 is functional in these cells.

In this study, upon probing membranes using a H2AK119ub-specific antibody, the level of H2AK119ub decreased in the cells transfected with siCBX2-4 in MDA-MB-231 cells but not siCBX2-1 and siCBX2-3 compared with a H2APan loading control. It should be noted that the H2Apan levels were not equal for the siCBX2-4 lysate so this result is not conclusive. Reduction in H2AK119ub following CBX2 knockdown may indicate functional

CBX2 as if there is less CBX2 present, the PRC1 complex will not be recruited to monoubiquitinate H2AK119 as frequently. We know that siCBX2-1 does not knock down *CBX2* mRNA as efficiently and effectively as siCBX2-3 and siCBX2-4 (as shown by qPCR analysis) therefore the lack of effect on H2AK119ub by this siRNA may be reflective of this. Only siCBX2-4 has an effect on H2AK119ub in HS-578T cells. Again, siCBX2-4 is the most efficient siRNA at knocking down *CBX2* mRNA so the effect on HS-578T H2AK119ub may be reflective of this.

Upon probing membranes for an H3K27me3-specific antibody, there was little change in the level of H3K27me3 seen. This may be an expected result considering that CBX2 recognises the mark and does not modify this mark. This was seen in both TNBC cell lines.

H3K27ac-specific antibodies were also used as this is a transcriptionally activating mark which occurs on the same lysine residue as the H3K27me3. Interestingly, in MDA-MB-231 cells, the level of H3K27ac decreased only in the lysate for the cells transfected with siCBX2-4, and remained equal in the cells transfected with siCBX2-1 and siCBX2-3 compared to the H3Pan loading control. In HS-578T cells, the level of H3K27ac decreased in all CBX2-targeted conditions, siCBX2-1, siCBX2-3 and siCBX2-4 compared to the H3Pan loading control. This result is not necessarily expected as when CBX2 is knocked down the expected result may be a higher level of transcriptionally active marks. It may be that CBX2 could be affecting expression of either a HAT or a HDAC that affects the H3K27ac modification, but further investigation is needed to accurately determine why this result is seen.

5.3 CBX2 knockdown reduces TNBC cell growth and viability

In this study, we have investigated the role of CBX2 in promoting proliferation. In order to do this, we first performed an MTS assay in MDA-MB-231 and HS-578T TNBC cell lines. The plates were set up allowing for a border of media to prevent evaporation to ensure all cells were under the same growth conditions. Cells underwent a reverse transfection with either a control siRNA or CBX2-targeting siRNA. A non-transfected condition was included in these experiments to ensure that any results seen were not as a result of the transfection procedure. siCBX2-1 was not used in these experiments due to the fact that the CBX2 knockdown using this siRNA was not as effective as with the other CBX2-targeting siRNAs. In MDA-MB-231 cells, after 48 hours, the cells transfected with siCBX2-

3 and siCBX2-4 grew slower whereas the non-transfected cells and cells transfected with siSCR continued to grow, although the difference was not significant. This is suggestive that CBX2 promotes growth and proliferation. The same experiment was performed using HS-578T cells and the cells transfected with siSCR were only growing slightly more than the cells with CBX2 knocked down indicating that the transfection process may have caused a decrease in growth. In the future, a forward transfection could be used with HS-578T cells instead to account for this issue.

Neither of these cell lines produced significant results with regard to proliferation, so next, phase contrast microscopy was used to observe the effect of CBX2 knockdown on growth of TNBC cells. In these images, it can be observed that there is a far larger difference between the cells transfected with siSCR and the cells transfected with the CBX2-targeting siRNAs, although this has not been quantified. The size and shape of the cells changes with the cells becoming more rounded and larger when CBX2 is knocked down, and the observation of floating cells is much higher in these cells. The growth appears to be greatly reduced in the cells transfected with the CBX2-targeting siRNAs indicating that perhaps the results seen with the MTS assay do not accurately represent the growth changes following CBX2 knockdown. In the future, other assays could be used to attempt to show the effect of CBX2 knockdown on cell growth in a more representative manner. Methods which could be used are a luminescent ATP assay or a Ki67 assay to measure cell viability and proliferation.

Just prior to writing up this thesis, Zheng et al., (2019) reported that CBX2 is significantly overexpressed in breast cancer, supporting other studies showing the same (Chen et al., (2017), Mao et al., (2019). The study also showed that CBX2 is required for TNBC cell proliferation *in vitro* and *in vivo* and that this is via the promotion of the PI3K-AKT signalling pathway. They showed this using MDA-MB-231 TNBC cells and performed a CCK-8 cell viability assay. The results indicated that CBX2 knockdown significantly reduced proliferation in this cell line. In addition, an EDU live cell proliferation assay showed that CBX2 knockdown decreased the growth of BC cells. They investigated the role of CBX2 in the PI3K-AKT signalling pathway and found that the PI3K-AKT pathway functions downstream of CBX2, and found a correlation between CBX2 expression and the expression of members of the PI3K-AKT signalling pathway; PIK3CA, PIK3CD and AKT. They also found that there was a significant positive correlation between the expression

of CBX2 and the activation of the PI3K-AKT signalling pathway (Zheng et al., 2019). This therefore supports our findings, however, the study by Zheng et al (2019) only used a single shRNA sequence whereas we used multiple siRNAs which may produce more reliable results. We used multiple siRNAs all targeted at CBX2 to ensure that any effects that we saw were not due to off target effects. This may, therefore, have been more reliable than using only one shRNA as used in the aforementioned study. In addition to this, the study showed CBX2 at 56kDa which we do not believe to be the active form of CBX2.

We also investigated the effect of CBX2 on cell viability via apoptosis assays. There is data suggesting that CBX2 knockdown could induce apoptosis in other cell lines including hepatocellular carcinoma cell lines Huh7, Bel-7402, Bel7402/5FU, Hep3B, SK-Hep-1, and 97-H. Mao et al., (2019) showed that in hepatocellular carcinoma cell lines Huh7 and Bel-7402, CBX2 knockdown induced apoptosis. Clermont et al., (2016) also showed that CBX2 plays a role in apoptosis. The study focussed on prostate cancer and showed that, in LNCaP and C4-2 cell lines, upon CBX2 knockdown, caspase-3-mediated apoptosis was induced. In this study, we used MDA-MB-231 cells and upon Western blot analysis and probed the membrane with an apoptosis antibody cocktail. This showed that the level of cleaved PARP increased in cells transfected with siCBX2-3 and siCBX2-4 after 48 hours and mainly after 72 hours. PARP is cleaved during apoptosis by caspase 3, meaning that cleaved PARP is a good marker of apoptosis (Boulares et al., 1999). We consistently observed that siCBX2-1 was not as efficient at knocking down *CBX2* mRNA, and this could explain why a lower amount of cleaved PARP was observed in the cell lysates from those cells transfected with siCBX2-1. This indicates that CBX2 knockdown may induce apoptosis, but this needs to be investigated further in other TNBC cell lines due to lack of independent repeats as a result of time constraints.

MCF-10A, a non-tumorigenic, non-transformed cell line was also used to determine the effect of CBX2 knockdown in “normal” breast epithelial cells. This is important because if CBX2 knockdown caused apoptosis or a reduction in proliferation or viability in a non-tumorigenic cell line it may affect its potential use as a therapy for TNBC tumours. In this study, we observed a decrease in the growth and proliferation of MCF-10A cells following CBX2 knockdown. MTS analysis was performed on this cell line and showed a decrease in growth of cells transfected with siCBX2-3 and siCBX2-4 over a period of 96

hours. Interestingly, there was also a decrease in cell viability in the siSCR cells, which could suggest that the decrease in cell viability was not due to CBX2 knockdown alone, but also due to the transfection process. In the future, a forward transfection could be performed on these cells to allow 24 hours of growth prior to transfection, giving a potentially more reliable result. Whilst this result was not significant, the effect of CBX2 knockdown on these cells was again more obvious in phase-contrast microscopy images. Images show that cells transfected with siCBX2-3 and siCBX2-4 were rounder, and there were more floating cells present in these conditions. Finally, cell counts were performed on MCF-10A cells, and showed a decrease in the amount of cells transfected with siCBX2-3 and siCBX2-4 after 72 hours. This could suggest that CBX2 as a therapy would not be viable due to the effect seen on non-tumorigenic cells, and not just on TNBC cells. However, the MCF-10A cell line is not a fully representative normal breast epithelial cell line as it is immortalised and has therefore undergone mutation. This means that any results gained may not be transferrable to the healthy cells as seen *in vivo*. In addition to this, only one non-tumorigenic cell line was used in this study meaning that these results are not conclusive, and may not apply to all non-tumorigenic cell lines. Further investigation is therefore required into this area. In the future, other non-tumorigenic cell lines could be used to increase reliability. In addition to this, analysis of *ex vivo* patient samples could be performed as this would be more reflective of *in vivo* tissues.

5.4 CBX2-regulated transcriptomic profile

We hypothesised that CBX2 could be causing a reduction in cell proliferation or causing cell death and next wanted to investigate whether this could have been through regulation of cell cycle regulatory genes. We therefore analysed changes in *CDK1, CDK4, CCND1, CCND3* and *CCNA2* gene expression following CBX2 knockdown due to their involvement in the cell cycle. Cyclins (CCND1 and CCND3) control the progression of cells through the cell cycle, and complex with cyclin dependent kinases (CDK1 and CDK4) to facilitate this. CCNA2 is involved in both the G1-S progression through the cell cycle and the G2-M progression (Mende et al., 2015).

Upon CBX2 knockdown, the expression of *CCND1, CCND3, CDK1, CDK4* and *CCNA2* decreased in MDA-MB-231 TNBC cells. Cyclins form complexes with cyclin-dependent kinases. An example of this is when *CCND1* forms a complex with CDK4 and facilitates the G1 to S transition in the cell cycle (Mende et al., 2015). When CCND1 expression

decreased following CBX2 knockdown it could reduce the association of CCND1 with CDK4. In addition the *CDK4* expression also decreased meaning that the cells could not progress through the cell cycle. CCND3 also complexes with CDK4 and is also required for G1-S transition. CCNA2 forms complexes with CDK1 facilitating progression through both the G1-S phase of the cell cycle and progression through the G2-M phase of the cell cycle (Pagano et al., 1992). If CCNA2 expression is reduced, these complexes may not form meaning the cells may not progress through the cell cycle. In summary, the reduction of a number of crucial cell cycle regulatory genes following CBX2 knockdown correlates with phenotypic observations that knockdown reduces cell growth and increases cell death.

In order to determine the global CBX2-regulated transcriptome, RNA samples of MDA-MB-231 cells transfected with siSCR, siCBX2-3 and siCBX2-4 were sent to Novogene™ for sequencing. This was done to analyse the effect CBX2 has on gene expression, along with the role of CBX2 in regulating different signalling pathways. The analysis was received shortly before the end of this project, and therefore only the initial analysis between siSCR and siCBX2-3 transfected cells has been reported here. There were 4864 genes upregulated and 1986 genes downregulated following CBX2 knockdown in comparison with siSCR-transfected cells. This pattern of differential gene expression may correspond with the fact that CBX2 is a transcriptional repressor, therefore it is understandable that there would be more genes upregulated upon CBX2 knockdown. Of the top 20 pathways identified to be enriched for genes differentially regulated by CBX2 knockdown in the RNA-seq analysis, the signalling pathways of interest were 'Pathways in Cancer', 'PI3K-AKT signalling pathway', 'mTOR signalling pathway' and 'Cell Cycle'. As some of these differentially expressed genes were found to be involved in the cell cycle, this supports the qPCR and phenotypic data gained in this study.

Further oncogenic signalling pathways of interest are the PI3K-AKT signalling pathway and the mTOR signalling pathway, which form the PI3K/AKT/mTOR signalling cascade (Yu and Cui, 2016). The PI3K/AKT/mTOR signalling cascade regulates cell proliferation, survival, angiogenesis and metabolism (Yu and Cui, 2016). This is facilitated by the phosphorylation of serines and/or threonines on downstream substrates (Ardito et al., 2017). The tumour suppressor gene *PTEN* is a negative regulator of this signalling pathway and *PTEN* is usually downregulated in cancer. Our RNA-seq data has indicated

that PTEN expression is upregulated when CBX2 is knocked down suggesting that CBX2 may be a repressor of this TSG. This is a potentially important and novel finding which could suggest how CBX2 promotes PI3K-AKT signalling as identified in other studies and in other cancers (Clermont et al., 2016 and Zheng et al., 2019). Our RNA-seq data suggests that CBX2 has a role in the PI3K-AKT signalling pathway and this is supported by a recent study performed by Zheng et al (2019). They showed that CBX2 regulates the PI3K-AKT signalling pathway as when CBX2 was expressed, the expression of PIK3CA, PIK3CD and AKT increased, along with a significant positive correlation between the expression of CBX2 and the activation of the PI3K-AKT signalling pathway. In addition to this, Clermont et al., (2016) found that CBX2 promotes the activation of the PI3K-AKT signalling pathway, and that CBX2 represses the transcription of PIK3R1 and INP55A which are PI3K antagonists. This allows activation of the PI3K-AKT signalling pathway and therefore promotes proliferation and metastasis. They found that when CBX2 was knocked down, the expression of PIK3R1 and INP55A increased, potentially inhibiting the PI3K-AKT signalling pathway and therefore slowing growth and metastasis indicating the possible role of CBX2 in the PI3K-AKT signalling pathway. A direct role for CBX2 in regulating these genes was not however established.

mTOR is involved in two complexes; mTORC1 and mTORC2. mTORC1 is responsible for the regulation of cell growth while mTORC2 is responsible for cell survival and proliferation (Saxton and Sabatini, 2017). mTORC2 controls survival and proliferation by phosphorylating and activating AKT. In turn, this phosphorylates and inhibits several upstream components in the mTORC1 pathway. One of these is TSC2, which is a negative regulator of mTORC1. Upstream of mTORC1, AMPK phosphorylates and activates TSC2 which in turn inhibits mTORC1 (Saxton and Sabatini, 2017). When these TSGs are downregulated, such as in cancer, the mTORC1 signalling pathway can facilitate more unrestricted cell growth, proliferation and survival (Popúlo et al., 2012). Upon CBX2 knockdown, the expression of AMPK, TSC1 and TSC2 are upregulated. This indicates that CBX2 may be regulating the expression of these TSGs and indicates a possible reason for the decrease in cell growth and proliferation observed on CBX2 knockdown through phenotypic and proliferative assays.

6. Conclusion and future prospects

In conclusion, this study has found that CBX2 is involved in many cellular processes especially those regulating cell growth and proliferation. This study has also identified that CBX2 is a regulator of several critical cell cycle regulatory genes highlighting the importance of targeting CBX2 to reduce tumour cell growth and progression through the cell cycle. Importantly, the aims of this study were completed, and as a result of this, further areas of research surrounding CBX2 have been identified.

It is important to further validate CBX2 as a therapeutic target for TNBC. Firstly, some experiments performed in this study should be repeated. This could include the dephosphorylation experiments using CIP to attempt to gain a more conclusive result. A higher cell density could also be used to ensure a clear result as the bands were faint in this study. The remaining RNA-Seq data will be analysed and validated using additional siRNAs targeted to CBX2 along with alternative and additional TNBC cell lines. In addition to this, chromatin immunoprecipitation (ChIP) should be performed to determine the localisation of CBX2 and therefore determine which genes identified by RNA-seq are directly regulated by CBX2 and the PRC1 complex. This analysis can be done at specific genomic loci, or ideally, globally by ChIP-sequencing analysis. Another area needing further investigation would be the role of CBX2 in “normal” breast epithelial cells. To do this, more non-transformed cell lines would be used and the protein and mRNA levels of CBX2 would be tested using western blotting and qPCR. *Ex vivo* tissues could also be used as a more reliable model to investigate the role of CBX2 in TNBC and non-transformed cells. One way of using *ex vivo* tissues is to use microfluidic chips. This would allow cell growth of real patient tissue to be analysed and could be a useful method of comparison between TNBC and non-transformed cells. This is important to determine the suitability of CBX2 as a therapeutic target in TNBC cells, as if CBX2 knockdown does not impact proliferation, growth or viability in non-transformed “normal” cells, there is more of a chance that CBX2 could be therapeutically targeted.

7. References

Abramson, V.G., Mayer, I.A., 2014. Molecular Heterogeneity of Triple Negative Breast Cancer. Curr Breast Cancer Rep 6, 154–158. https://doi.org/10.1007/s12609-014-0152-1

acs.jmedchem.pdf, n.d.

Alexander, S., Fabbro, D., Kelly, E., Marrion, N., Peters, J., Faccenda, E., Harding, S., Pawson, A., Sharman, J., Southan, C., Davies, J., n.d. Chromatin modifying enzymes | Enzymes | IUPHAR/BPS Guide to PHARMACOLOGY [WWW Document]. URL http://www.guidetopharmacology.org/GRAC/FamilyDisplayForward?familyId=865 (accessed 11.21.18).

Alluri, P., Newman, L., 2014. Basal-like and Triple Negative Breast Cancers: Searching For Positives Among Many Negatives. Surg Oncol Clin N Am 23, 567–577. https://doi.org/10.1016/j.soc.2014.03.003

Aloia, L., Di Stefano, B., Di Croce, L., 2013. Polycomb complexes in stem cells and embryonic development. Development 140, 2525–2534. https://doi.org/10.1242/dev.091553

Anderson, W.F., Rosenberg, P.S., Prat, A., Perou, C.M., Sherman, M.E., 2014. How many etiological subtypes of breast cancer: two, three, four, or more? J. Natl. Cancer Inst. 106. https://doi.org/10.1093/jnci/dju165

Anti-CBX2 antibody (ab80044) | Abcam [WWW Document], n.d. URL https://www.abcam.com/cbx2-antibody-ab80044.html (accessed 9.3.19).

Ardito, F., Giuliani, M., Perrone, D., Troiano, G., Muzio, L.L., 2017. The crucial role of protein phosphorylation in cell signaling and its use as targeted therapy (Review). Int J Mol Med 40, 271–280. https://doi.org/10.3892/ijmm.2017.3036

Arnould, L., Gelly, M., Penault-Llorca, F., Benoit, L., Bonnetain, F., Migeon, C., Cabaret, V., Fermeaux, V., Bertheau, P., Garnier, J., Jeannin, J.-F., Coudert, B., 2006. Trastuzumab-based treatment of HER2-positive breast cancer: an antibody-dependent cellular cytotoxicity mechanism? Br J Cancer 94, 259–267. https://doi.org/10.1038/sj.bjc.6602930

Audia, J.E., Campbell, R.M., 2016. Histone Modifications and Cancer. Cold Spring Harb Perspect Biol 8, a019521. https://doi.org/10.1101/cshperspect.a019521

Baldan, F., Allegri, L., Lazarevic, M., Catia, M., Milosevic, M., Damante, G., Milasin, J., 2019. Biological and molecular effects of bromodomain and extra-terminal (BET) inhibitors JQ1, IBET-151, and IBET-762 in OSCC cells. Journal of Oral Pathology & Medicine 48, 214–221. https://doi.org/10.1111/jop.12824

Bannister, A.J., Kouzarides, T., 2011. Regulation of chromatin by histone modifications. Cell Res 21, 381–395. https://doi.org/10.1038/cr.2011.22

Barski, A., Cuddapah, S., Cui, K., Roh, T.-Y., Schones, D.E., Wang, Z., Wei, G., Chepelev, I., Zhao, K., 2007. High-Resolution Profiling of Histone Methylations in the Human Genome. Cell 129, 823–837. https://doi.org/10.1016/j.cell.2007.05.009

Béguelin, W., Rivas, M.A., Calvo Fernández, M.T., Teater, M., Purwada, A., Redmond, D., Shen, H., Challman, M.F., Elemento, O., Singh, A., Melnick, A.M., 2017. EZH2 enables germinal centre formation through epigenetic silencing of CDKN1A and an Rb-E2F1 feedback loop. Nat Commun 8. https://doi.org/10.1038/s41467-017-01029-x

Berrocal, J.K., Chagpar, A.B., 2017. Current Approaches to Triple-Negative Breast Cancer. American Journal of Hematology / Oncology® 13.

Biswas, S., Rao, C.M., 2018. Epigenetic tools (The Writers, The Readers and The Erasers) and their implications in cancer therapy. European Journal of Pharmacology 837, 8–24. https://doi.org/10.1016/j.ejphar.2018.08.021

Boulares, A.H., Yakovlev, A.G., Ivanova, V., Stoica, B.A., Wang, G., Iyer, S., Smulson, M., 1999. Role of Poly(ADP-ribose) Polymerase (PARP) Cleavage in Apoptosis CASPASE 3-RESISTANT PARP MUTANT INCREASES RATES OF APOPTOSIS IN TRANSFECTED CELLS. J. Biol. Chem. 274, 22932–22940. https://doi.org/10.1074/jbc.274.33.22932

Bowman, G.D., Poirier, M.G., 2015. Post-Translational Modifications of Histones That Influence Nucleosome Dynamics. Chem Rev 115, 2274–2295. https://doi.org/10.1021/cr500350x

Bracken, A.P., Pasini, D., Capra, M., Prosperini, E., Colli, E., Helin, K., 2003. EZH2 is downstream of the pRB-E2F pathway, essential for proliferation and amplified in cancer. EMBO J. 22, 5323–5335. https://doi.org/10.1093/emboj/cdg542

Brd4 activates P-TEFb for RNA polymerase II CTD phosphorylation [WWW Document], n.d. URL https://www.ncbi.nlm.nih.gov/pmc/articles/PMC4081074/ (accessed 5.2.19).

Bulut, N., Altundag, K., 2015. Does estrogen receptor determination affect prognosis in early stage breast cancers? Int J Clin Exp Med 8, 21454–21459.

Burstein, M.D., Tsimelzon, A., Poage, G.M., Covington, K.R., Contreras, A., Fuqua, S.A.W., Savage, M.I., Osborne, C.K., Hilsenbeck, S.G., Chang, J.C., Mills, G.B., Lau, C.C., Brown, P.H., 2015. Comprehensive Genomic Analysis Identifies Novel Subtypes and Targets of Triple-negative Breast Cancer. Clin Cancer Res 21, 1688–1698. https://doi.org/10.1158/1078-0432.CCR-14-0432

Cancer mortality for common cancers [WWW Document], 2015. . Cancer Research UK. URL https://www.cancerresearchuk.org/health-professional/cancer-statistics/mortality/common-cancers-compared (accessed 8.13.19).

Cancer Risk Factors | SEER Training [WWW Document], n.d. URL https://training.seer.cancer.gov/disease/cancer/risk.html (accessed 11.21.18).

Cao, J., Yan, Q., 2012. Histone Ubiquitination and Deubiquitination in Transcription, DNA Damage Response, and Cancer. Front Oncol 2. https://doi.org/10.3389/fonc.2012.00026

Cao, R., Tsukada, Y.-I., Zhang, Y., 2005. Role of Bmi-1 and Ring1A in H2A ubiquitylation and Hox gene silencing. Mol. Cell 20, 845–854. https://doi.org/10.1016/j.molcel.2005.12.002

Carter, P., Presta, L., Gorman, C.M., Ridgway, J.B., Henner, D., Wong, W.L., Rowland, A.M., Kotts, C., Carver, M.E., Shepard, H.M., 1992. Humanization of an anti-p185HER2 antibody for human cancer therapy. Proc. Natl. Acad. Sci. U.S.A. 89, 4285–4289. https://doi.org/10.1073/pnas.89.10.4285

CBX2 - Chromobox protein homolog 2 - Homo sapiens (Human) - CBX2 gene & protein [WWW Document], n.d. URL https://www.uniprot.org/uniprot/Q14781 (accessed 9.3.19).

Chan, H.L., Beckedorff, F., Zhang, Y., Garcia-Huidobro, J., Jiang, H., Colaprico, A., Bilbao, D., Figueroa, M.E., LaCava, J., Shiekhattar, R., Morey, L., 2018. Polycomb complexes associate with enhancers and promote oncogenic transcriptional programs in cancer

through multiple mechanisms. Nat Commun 9, 1–16. https://doi.org/10.1038/s41467-018-05728-x

Cheang, M.C.U., Chia, S.K., Voduc, D., Gao, D., Leung, S., Snider, J., Watson, M., Davies, S., Bernard, P.S., Parker, J.S., Perou, C.M., Ellis, M.J., Nielsen, T.O., 2009. Ki67 Index, HER2 Status, and Prognosis of Patients With Luminal B Breast Cancer. J Natl Cancer Inst 101, 736–750. https://doi.org/10.1093/jnci/djp082

Chen, G., Subedi, K., Chakraborty, S., Sharov, A., Lu, J., Kim, J., Mi, X., Wersto, R., Sung, M.-H., Weng, N.-P., 2018. Ezh2 Regulates Activation-Induced CD8+ T Cell Cycle Progression via Repressing Cdkn2a and Cdkn1c Expression. Front Immunol 9, 549. https://doi.org/10.3389/fimmu.2018.00549

Chen, W.Y., Zhang, X.Y., Liu, T., Liu, Y., Zhao, Y.S., Pang, D., 2017. Chromobox homolog 2 protein: A novel biomarker for predicting prognosis and Taxol sensitivity in patients with breast cancer. Oncol Lett 13, 1149–1156. https://doi.org/10.3892/ol.2016.5529

Chow, A., n.d. Cell Cycle Control, Oncogenes, Tumor Suppressors | Learn Science at Scitable [WWW Document]. URL https://www.nature.com/scitable/topicpage/cell-cycle-control-by-oncogenes-and-tumor-14191459/ (accessed 9.24.19).

Clermont, P.-L., Crea, F., Chiang, Y.T., Lin, D., Zhang, A., Wang, J.Z.L., Parolia, A., Wu, R., Xue, H., Wang, Yuwei, Ding, J., Thu, K.L., Lam, W.L., Shah, S.P., Collins, C.C., Wang, Yuzhuo, Helgason, C.D., 2016. Identification of the epigenetic reader CBX2 as a potential drug target in advanced prostate cancer. Clin Epigenetics 8. https://doi.org/10.1186/s13148-016-0182-9

Clermont, P.-L., Sun, L., Crea, F., Thu, K.L., Zhang, A., Parolia, A., Lam, W.L., Helgason, C.D., 2014. Genotranscriptomic meta-analysis of the Polycomb gene CBX2 in human cancers: initial evidence of an oncogenic role. Br J Cancer 111, 1663–1672. https://doi.org/10.1038/bjc.2014.474

Clynes, R.A., Towers, T.L., Presta, L.G., Ravetch, J.V., 2000. Inhibitory Fc receptors modulate in vivo cytoxicity against tumor targets. Nature Medicine 6, 443. https://doi.org/10.1038/74704

Conway, E.M., Bracken, A.P., 2017. Chapter 4 - Unraveling the Roles of Canonical and Noncanonical PRC1 Complexes, in: Pirrotta, V. (Ed.), Polycomb Group Proteins. Academic Press, pp. 57–80. https://doi.org/10.1016/B978-0-12-809737-3.00004-0

Dai, X., Li, T., Bai, Z., Yang, Y., Liu, X., Zhan, J., Shi, B., 2015. Breast cancer intrinsic subtype classification, clinical use and future trends. Am J Cancer Res 5, 2929–2943.

Dikic, I., Robertson, M., 2012. Ubiquitin ligases and beyond. BMC Biology 10, 22. https://doi.org/10.1186/1741-7007-10-22

Donati, B., Lorenzini, E., Ciarrocchi, A., 2018. BRD4 and Cancer: going beyond transcriptional regulation. Molecular Cancer 17, 164. https://doi.org/10.1186/s12943-018-0915-9

Egger, G., Liang, G., Aparicio, A., Jones, P.A., 2004. Epigenetics in human disease and prospects for epigenetic therapy. Nature 429, 457–463. https://doi.org/10.1038/nature02625

Feher, J., 2012. 2.8 - Cell Signaling, in: Feher, J. (Ed.), Quantitative Human Physiology. Academic Press, Boston, pp. 158–170. https://doi.org/10.1016/B978-0-12-382163-8.00019-0

Feinberg, A.P., Vogelstein, B., 1983. Hypomethylation distinguishes genes of some human cancers from their normal counterparts. Nature 301, 89–92. https://doi.org/10.1038/301089a0

Genotranscriptomic meta-analysis of the Polycomb gene CBX2 in human cancers: initial evidence of an oncogenic role [WWW Document], n.d. URL https://www.ncbi.nlm.nih.gov/pmc/articles/PMC4200100/ (accessed 11.21.18).

Gil, J., O'Loghlen, A., 2014. PRC1 complex diversity: where is it taking us? Trends in Cell Biology 24, 632–641. https://doi.org/10.1016/j.tcb.2014.06.005

Grau, D.J., Chapman, B.A., Garlick, J.D., Borowsky, M., Francis, N.J., Kingston, R.E., 2011. Compaction of chromatin by diverse Polycomb group proteins requires localized regions of high charge. Genes Dev 25, 2210–2221. https://doi.org/10.1101/gad.17288211

Greer, E.L., Shi, Y., 2012. Histone methylation: a dynamic mark in health, disease and inheritance. Nature Reviews Genetics 13, 343–357. https://doi.org/10.1038/nrg3173

Guo, X., Shi, M., Sun, L., Wang, Y., Gui, Y., Cai, Z., Duan, X., 2011. The expression of histone demethylase JMJD1A in renal cell carcinoma. Neoplasma 58, 153–157.

Gutierrez, C., Schiff, R., 2011. HER 2: Biology, Detection, and Clinical Implications. Arch Pathol Lab Med 135, 55–62. https://doi.org/10.1043/2010-0454-RAR.1

Hałasa, M., Wawruszak, A., Przybyszewska, A., Jaruga, A., Guz, M., Kałafut, J., Stepulak, A., Cybulski, M., 2019. H3K18Ac as a Marker of Cancer Progression and Potential Target of Anti-Cancer Therapy. Cells 8. https://doi.org/10.3390/cells8050485

Hatano, A., Matsumoto, M., Higashinakagawa, T., Nakayama, K.I., 2010. Phosphorylation of the chromodomain changes the binding specificity of Cbx2 for methylated histone H3. Biochem. Biophys. Res. Commun. 397, 93–99. https://doi.org/10.1016/j.bbrc.2010.05.074

Hergeth, S.P., Schneider, R., 2015. The H1 linker histones: multifunctional proteins beyond the nucleosomal core particle. EMBO Rep 16, 1439–1453. https://doi.org/10.15252/embr.201540749

Hon, J.D.C., Singh, B., Sahin, A., Du, G., Wang, J., Wang, V.Y., Deng, F.-M., Zhang, D.Y., Monaco, M.E., Lee, P., 2016. Breast cancer molecular subtypes: from TNBC to QNBC. Am J Cancer Res 6, 1864–1872.

Is qPCR For You? | An Introduction to qPCR Methods | Promega [WWW Document], n.d. URL https://www.promega.co.uk/resources/pubhub/features/is-qpcr-for-you/ (accessed 6.24.19).

Itzen, F., Greifenberg, A.K., Bösken, C.A., Geyer, M., 2014. Brd4 activates P-TEFb for RNA polymerase II CTD phosphorylation. Nucleic Acids Res 42, 7577–7590. https://doi.org/10.1093/nar/gku449

Jin, B., Li, Y., Robertson, K.D., 2011. DNA Methylation. Genes Cancer 2, 607–617. https://doi.org/10.1177/1947601910393957

Jones, P.A., Baylin, S.B., 2002. The fundamental role of epigenetic events in cancer. Nature Reviews Genetics 3, 415–428. https://doi.org/10.1038/nrg816

Junttila, T.T., Akita, R.W., Parsons, K., Fields, C., Phillips, G.D.L., Friedman, L.S., Sampath, D., Sliwkowski, M.X., 2009. Ligand-Independent HER2/HER3/PI3K Complex Is Disrupted by

Trastuzumab and Is Effectively Inhibited by the PI3K Inhibitor GDC-0941. Cancer Cell 15, 429–440. https://doi.org/10.1016/j.ccr.2009.03.020

Katz, T.A., Huang, Y., Davidson, N.E., Jankowitz, R.C., 2014. Epigenetic reprogramming in breast cancer: From new targets to new therapies. Annals of Medicine 46, 397–408. https://doi.org/10.3109/07853890.2014.923740

Kawaguchi, T., Machida, S., Kurumizaka, H., Tagami, H., Nakayama, J., 2017. Phosphorylation of CBX2 controls its nucleosome-binding specificity. J Biochem 162, 343–355. https://doi.org/10.1093/jb/mvx040

Kawazu, M., Saso, K., Tong, K.I., McQuire, T., Goto, K., Son, D.-O., Wakeham, A., Miyagishi, M., Mak, T.W., Okada, H., 2011. Histone demethylase JMJD2B functions as a co-factor of estrogen receptor in breast cancer proliferation and mammary gland development. PLoS ONE 6, e17830. https://doi.org/10.1371/journal.pone.0017830

Klapper, L.N., Waterman, H., Sela, M., Yarden, Y., 2000. Tumor-inhibitory Antibodies to HER-2/ErbB-2 May Act by Recruiting c-Cbl and Enhancing Ubiquitination of HER-2. Cancer Res 60, 3384–3388.

Kouzarides, T., 2007. Chromatin modifications and their function. Cell 128, 693–705. https://doi.org/10.1016/j.cell.2007.02.005

Kumar, P., Aggarwal, R., 2016. An overview of triple-negative breast cancer. Arch Gynecol Obstet 293, 247–269. https://doi.org/10.1007/s00404-015-3859-y

Lee, E.Y.H.P., Muller, W.J., 2010. Oncogenes and Tumor Suppressor Genes. Cold Spring Harb Perspect Biol 2. https://doi.org/10.1101/cshperspect.a003236

Liang, Y.-K., Lin, H.-Y., Chen, C.-F., Zeng, D., 2017. Prognostic values of distinct CBX family members in breast cancer. Oncotarget 8, 92375–92387. https://doi.org/10.18632/oncotarget.21325

Lim, S., Janzer, A., Becker, A., Zimmer, A., Schüle, R., Buettner, R., Kirfel, J., 2010. Lysine-specific demethylase 1 (LSD1) is highly expressed in ER-negative breast cancers and a biomarker predicting aggressive biology. Carcinogenesis 31, 512–520. https://doi.org/10.1093/carcin/bgp324

Lodish, H., Berk, A., Zipursky, S.L., Matsudaira, P., Baltimore, D., Darnell, J., 2000. Proto-Oncogenes and Tumor-Suppressor Genes. Molecular Cell Biology. 4th edition.

Mandal, A., 2010. What are Oncogenes? [WWW Document]. News-Medical.net. URL https://www.news-medical.net/life-sciences/What-are-Oncogenes.aspx (accessed 11.21.18).

Mao, J., Tian, Y., Wang, C., Jiang, K., Li, R., Yao, Y., Zhang, R., Sun, D., Liang, R., Gao, Z., Wang, Q., Wang, L., 2019. CBX2 Regulates Proliferation and Apoptosis via the Phosphorylation of YAP in Hepatocellular Carcinoma. J. Cancer 10, 2706–2719. https://doi.org/10.7150/jca.31845

Martin, C., Zhang, Y., 2005. The diverse functions of histone lysine methylation. Nature Reviews Molecular Cell Biology 6, 838–849. https://doi.org/10.1038/nrm1761

mda-mb-231-cell-line-profile.pdf, n.d.

Mende, N., Kuchen, E.E., Lesche, M., Grinenko, T., Kokkaliaris, K.D., Hanenberg, H., Lindemann, D., Dahl, A., Platz, A., Höfer, T., Calegari, F., Waskow, C., 2015. CCND1–CDK4–mediated cell cycle progression provides a competitive advantage for human hematopoietic stem cells in vivo. J Exp Med 212, 1171–1183. https://doi.org/10.1084/jem.20150308

Mills, M.N., Yang, G.Q., Oliver, D.E., Liveringhouse, C.L., Ahmed, K.A., Orman, A.G., Laronga, C., Hoover, S.J., Khakpour, N., Costa, R.L.B., Diaz, R., 2018. Histologic heterogeneity of triple negative breast cancer: A National Cancer Centre Database analysis. Eur. J. Cancer 98, 48–58. https://doi.org/10.1016/j.ejca.2018.04.011

Moore, L.D., Le, T., Fan, G., 2013. DNA Methylation and Its Basic Function. Neuropsychopharmacology 38, 23–38. https://doi.org/10.1038/npp.2012.112

MTS Assay Kit (ab197010) | Abcam [WWW Document], n.d. URL https://www.abcam.com/mts-assay-kit-cell-proliferation-colorimetric-ab197010.html (accessed 5.1.19).

Nagata, Y., Lan, K.-H., Zhou, X., Tan, M., Esteva, F.J., Sahin, A.A., Klos, K.S., Li, P., Monia, B.P., Nguyen, N.T., Hortobagyi, G.N., Hung, M.-C., Yu, D., 2004. PTEN activation contributes

to tumor inhibition by trastuzumab, and loss of PTEN predicts trastuzumab resistance in patients. Cancer Cell 6, 117–127. https://doi.org/10.1016/j.ccr.2004.06.022

Negrini, S., Gorgoulis, V.G., Halazonetis, T.D., 2010. Genomic instability — an evolving hallmark of cancer. Nature Reviews Molecular Cell Biology 11, 220–228. https://doi.org/10.1038/nrm2858

Nichol, J.N., Dupéré-Richer, D., Ezponda, T., Licht, J.D., Miller, W.H., 2016. Chapter Three - H3K27 Methylation: A Focal Point of Epigenetic Deregulation in Cancer, in: Tew, K.D., Fisher, P.B. (Eds.), Advances in Cancer Research. Academic Press, pp. 59–95. https://doi.org/10.1016/bs.acr.2016.05.001

Noguchi, K., Shiurba, R., Higashinakagawa, T., 2002. Nuclear Translocation of Mouse Polycomb M33 Protein in Regenerating Liver. Biochemical and Biophysical Research Communications 291, 508–515. https://doi.org/10.1006/bbrc.2002.6480

Orphanides, G., Reinberg, D., 2000. RNA polymerase II elongation through chromatin. Nature 407, 471–476. https://doi.org/10.1038/35035000

Pagano, M., Pepperkok, R., Verde, F., Ansorge, W., Draetta, G., 1992. Cyclin A is required at two points in the human cell cycle. EMBO J. 11, 961–971.

Parris, T., Danielsson, A., Nemes, S., Kovács, A., Delle, U., Fallenius, G., Möllerström, E., Karlsson, P., Helou, K., n.d. Clinical Implications of Gene Dosage and Gene Expression Patterns in Diploid Breast Carcinoma | Clinical Cancer Research [WWW Document]. URL http://clincancerres.aacrjournals.org/content/16/15/3860.long (accessed 11.21.18).

(PDF) Epigenetic Approaches in Neuroblastoma Disease Pathogenesis [WWW Document], n.d. . ResearchGate. URL https://www.researchgate.net/publication/320671837_Epigenetic_Approaches_in_Neuroblastoma_Disease_Pathogenesis (accessed 7.22.19).

Penagarikano, O., Mulle, J.G., Warren, S.T., 2007. The Pathophysiology of Fragile X Syndrome. Annual Review of Genomics and Human Genetics 8, 109–129. https://doi.org/10.1146/annurev.genom.8.080706.092249

PI3K-AKT Signaling Pathway - Creative Diagnostics [WWW Document], n.d. URL https://www.creative-diagnostics.com/PI3K-AKT-Signaling-Pathway.htm (accessed 9.10.19).

Pieterman, C.R.C., Conemans, E.B., Dreijerink, K.M.A., Laat, J.M. de, Timmers, H.T.M., Vriens, M.R., Valk, G.D., 2014. Thoracic and duodenopancreatic neuroendocrine tumors in multiple endocrine neoplasia type 1: natural history and function of menin in tumorigenesis. Endocrine-Related Cancer 21, R121–R142. https://doi.org/10.1530/ERC-13-0482

Piqué, D.G., Montagna, C., Greally, J.M., Mar, J.C., 2019. A novel approach to modelling transcriptional heterogeneity identifies the oncogene candidate CBX2 in invasive breast carcinoma. British Journal of Cancer 120, 746. https://doi.org/10.1038/s41416-019-0387-8

Pópulo, H., Lopes, J.M., Soares, P., 2012. The mTOR Signalling Pathway in Human Cancer. Int J Mol Sci 13, 1886–1918. https://doi.org/10.3390/ijms13021886

Proto-Oncogenes and Tumor-Suppressor Genes - Molecular Cell Biology - NCBI Bookshelf [WWW Document], n.d. URL https://www.ncbi.nlm.nih.gov/books/NBK21662/ (accessed 5.29.19).

Robertson, K.D., 2002. DNA methylation and chromatin – unraveling the tangled web. Oncogene 21, 5361–5379. https://doi.org/10.1038/sj.onc.1205609

Ropero, S., Esteller, M., 2007. The role of histone deacetylases (HDACs) in human cancer. Mol Oncol 1, 19–25. https://doi.org/10.1016/j.molonc.2007.01.001

Russo, J., Russo, I.H., 2006. The role of estrogen in the initiation of breast cancer. J. Steroid Biochem. Mol. Biol. 102, 89–96. https://doi.org/10.1016/j.jsbmb.2006.09.004

Saksouk, N., Simboeck, E., Déjardin, J., 2015. Constitutive heterochromatin formation and transcription in mammals. Epigenetics Chromatin 8. https://doi.org/10.1186/1756-8935-8-3

Santonja, A., Sánchez-Muñoz, A., Lluch, A., Chica-Parrado, M.R., Albanell, J., Chacón, J.I., Antolín, S., Jerez, J.M., de la Haba, J., de Luque, V., Fernández-De Sousa, C.E., Vicioso, L., Plata, Y., Ramírez-Tortosa, C.L., Álvarez, M., Llácer, C., Zarcos-Pedrinaci, I., Carrasco, E.,

Caballero, R., Martín, M., Alba, E., 2018. Triple negative breast cancer subtypes and pathologic complete response rate to neoadjuvant chemotherapy. Oncotarget 9, 26406–26416. https://doi.org/10.18632/oncotarget.25413

Saraiva, D.P., Cabral, M.G., Jacinto, A., Braga, S., 2017. How many diseases is triple negative breast cancer: the protagonism of the immune microenvironment. ESMO Open 2, e000208. https://doi.org/10.1136/esmoopen-2017-000208

Saxton, R.A., Sabatini, D.M., 2017. mTOR Signaling in Growth, Metabolism, and Disease. Cell 168, 960–976. https://doi.org/10.1016/j.cell.2017.02.004

Seligson, D.B., Horvath, S., Shi, T., Yu, H., Tze, S., Grunstein, M., Kurdistani, S.K., 2005. Global histone modification patterns predict risk of prostate cancer recurrence. Nature 435, 1262–1266. https://doi.org/10.1038/nature03672

Shagufta, Ahmad, I., 2018. Tamoxifen a pioneering drug: An update on the therapeutic potential of tamoxifen derivatives. European Journal of Medicinal Chemistry 143, 515–531. https://doi.org/10.1016/j.ejmech.2017.11.056

Shu, S., Lin, C.Y., He, H.H., Witwicki, R.M., Tabassum, D.P., Roberts, J.M., Janiszewska, M., Huh, S.J., Liang, Y., Ryan, J., Doherty, E., Mohammed, H., Guo, H., Stover, D.G., Ekram, M.B., Brown, J., D'Santos, C., Krop, I.E., Dillon, D., McKeown, M., Ott, C., Qi, J., Ni, M., Rao, P.K., Duarte, M., Wu, S.-Y., Chiang, C.-M., Anders, L., Young, R.A., Winer, E., Letai, A., Barry, W.T., Carroll, J.S., Long, H., Brown, M., Liu, X.S., Meyer, C.A., Bradner, J.E., Polyak, K., 2016. Response and resistance to BET bromodomain inhibitors in triple negative breast cancer. Nature 529, 413–417. https://doi.org/10.1038/nature16508

Sørlie, T., Perou, C.M., Tibshirani, R., Aas, T., Geisler, S., Johnsen, H., Hastie, T., Eisen, M.B., van de Rijn, M., Jeffrey, S.S., Thorsen, T., Quist, H., Matese, J.C., Brown, P.O., Botstein, D., Lønning, P.E., Børresen-Dale, A.-L., 2001. Gene expression patterns of breast carcinomas distinguish tumor subclasses with clinical implications. Proc Natl Acad Sci U S A 98, 10869–10874. https://doi.org/10.1073/pnas.191367098

Stuckey, J.I., Dickson, B.M., Cheng, N., Liu, Y., Norris, J.L., Cholensky, S.H., Tempel, W., Qin, S., Huber, K.G., Sagum, C., Black, K., Li, F., Huang, X.-P., Roth, B.L., Baughman, B.M., Senisterra, G., Pattenden, S.G., Vedadi, M., Brown, P.J., Bedford, M.T., Min, J., Arrowsmith, C.H., James, L.I., Frye, S.V., 2016. A cellular chemical probe targeting the

chromodomains of Polycomb repressive complex 1. Nat. Chem. Biol. 12, 180–187. https://doi.org/10.1038/nchembio.2007

TechNote: What are the differences between PCR, RT-PCR, qPCR, and RT-qPCR? [WWW Document], n.d. URL http://www.enzolifesciences.com/science-center/technotes/2017/march/what-are-the-differences-between-pcr-rt-pcr-qpcr-and-rt-qpcr?/ (accessed 6.24.19).

Tumor Suppressor Genes - The Cell - NCBI Bookshelf [WWW Document], n.d. URL https://www.ncbi.nlm.nih.gov/books/NBK9894/ (accessed 5.29.19).

Turashvili, G., Brogi, E., 2017. Tumor Heterogeneity in Breast Cancer. Front Med (Lausanne) 4. https://doi.org/10.3389/fmed.2017.00227

Uemura, M., Yamamoto, H., Takemasa, I., Mimori, K., Hemmi, H., Mizushima, T., Ikeda, M., Sekimoto, M., Matsuura, N., Doki, Y., Mori, M., 2010. Jumonji domain containing 1A is a novel prognostic marker for colorectal cancer: in vivo identification from hypoxic tumor cells. Clin. Cancer Res. 16, 4636–4646. https://doi.org/10.1158/1078-0432.CCR-10-0407

Vidal, M., 2009. Role of polycomb proteins Ring1A and Ring1B in the epigenetic regulation of gene expression. Int. J. Dev. Biol. 53, 355–370. https://doi.org/10.1387/ijdb.082690mv

Vu, T., Claret, F.X., 2012. Trastuzumab: Updated Mechanisms of Action and Resistance in Breast Cancer. Front Oncol 2. https://doi.org/10.3389/fonc.2012.00062

Wang, H.-Y., Long, Q.-Y., Tang, S.-B., Xiao, Q., Gao, C., Zhao, Q.-Y., Li, Q.-L., Ye, M., Zhang, L., Li, L.-Y., Wu, M., 2019. Histone demethylase KDM3A is required for enhancer activation of hippo target genes in colorectal cancer. Nucleic Acids Res 47, 2349–2364. https://doi.org/10.1093/nar/gky1317

Weaver, I.C.G., Korgan, A.C., Lee, K., Wheeler, R.V., Hundert, A.S., Goguen, D., 2017. Stress and the Emerging Roles of Chromatin Remodeling in Signal Integration and Stable Transmission of Reversible Phenotypes. Front. Behav. Neurosci. 11. https://doi.org/10.3389/fnbeh.2017.00041

Wen, X., Klionsky, D.J., 2017. BRD4 is a newly characterized transcriptional regulator that represses autophagy and lysosomal function. Autophagy 13, 1801–1803. https://doi.org/10.1080/15548627.2017.1364334

What Is Breast Cancer? [WWW Document], 2018. . Breastcancer.org. URL https://www.breastcancer.org/symptoms/understand_bc/what_is_bc (accessed 11.21.18).

What is cancer? [WWW Document], 2014. . Cancer Research UK. URL https://www.cancerresearchuk.org/about-cancer/what-is-cancer (accessed 11.21.18).

Worldwide cancer data [WWW Document], 2018. . World Cancer Research Fund. URL https://www.wcrf.org/dietandcancer/cancer-trends/worldwide-cancer-data (accessed 11.21.18).

You, J.S., Jones, P.A., 2012. Cancer Genetics and Epigenetics: Two Sides of the Same Coin? Cancer Cell 22, 9–20. https://doi.org/10.1016/j.ccr.2012.06.008

Yu, J.S.L., Cui, W., 2016. Proliferation, survival and metabolism: the role of PI3K/AKT/mTOR signalling in pluripotency and cell fate determination. Development 143, 3050–3060. https://doi.org/10.1242/dev.137075

Zhang, K., Dent, S.Y.R., 2005. Histone modifying enzymes and cancer: Going beyond histones. Journal of Cellular Biochemistry 96, 1137–1148. https://doi.org/10.1002/jcb.20615

Zhang, P., Torres, K., Liu, X., Liu, C., Pollock, R.E., 2016. An Overview of Chromatin-Regulating Proteins in Cells. Curr Protein Pept Sci 17, 401–410.

Zhang, S., Huang, W.-C., Li, P., Guo, H., Poh, S.-B., Brady, S.W., Xiong, Y., Tseng, L.-M., Li, S.-H., Ding, Z., Sahin, A.A., Esteva, F.J., Hortobagyi, G.N., Yu, D., 2011. Combating trastuzumab resistance by targeting SRC, a common node downstream of multiple resistance pathways. Nat Med 17. https://doi.org/10.1038/nm.2309

Zheng, S., Lv, P., Su, J., Miao, K., Xu, H., Li, M., 2019. Overexpression of CBX2 in breast cancer promotes tumor progression through the PI3K/AKT signaling pathway. Am J Transl Res 11, 1668–1682.

Appendices

Supplementary data

Supplementary table 1.1: Reagents

Reagent	Catalogue number	Company
MDA-MB-231 cells	HTB-26	ATCC
HS578T cells	HTB-126	ATCC
MCF10A cells	CRL-10317	ATCC
RPMI 1640 media	52400041	Gibco
DMEM media	11966025	Gibco
DMEM F12 media	1133057	Thermofisher
Cholera toxin	C8052	Sigma
hEGF	PHG0315	Gibco
Insulin	I0515-5mL	Sigma
Hydrocortisone	H0888	Sigma
Horse serum	16050122	Thermofisher
Glutamine	25030081	Gibco

Penicillin/streptomycin	10378016	Gibco
PVDF membrane	10600023	GE Healthcare
Clarity ECL	1705061	Biorad
Spectra protein ladder	26634	Thermofisher
Page ruler protein ladder	26620	Thermofisher
Whatman paper		GE Healthcare
MTS reagent	Ab197010	Abcam
Dynabeads protein A	10001D	Invitrogen

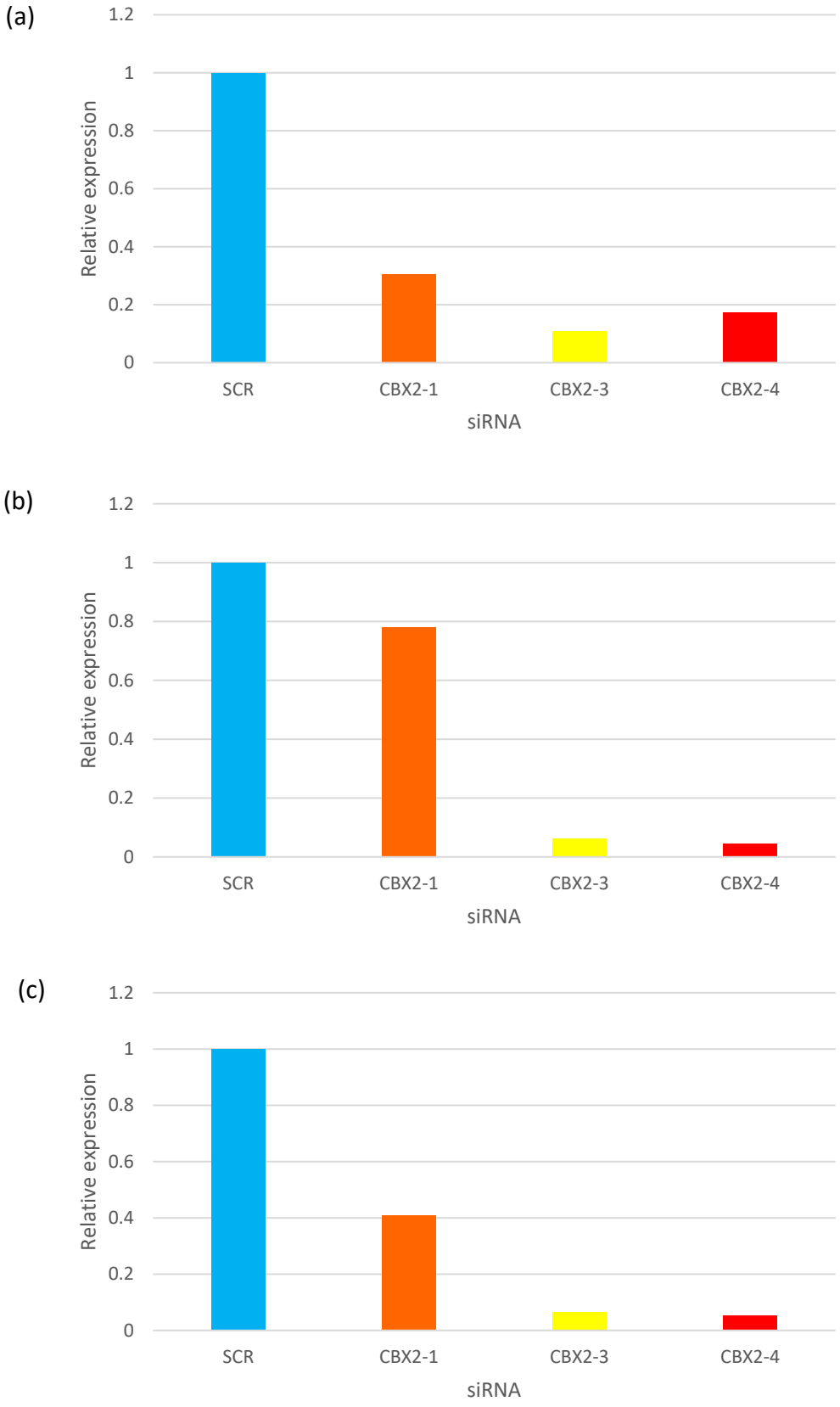

Supplementary figure 1.1. qPCR graphs showing 3 independent repeats of CBX2 mRNA expression in MDA-MB-231 cells. Expression of CBX2 was decreased in siCBX2-1, siCBX2-3 and siCBX2-4, with siCBX2-1 not knocking down CBX2 as efficiently as siCBX2-3 and siCBX2-4. (a) = n1, (b) = n2, (c) = n3.

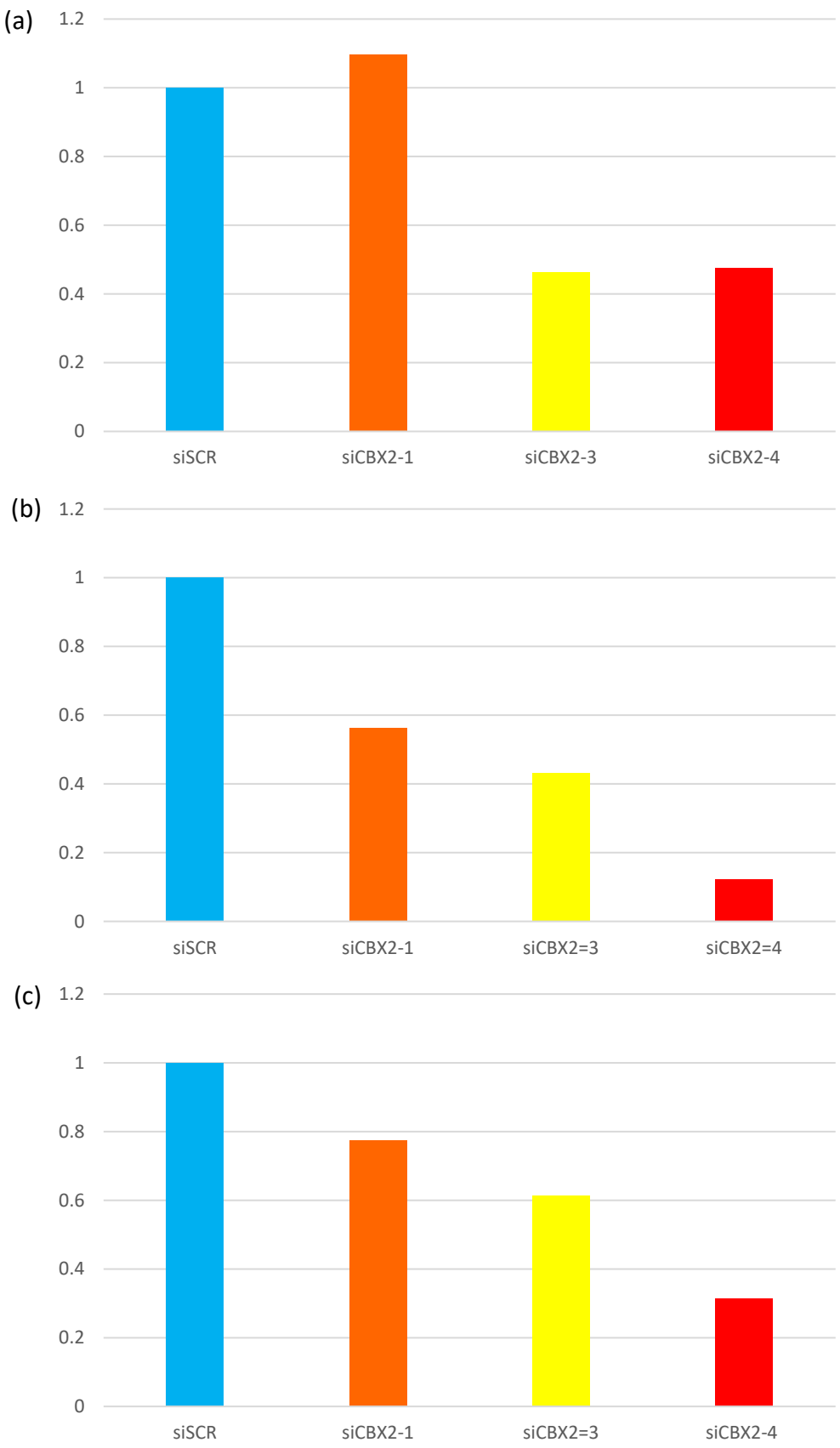

Supplementary figure 1.2. qPCR graphs showing 3 independent repeats of CBX2 mRNA expression in HS-578T cells. Expression of CBX2 was consistently decreased in siCBX2-3 and siCBX2-4, with siCBX2-1 not knocking down CBX2 as efficiently as siCBX2-3 and siCBX2-4. (a) = n1, (b) = n2, (c) = n3.

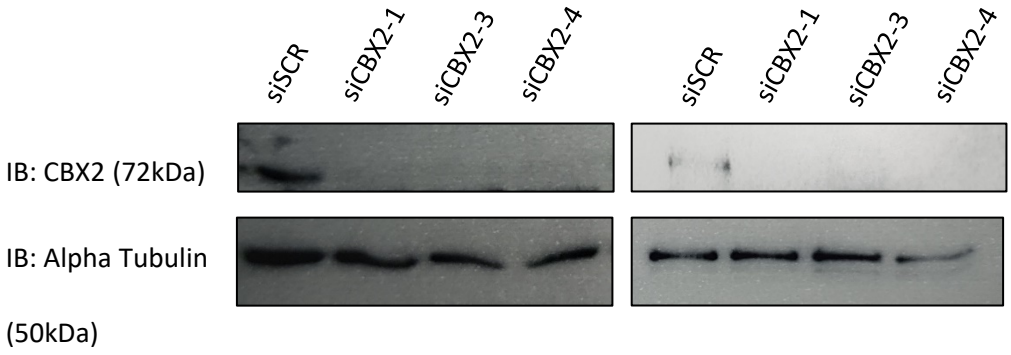

MDA-MB-231

Supplementary figure 1.3. Western blots showing 2 other independent repeats of CBX2 protein levels and alpha tubulin levels in MDA-MB-231 cells. Alpha tubulin shows equal loading. Representative blot of N=3 in Results.

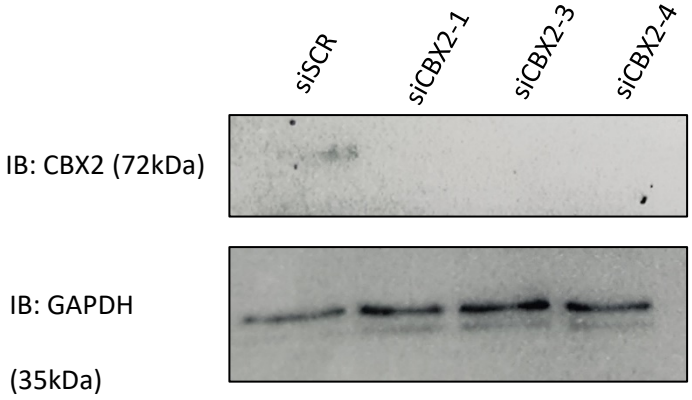

HS-578T

Supplementary figure 1.4. Western blots showing independent repeat of CBX2 protein levels an GAPDH levels in HS-578T cells. Representative blot of N=2 in Results.

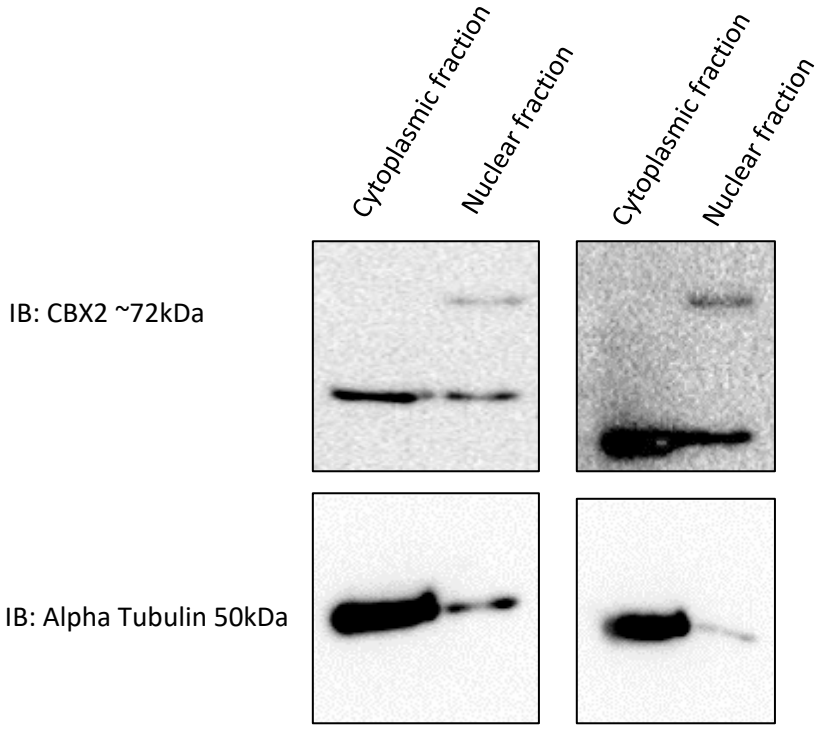

Supplementary figure 1.5. Western blots showing 2 other independent repeats of cell fractionations in MDA-MB-231 cells. Representative blot of N=3 in Results.

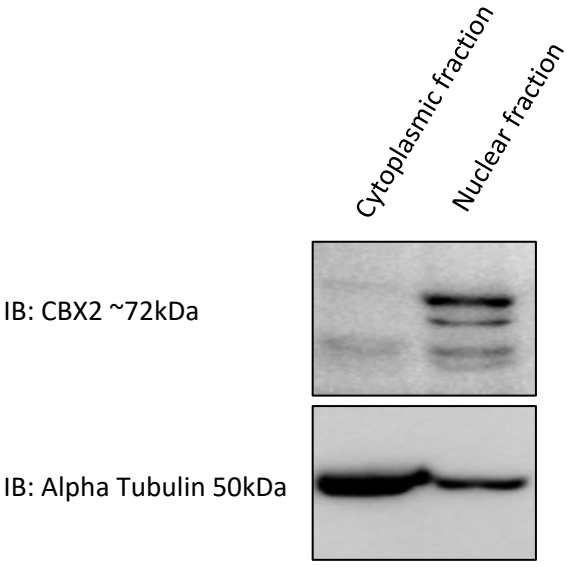

Supplementary figure 1.6. Western blots showing 1 other independent repeat of cell fractionations in HS-578T cells. Representative blot of N=2 in Results.

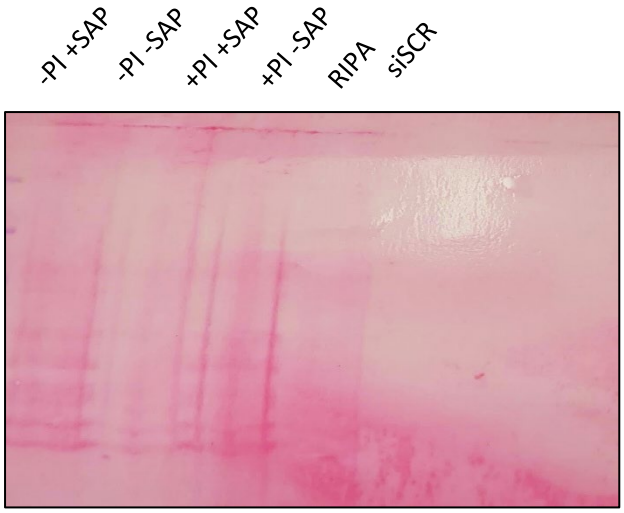

Supplementary figure 1.7. Ponceau stain on SAP experiment membrane in MDA-MB-231 cells. This stain shows the presence of protein and was performed as a troubleshooting measure.

(a)

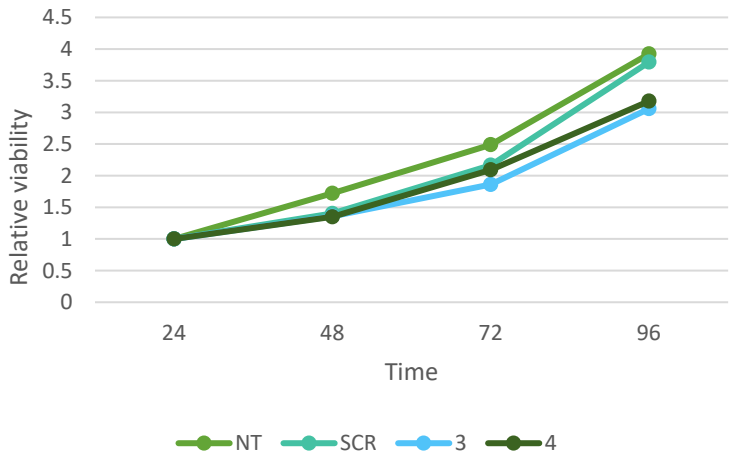

(b)

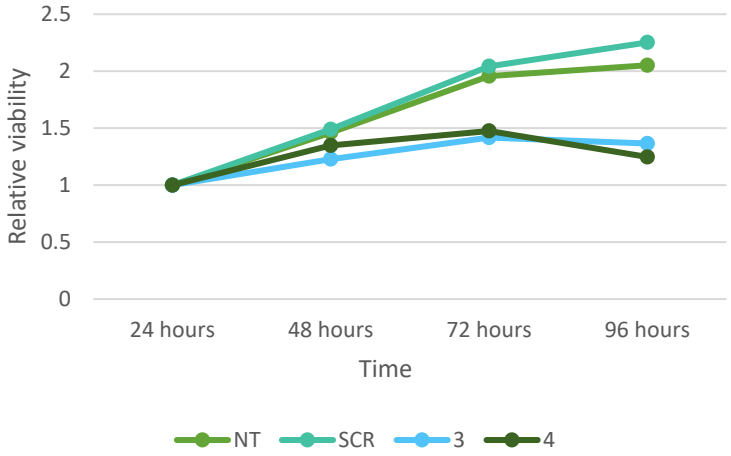

(c)

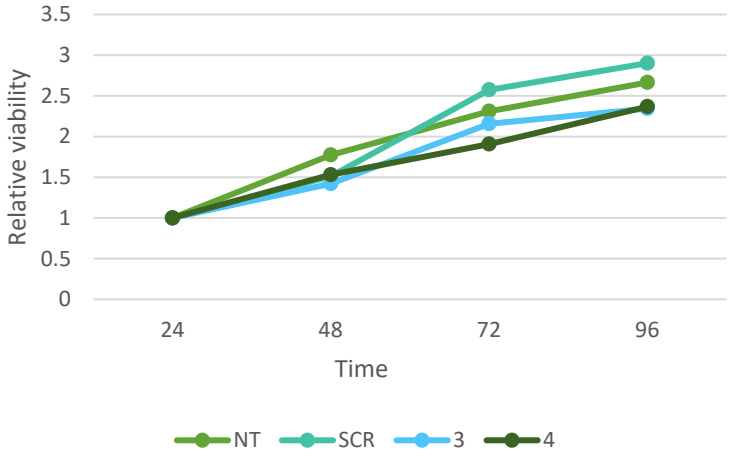

Supplementary figure 1.8. MTS graphs showing 3 independent repeats of cell viability in MDA-MB-231 cells. (a) = n1, (b) = n2, (c) = n3.

(a)

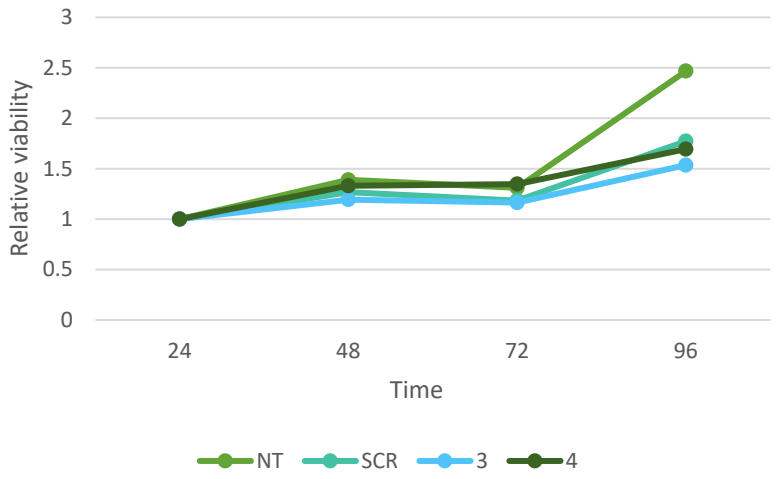

(b)

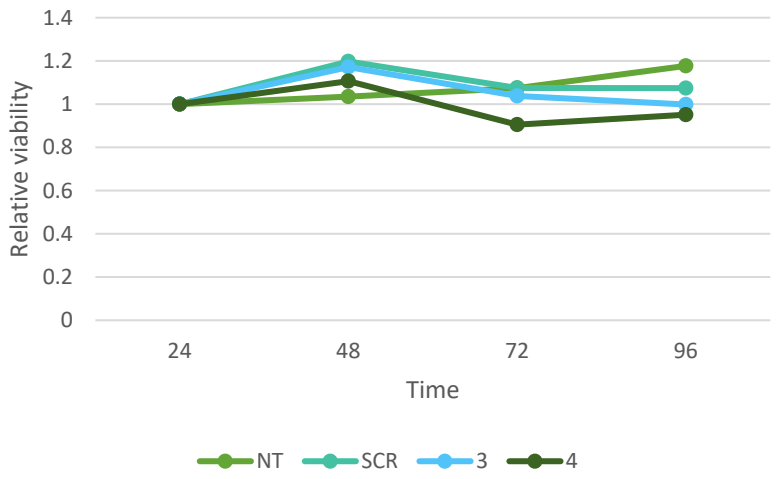

Supplementary figure 1.9. MTS graphs showing 2 independent repeats of cell viability in HS-578T cells. (a) = n1, (b) = n2.

(a)

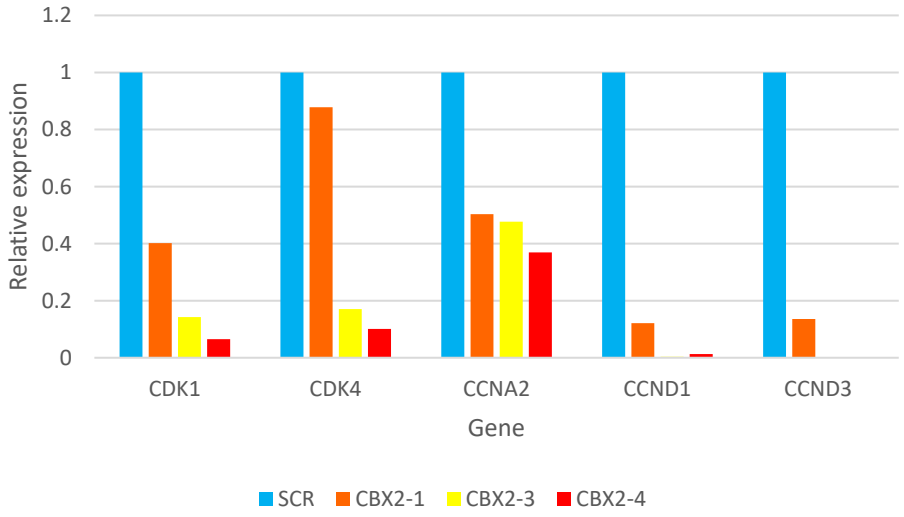

(b)

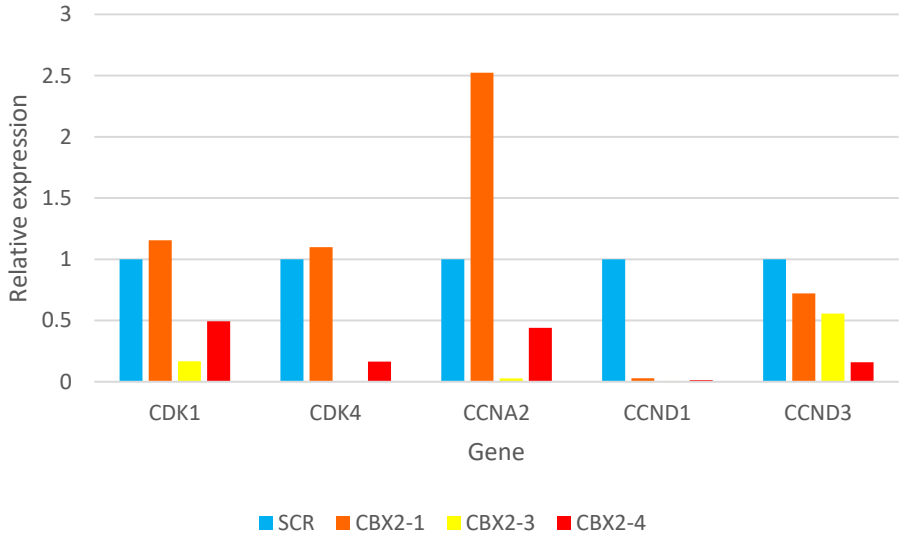

(c)

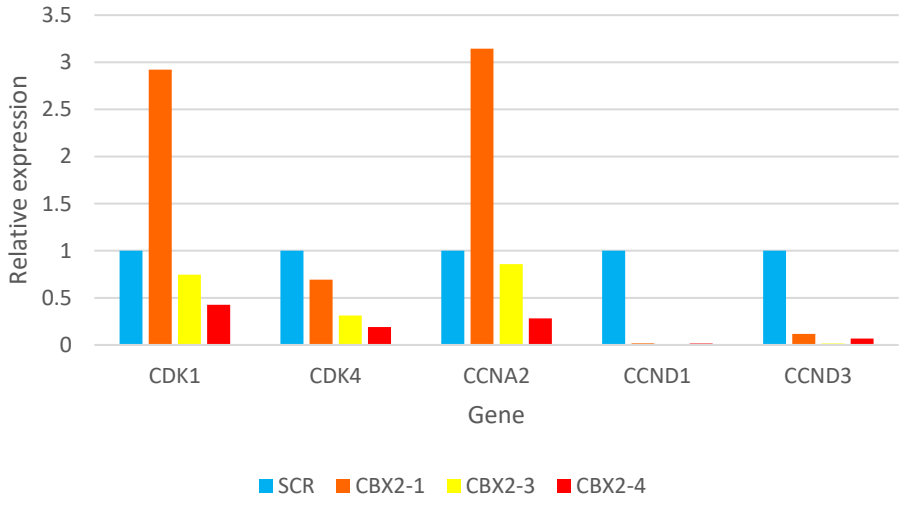

Supplementary figure 1.10. qPCR graphs showing 3 independent repeats of cell cycle regulatory genes in MDA-MB-231 cells. (a) = n1, (b) = n2, (c) = n3.

(a)

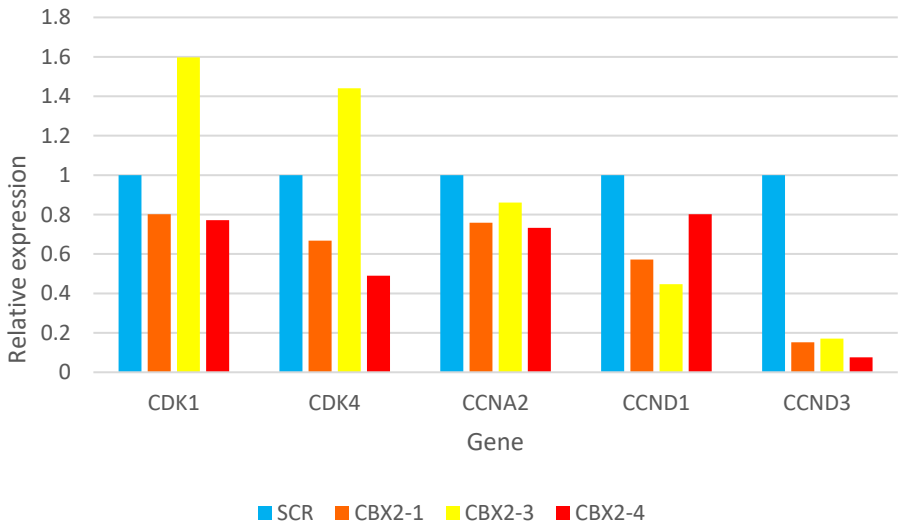

(b)

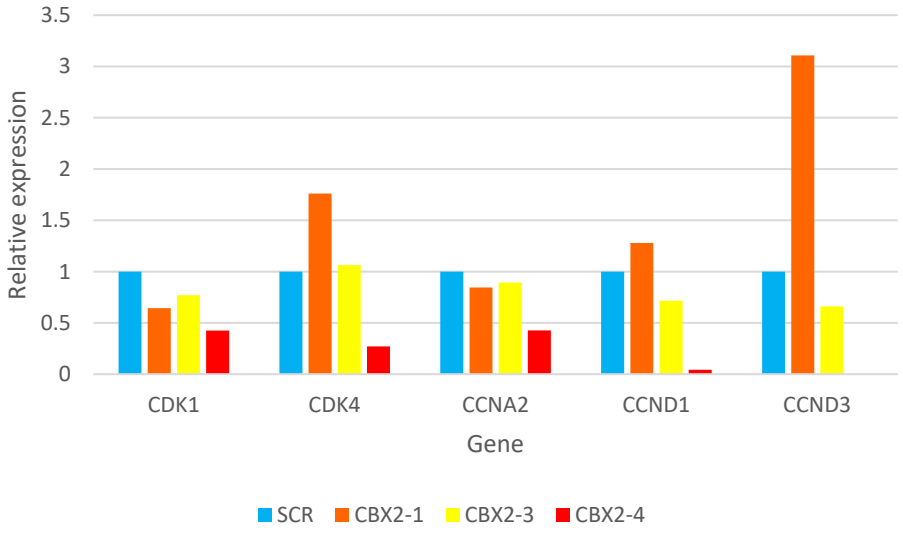

(c)

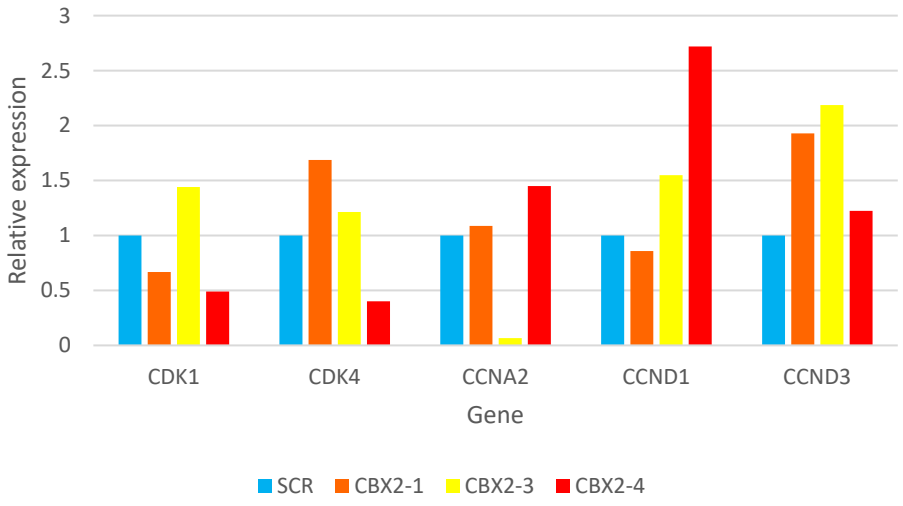

Supplementary figure 1.11. qPCR graphs showing 3 independent repeats of cell cycle regulatory genes in HS-578T cells. (a) = n1, (b) = n2, (c) = n3.

(a)

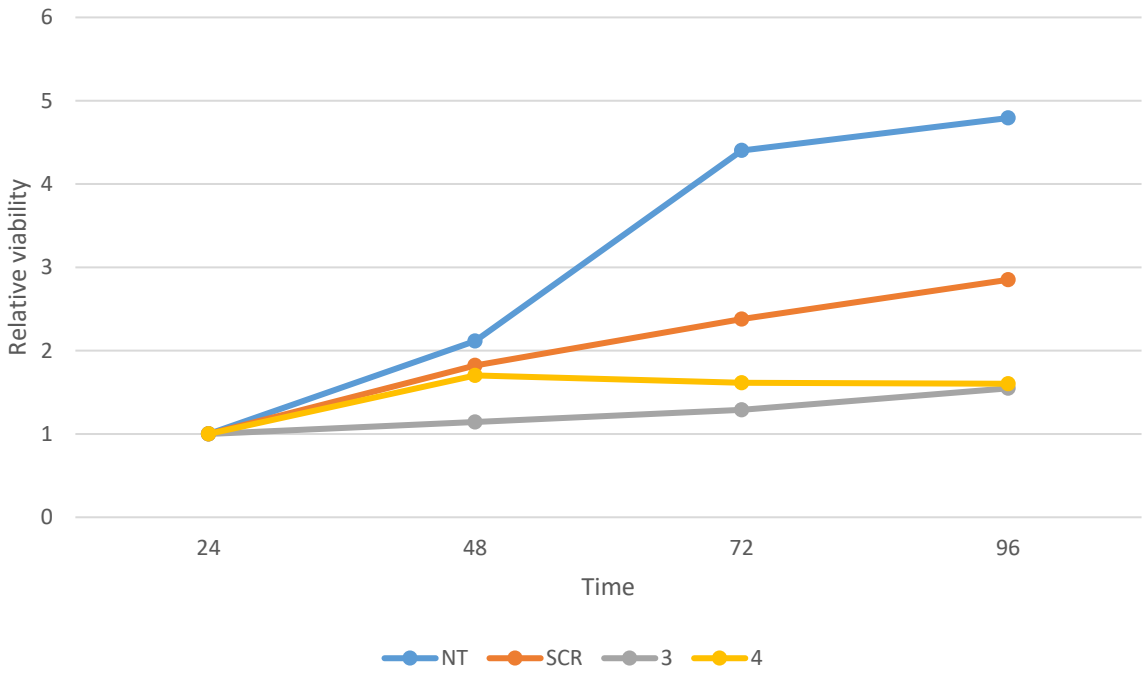

(b)

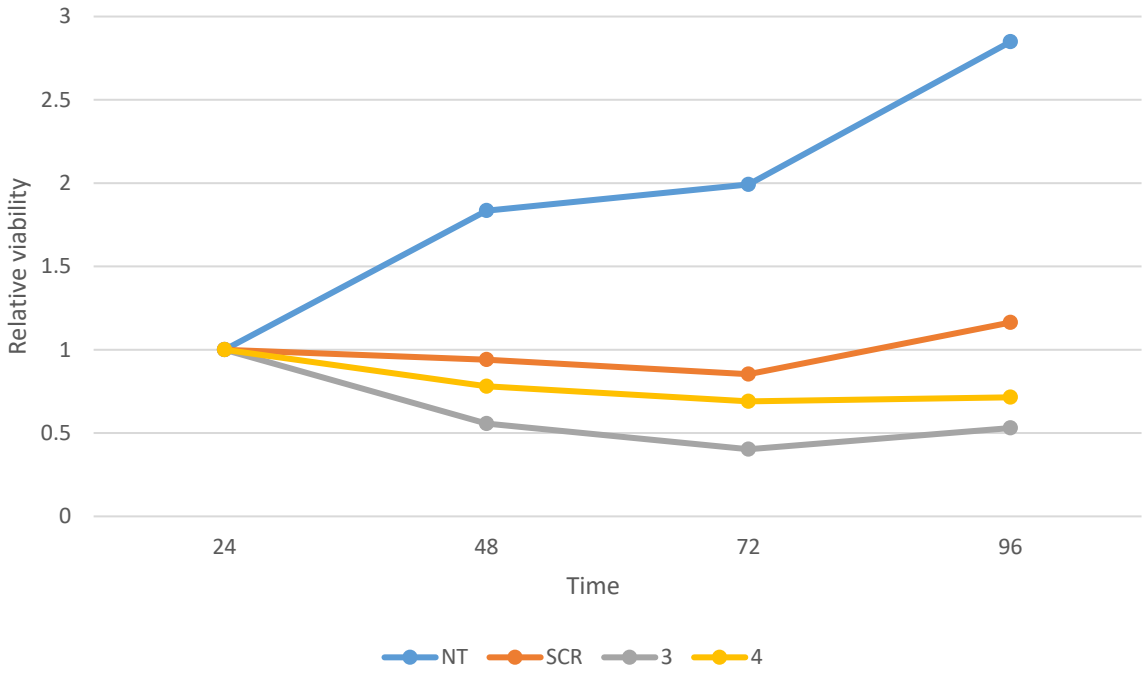

Supplementary figure 1.12. 3 independent MTS graphs showing cell viability in MCF-10A cells. Representative graph in results. (a) = n1, (b) = n2.

Supplementary table 1.2. Table showing 3 independent repeats of cell counts in MCF-10A cells. Within each repeat, the counts were taken in triplicate (left hand side of table).

	1				2				3			
	siSCR	siCBX2-1	siCBX2-3	siCBX2-4	siSCR	siCBX2-1	siCBX2-3	siCBX2-4	siSCR	siCBX2-1	siCBX2-3	siCBX2-4
Repeat 1	21	18	18	13	41	34	19	24	35	21	20	21
Repeat 2	21	18	16	14	33	30	20	21	30	28	17	18
Repeat 3	19	14	15	14	45	23	16	19	26	27	14	24

(a)

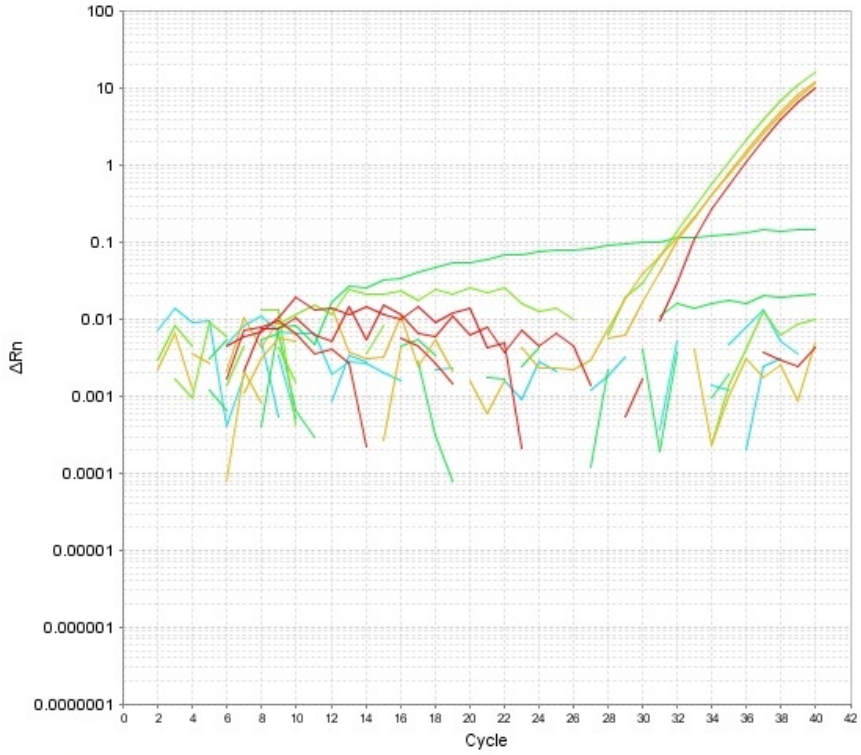
100
10
1
0.1
0.01
0.001
0.0001
0.00001
0.000001
0.0000001
ΔRn
0 2 4 6 8 10 12 14 16 18 20 22 24 26 28 30 32 34 36 38 40 42
Cycle

(b)

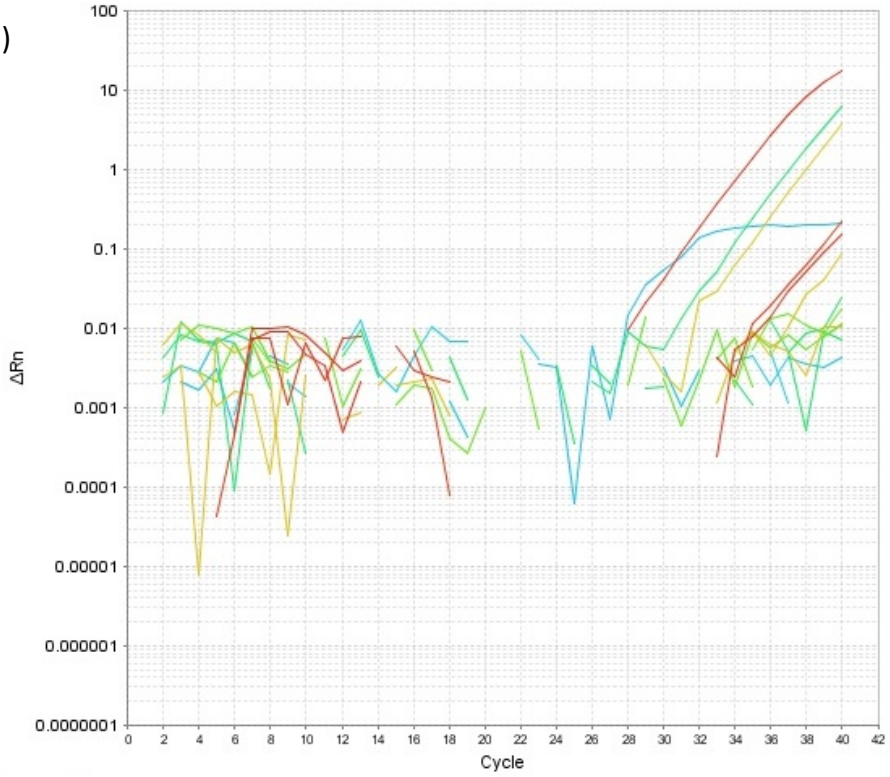
100
10
1
0.1
0.01
0.001
0.0001
0.00001
0.000001
0.0000001
ΔRn
0 2 4 6 8 10 12 14 16 18 20 22 24 26 28 30 32 34 36 38 40 42
Cycle

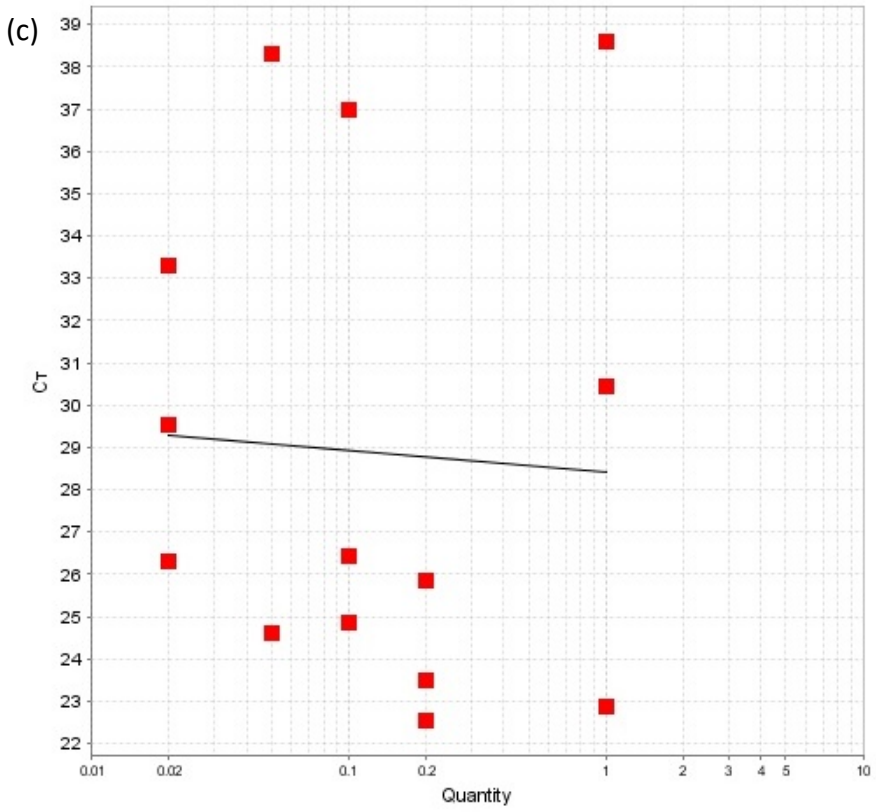

Supplementary figure 1.13. qPCR graphs showing that p16 and p21 were not expressed in MDA-MB-231 cells. (a) = p16 amplification plot, (b) = p21 amplification plot, (c) = p16 standard curve.